MECHANISM OF RESISTANCE TO FLOW OVER ARTIFICIAL ROUGHNESS ELEMENTS

By
K.G. RANGA RAJU

A Thesis

Submitted in fulfilment of the requirements for

the award of the degree of Doctor of Philosophy in

CIVIL ENGINEERING OF THE UNIVERSITY OF ROORKEE

DEPARTMENT OF CIVIL ENGINEERING
UNIVERSITY OF ROORKEE
ROORKEE
1967

CERTIFICATE

Certified that the thesis entitled 'MECHANISM OF RESISTANCE TO FLOW OVER ARTIFICIAL ROUGHNESS ELEMENTS' which is being submitted by Mr. K.G. Ranga Raju in fulfilment of the requirements for the award of the Degree of Doctor of Philosophy in Civil Engineering of the University of Roorkee is a record of the student's own work carried out by him under my supervision and guidance. The matter embodied in this thesis has not been submitted for the award of any other Degree.

This is further to certify that he has worked for a period of 2 years and 10 months from July 1964 to April 1967 for preparing this thesis.

R.J. Garde

(R.J. Garde)
Professor of Civil Engineering,
University of Roorkee,
Roorkee, U.P.

Roorkee.

Dated Ist May, 1967.

****

ABSTRACT

This thesis presents the results of an experimental investigation concerning the mechanism of resistance to flow over two-dimensional sharp-edged roughness elements of negligible thickness. The studies were carried out in a tilting flume with water and also in two wind tunnels, one of them being an open circuit tunnel & other of the closed-circuit type. Experiments were carried out to cover the following aspects of the problem :-

a) Effect of contraction of the stream on the drag coefficient of sharp-edged plates.

b) Effect of submergence of a normal plate in a turbulent boundary on the drag coefficient of the plate.

c) Form resistance of an element kept in series on a plane boundary and the total resistance of the plane boundary.

d) Effect of introduction of a small roughness element in the wake of a large one on the resistance characteristics of both the elements.

In addition to the aspects mentioned above, information has also been obtained on the nature of velocity distribution in the flow over artificial roughness elements and on the location of datum as related to the relative spacing of the roughness

elements . Also the applicability of the method suggested by Morris to the type of roughness elements used in this study has been examined.

The conclusions derived on the basis of the analysis of data concerning the various aspects mentioned above afford a better insight into the problem of resistance of artificial roughness elements.

***

ACKNOWLEDGEMENTS

The author is extremely grateful to Dr. R.J.Garde, Professor in Civil Engineering, University of Roorkee, for his invaluable guidance throughout the present investigation. He was the author's supervisor and guide during this investigation and his suggestions at various stages of the work proved to be highly beneficial. The author also expresses his thanks to Dr. O.P. Jain, Head of Department of Civil Engineering for his constant encouragement.

The assistance given by Mr. B.R. Sethi and his Laboratory Staff during the experimental investigation is highly appreciated.

-:o:-

TABLE OF CONTENTS

CHAPTER		PAGE
	LIST OF SYMBOLS	6-10
	LIST OF FIGURES	11-13
I	INTRODUCTION	14-20
II	REVIEW OF LITERATURE	21-42
III	ANALYTICAL CONSIDERATIONS	43-55
IV	EXPERIMENTAL EQUIPMENT AND PROCEDURE	56-69
V	ANALYSIS OF DATA - I - RESISTANCE OF A SINGLE ELEMENT	70-89
VI	ANALYSIS OF DATA - II - RESISTANCE OF A SERIES OF ELEMENTS	90-114
VII	ANALYSIS OF DATA - III - COMBINATION OF ELEMENTS OF DIFFERENT HEIGHTS	115-120
VIII	CONCLUSIONS	121-124
	REFERENCES	125-128
	FIGURES	129-170
	APPENDIX	171-183

-:o:-

LIST OF SYMBOLS

Symbol		Meaning	Units	Dimension
A	=	Projected area of a body on a plane normal to the direction of motion	Metre^2	L^2
A_1, B_1	=	Constants in resistance equation	Dimensionless	-
B	=	Width of channel	Metres	L
β	=	Momentum correction factor	Dimensionless	-
C	=	Chezy's coefficient	$m^{1/2}/sec$	$\frac{L^{1/2}}{T}$
C_D	=	Drag coefficient based on the average velocity	Dimensionless	-
C_{D_o}	=	Drag coefficient based on the average velocity, but corresponding to an infinite stream	"	-
C_{D_1}	=	Drag coefficient based on the free stream velocity	"	-
C'_D	=	Drag coefficient based on the velocity at the crest level of the element, under infinite stream conditions	"	-
C_{D_c}	=	Drag coefficient corrected for blockage according to Maskell	"	-
C_{D_p}	=	Drag coefficient of an element in the primary series	"	-
C_{D_s}	=	Drag coefficient of an element in the secondary series.	"	-

Symbol		Meaning	Units	Dimension
C_1, C_2	=	Constants used in the resistance equation.	Dimensionless	-
C_{Pbc}	=	Theoretical base pressure corrected for blockage used by Maskell	''	-
C_w	=	Constant used by Morris	''	-
D	=	Depth of test section of the wind tunnel or depth of flow in the flume measured from the floor	cms or metres	L
D_c	=	Diameter of the conduit	''	L
d_{50}	=	Sediment size for which 50 percent of the material, by weight, is finer.	Metres	L
d_{65}	=	Sediment size for which 65 percent of the material, by weight, is finer	''	L
d_{90}	=	Sediment size for which 90 percent of the material, by weight, is finer	''	L
δ	=	Thickness of the boundary layer defined so that the velocity at the edge of the boundary layer is equal to 99 percent of the free stream velocity	cms	L
e	=	Lateral spacing between roughness elements	cms	L
ρ	=	Mass density of the flowing fluid	Metric slug/m^3	M/L^3
ϵ	=	Blockage coefficient used by Maskell	Dimensionless	-
F	=	Force acting on a unit length of a two-dimensional element	kgm/metre	M/T^2
F_d	=	Force acting on a body of area 'A'	kgm	ML/T^2

Symbol		Meaning	Unit	Dimension
F_B	=	Force acting on a strip element of width B	kgm	ML/T^2
Fr	=	Froude number of the flow	Dimensionless	-
F_{r-n}	=	Froude number corresponding to neutral stability	''	-
f	=	Darcy-Weisbach resistance coefficient	''	-
f_s	=	Darcy-Weisbach resistance coefficient for the smooth bed	''	-
g	=	Acceleration due to gravity	Metre/scc^2	L/T^2
h	=	Height of roughness element	cms	L
h'	=	Height of roughness element in the secondary series	cms	L
h_f	=	Head loss in a length of conduit L_c	metres or cms	L
j	=	Width of groove in a bed with roughness elements	metres	L
K	=	Karman's constant	Dimensionless	-
K_s	=	Equivalent Sandgrain roughness of the bed	metres	L
K_s'	=	Resistance parameter which is a function of the roughness geometry	Metres	L
ℓ	=	Mixing length	Metres	L
L	=	Spacing between the roughness elements	cms	L
L_c	=	Length of conduit	Metres	L

Symbol		Meaning	Unit	Dimension
L_1	=	Distance of the small element from the large element	cms	L
L'	=	Spacing of elements in the secondary series	cms	L
λ	=	Roughness concentration, defined as ratio of projected area of roughness elements to the area of the bed.	Dimensionless	-
μ	=	Dynamic viscosity of the flowing fluid	$\frac{\text{kgm sec}}{m^2}$	$\frac{M}{LT}$
n	=	Manning's roughness coefficient	$\text{metre}^{-1/3}\ \text{sec}$	$T/L^{1/3}$
ν	=	Kinematic viscosity of the flowing fluid	m^2/sec	L^2/T
p	=	Perimeter of roughness elements in a cross section	metres	L
p_o	=	Ambient pressure	kgm/m^2	M/LT^2
p_u	=	Pressure on the upstream face of the element at a height y from the floor	''	''
$\bar{p}_u$	=	Average pressure on the upstream face of the element	''	''
p_d	=	Constant pressure on the downstream face of the element	''	''
P	=	Perimeter of channel	Metres	L
R	=	Hydraulic radius of channel	Metres	L
R_b	=	Hydraulic radius with respect to bed	Metres	L
R_e	=	Reynolds number of flow	Dimensionless	-
r	=	Unit weight of the flowing fluid	kgm/m^3	M/L^2T^2

Symbol		Meaning	Unit	Dimension
$\triangle r_f$	=	Difference in unit weight of the flowing fluid in an open channel and the fluid above the free surface.	kgm/m^3	M/L^2T^2
S	=	Water surface slope	Dimension less	-
t	=	Thickness of the roughness element	cms	L
τ_o	=	Average shear stress on the bed	kgm/m^2	M/LT^2
U_o	=	Free stream velocity	metre/sec	L/T
u_h	=	Velocity at a height 'h' from the floor	"	"
u	=	Velocity at a height 'y' from the floor	"	"
V	=	Average velocity in the vertical centre line of the tunnel	"	"
V_o	=	Average velocity in the vertical centre line of the tunnel corrected for blockage	"	"
$\overline{V}$	=	Average velocity over the cross section of the channel	"	"
V_*	=	Shear velocity = $\sqrt{\tau_o/\rho}$	"	"
X,Y	=	Constants used in Koloseus's equations	Dimension less	-
y	=	Height measured from the floor	Metres	L
Z	=	Constant used in Koloseus's equation	Dimension less	-

-:o:-

LIST OF FIGURES

Fig.No. Description

2.1 - Pressure distribution around elements in midstream (Ref. 4)

2.2 - Variation of C_{D_1} with δ/h for normal plates

2.3 - Different zones of flow for the case of a normal plate in a turbulent boundary layer (Ref. 26)

2.4 - Criterion for prediction of type of flow, proposed by Morris (Ref. 17)

2.5 - Typical velocity profiles in corrugated metal pipes (Ref. 17)

2.6 - Variation of K with roughness concentration for strip roughnesses (Ref. 37)

2.7 - Relation between $1/\sqrt{f}$ and 4D/h at small values of D/h - cubical roughnesses (Ref. 24)

2.8 - Typical velocity profiles with strip roughnesses (Ref.2)

4.1 - Schematic diagram of the flume.

4.2 - Schematic diagram of the open-circuit wind tunnel

4.3 - Pressure variation along the length of test section of open-circuit tunnel.

4.4 - Typical velocity profile in boundary layer of open-circuit tunnel.

4.5 - Variation of δ along length of test section of Open-circuit tunnel.

4.6 - Velocity distribution in boundary layer in open-circuit tunnel .

Fig.No. Description

4.7 - Diagram showing placement of element in midstream .

4.8 - Diagram showing combination of two roughness series.

5.1 - Pressure distribution around elements in uniform flow.

5.2 - Variation of $(\bar{p}_u - p_o)\frac{1}{\rho V^2/2}$ and $(p_d - p_o)\frac{1}{\rho V^2/2}$ with h/D for elements in uniform flow.

5.3 - Variation of C_D with (1 - h/D) for elements in uniform flow.

5.4 - Variation of C_D with $p_d - p_o / \rho V^2/2$ for elements in uniform flow.

5.5 - Pressure distribution around elements in boundary layer

5.6 - Variation of $\frac{\bar{p}_u - p_o}{\rho V^2/2}$ and $\frac{p_d - p_o}{\rho V^2/2}$ with δ/h .

5.7 - Variation of C_D with D/h and δ/h for element in boundary layer.

5.8 - Variation of C_{D_o} (Drag Coefficient corrected for blockage) with δ/h-

5.9 - Variation of C_D'(Drag coefficient with respect to velocity at crest level, in infinite stream) with δ/h.

5.10 - Relation between C_D and $\frac{p_d - p_o}{\rho V^2/2}$ for elements in boundary layer.

5.11 - Variation of C_D with D/h for element on bed of an open channel.

6.1 - Flume data plotted on Morris's curve (Ref.17) for wake-interference type of roughness

6.2 - Comparison of observed and predicted friction. factors (by Morris's method -Ref 17) for isolated-roughness flow.

Fig.No. Description

6.3 - Variation of C_D along the length for elements in series.

6.4 - Pressure distribution around element - Elements in series.

6.5 - Variation of C_D with h/L and D/h for tunnel data.

6.6 - Variation of C_{D_o} (obtained from Eq. 5.2) with h/L and D/h for tunnel data.

6.7 - Velocity profiles along the length of tunnel for elements in series.

6.8 - Comparison of velocity profiles in tunnel and flume.

6.9 - Variation of $1/\sqrt{C_D}$ with D/h and L/h for tunnel and flume data.

6.10 - Variation of C_1 with L/h for elements in series.

6.11 - Variation of C_2 with L/h for elements in series.

6.12 - Comparison between observed and predicted resistance for Basha's data (Ref.6)

6.13 - Comparison of conventional resistance equation with observed variation.

6.14 - Plot of u/V_* vs Log_{10} y for tunnel and flume data.

7.1 - Variation of C_D with L_1 for case of 2 cm strip downstream of a 4 cm strip ($\delta/h = 0.28$)

7.2 - Variation of C_D with relative displacement of two series of roughnesses (Tunnel data).

7.3 - Variation of 'effective' C_D of an element in the primary series with D/h for combination of two roughness series.

7.4 - Variation of C_2 with L_1 for combination of two roughness series (Based on flume data).

-:o:-

CHAPTER - I

I N T R O D U C T I O N

1.1 Preliminary Remarks :

The problem of prediction of resistance to flow in open channels has attracted the attention of engineers for a long time. A knowledge of the resistance to flow in open channels is essential in the design of canals, preparation of stage-discharge curves for rivers and other related problems. However, an accurate solution of the problem of prediction of resistance in open channels is much more difficult than in the case of flow under pressure through pipes. Firstly, while one is concerned mostly with pipes of circular cross section, the cross section of open channels may be of any shape from circular to an irregular form as in the case of natural streams. Also , the configuration and arrangement of roughness elements encountered in case of natural open channels are almost infinite; as a result, the range of variation of the resistance coefficient is much larger in open channels than in pipes.

It is well known (38)* that in flow past a boundary with small roughness elements, the velocity distribution in the turbulent flow region is logarithmic for smooth, rough and the transition boundaries. However, deviations from the logarithmic velocity distribution law have been noticed (17,23) in the flow past a boundary with fairly large-sized roughness elements; this

---

* Numbers in paranthesis relate to References given at the end.

departure would necessarily introduce some inaccuracy in the resistance relation obtained by integrating the logarithmic velocity distribution equation.

Nevertheless, empirical resistance relations like the Chezy's and the Manning's equations have been developed and these are useful under a limited range of conditions. The Manning's equation, in particular, has become a widely accepted resistance relation for rigid-bed open channel. flow. In using this relation, the roughness coefficient 'n' for a channel is fixed by experience or by reference to standard tables (7) in most cases; however, in the particular case of flow over a hydrodynamically rough sandy bed without motion, the Strickler's equation, viz ;

$$n = \frac{d^{1/6}}{24} \quad \text{in metric units} \qquad \ldots\ldots\ldots (1.1)$$

is commonly used. In the above equation, d is the representative grain size in metres. But there appears to be no agreement on the effective or the representative size of the material to be used in the Strickler's equation. While Einstein (8) has used d_{65} (the size for which 65 percent of the material by weight is finer) and Meyer-Peter and Mueller (15) have used d_{90} (the size for which 90 percent of the material by weight is finer) - though with a slightly different numerical constant, - the size d_{50} (the size for which 50 percent of the material, by weight, is finer) has been used as the effective size by many others. Apparently when the effective resistance is the combined effect of a number of different roughness elements (as is the above case), there seems to be no reliable procedure of evaluating the total resistance accurately. The case of flow over an alluvial bed with motion is

another highly involved problem of this category. In this case at shear stresses large enough to cause movement of the sediment, sediment motion is accompanied by the formation of undulations on the bed which change in character and size with changes in discharge. The total resistance in this case is the effective sum of the grain resistance and the form resistance of the undulations and no accurate method is available at present to predict the resistance coefficient for such channels.

1.2 Studies on Artificial Roughness Elements :

The resistance characteristics of commercial pipe surfaces can be conveniently expressed in terms of an 'equivalent sand grain roughness' as a result of the experimental work carried out by Nikuradse on sand-coated pipes and by Colebrook and White on commercial pipes (38). Based on experiments on artificial roughness elements, a number of efforts have been made to evolve a roughness standard for open channels, similar to the sand grain roughness for commercial pipes. Notable among these are the works of Schlichting (38), Powell (28), Johnson (12), Basha (6), Adachi(2) and Sayre and Albertson (37). But they have not met with the same remarkable success as the work leading to the sand grain concept for natural pipe surfaces. An attempt by Basha (6) at comparing the resistance characteristics of alluvial channels and those of a channel with artificial roughness elements indicated merely a qualitative similarity. Further, all the above studies were concentrated on the total resistance of a plane boundary interspersed with a regular array of artificial roughness elements, without regard to the individual roughness effects.

A rational approach to the problem of resistance of a composite bed (defined here, as one comprising of different types and sizes of roughness elements) was suggested by Einstein and Banks (9). They carried out flume experiments with different combinations of various types of roughnesses and found that the total (effective) resistance could be obtained as the sum of the resistances offered by the individual roughness elements. Also for the roughness concentrations studied, it was found that the roughness elements could be treated as discrete and the standard values of drag coefficient (36) (for case of unlimited extent of stream without any velocity gradient)could be used to predict the resistance offered by the roughness elements.

1.3 Interference Effect :

The above findings would imply that the interference effect - namely, the effect of the presence of a roughness element on the resistance of the other roughness elements or on the resistance of the plane boundary - was not appreciable. In other words, according to this approach, the effective resistance can be obtained as the sum of the plane boundary friction over the whole area and the form resistance of the roughness elements calculated using the listed values of drag coefficient (36); thus, each element is being treated as if kept isolated in a stream of infinite extent and is also assumed to exert no influence on the plane boundary friction. However, over a wide range of roughness patterns and spacings, one would expect that the interference effect would be important and needs to be considered in the analysis. In fact, the drag coefficient of the element would be in general, a function of the depth of the stream, the type, size

and arrangement of the roughness elements, and the area on which plane boundary friction is effective would depend on the roughness pattern and size also. It may be mentioned that in the problem of alluvial channel resistance, an attempt at considering the effect of presence of bed forms on the grain resistance has been made by Tsubaki (39).

Thus, in applying the approach of Einstein and Banks (9), to a case where there are different types of roughnesses on the bed, it is very essential to evaluate the effect of interference on the resistance parameters. Considering the case of a plane smooth boundary on which artificial roughness elements are arranged at different concentrations, the following information is essential in thoroughly understanding the mechanism of resistance of the bed:

a) The drag coefficient of a representative roughness element and its variation with the roughness concentration and other flow parameters,

b) the effective area of the plane boundary on which skin friction would act and the variation of the friction coefficient for this area with the relevant parameters.

1.4 Drag Coefficient of the Roughness Element :

It may be mentioned that very little information is available on the two aspects of the problem, mentioned above. Though information on the drag coefficient of bodies held in an uniform stream of infinite extent (the term uniform has been used here to indicate a flow region in which there is no velocity

variation across the flow) is available (36) only limited studies have been reported (4,21,26) concerning the resistance of bodies placed on a boundary. The flow past a body placed on a boundary is different from that past a body held in uniform flow in two respects; firstly the wake behind an element kept on the boundary is of the non-oscillating type, while that behind a body in uniform flow is of the oscillating type. The plane boundary, apparently, places a restraint on the tendency of the vortices shed in the wake to oscillate. Secondly, an element placed on a boundary would be submerged in a boundary layer, while the element held in uniform flow is in a region where there is no velocity gradient. For these two reasons, one cannot use the available results for uniform flow without the plane boundary restraint on the vortices, in the present case. Further, information is also lacking concerning the variation of drag coefficient of a roughness element, when placed at various concentrations on the boundary. The skin friction on the plane boundary with artificial roughness elements is another aspect of the problem, which needs detailed study.

1.5 Scope of the Investigation :

This investigation was, therefore, carried out with a view to enable a better appreciation of the mechanism of resistance to flow over artificial roughness elements kept on a plane boundary by providing information on the two aspects mentioned earlier. It is hoped that the information would be useful in studies on artificial roughness elements aimed at evolving a roughness standard or in problems concerning the prediction of the resistance of a composite bed.

The problem posed for investigation was simplified by restricting the studies to two dimensional roughness elements, placed laterally across the width of the channel. Sharp-edged strips of negligible thickness were used as the roughness elements, since the drag coefficient of these strips would be independent of Reynolds' number over a large range of Reynolds number. The work was programmed to provide the following information :

a) Resistance of a single element kept on a boundary :- A single element kept on a boundary would form a limiting case of a plane boundary with artificial roughness elements at various concentrations. The results of this part of the study would also be of help in the estimation of wind forces on isolated structures.

b) Effect of variation of the spacing parameter of roughness elements in series on the total resistance coefficient and on the drag coefficient of the representative element in the series. The spacing parameter is defined as the ratio of the spacing, L, to the height of the element, h, and it was varied from 2.5 to 40.0. The ratio of the flow depth, D, to the height of the element was varied from 3.0 to 27.0 .

c) Resistance of a small roughness element placed in the wake of a large one and the effect of introduction of the additional roughness element on the resistance of the larger one:- The results of this part of the study would provide some preliminary information concerning the sheltering effect of the coarser particles on the small particles of the sandy bed of an alluvial channel.

-:o:-

CHAPTER - II

REVIEW OF LITERATURE :

2.1 Preliminary Remarks :

Many investigations concerning the problem of resistance to flow over artificial roughness elements have been carried out in the past. These investigations have been conducted by hydraulic engineers, as well as the aeronautical engineers. The studies conducted by the aeronautical engineers throw light on the characteristics of flow around single roughness elements, the variation of their drag coefficients, etc. The studies conducted by hydraulic engineers mainly relate to the case of a series of elements on the bed of an open channel and the effect of the roughness concentration on the resistance coefficient. The salient features of both the above categories of investigations are reviewed in this chapter to illustrate the various approaches that have been made in the past and to bring out clearly those aspects on which information is lacking.

For the purpose of this investigation, the review of literature has been divided into two categories :-

a) Studies on the resistance of a single roughness element, most of these studies having been conducted in a wind tunnel.

b) Studies on the total resistance of a plane boundary with a series of roughness elements placed on it, most of these studies being in open channels.

2.2 Studies on a Single Roughness Element :

Roshko (32) 1955, while studying the characteristics of flow past bluff bodies, found that the shedding frequency of vortices behind a cylinder and its drag coefficient are reduced by the provision of a tail plate parallel to the flow and along the plane of symmetry.

Arie and Rouse (4), 1956, studied the characteristics of two-dimensional flow over a plate kept normal to a plane boundary. The experiments were performed in the uniform test section of an open-circuit wind tunnel. The problem was simplified by eliminating the effect of the approach boundary layer by placing the plate vertically in midstream (away from the plane boundary); but the non-oscillating character of the wake was maintained by the provision of a tailplate which was symmetrical with respect to the test plate and normal to it . The tail plate extended in the downstream direction a distance slightly greater than the length of the standing eddy. The separating streamline downstream of the test plate was approximated by a Rankine oval and it was assumed that the streamlines at a considerable distance from the plate would approximate those in irrotational flow past the Rankine oval. Based on these ideas, the streamline configuration in the vicinity of the tunnel floor and ceiling were determined . The calculated co-ordinates of the streamlines were corrected taking into account the fact that a boundary layer would develop along the tunnel floor and ceiling. To obviate the effect of the presence of the tunnel floor and ceiling on the flow, false boundaries shaped to the corrected streamline profile were introduced at the top and bottom. These were then smoothly joined to the bell-mouth entrance.

However, since the flow over a plate fixed on a boundary departs from the irrotational flow past a Rankine oval due to the presence of turbulence in the wake, the corrections made in the boundary profile were found to be inadequate. Hence additional analytical corrections were made and the analysis of the experimental data led them to conclude that;

a) the use of measurements made on bodies placed in midstream to approximate conditions in which the wake is not free to oscillate can cause large error,

b) the drag coefficient for a flat plate kept in uniform flow region normal to the flow and with a tail plate is 1.38 and thus only two-thirds that for a normal plate in uniform flow without a tail plate; also, the relative pressure change. $\frac{p_d - p_o}{\rho U_o^2/2}$ (where p_o denotes the ambient pressure, p_d the constant pressure on the rear of the plate, ρ the mass density of the fluid and U_o the free stream velocity) in the former case is - 0.57 (vide Fig. 2.1) and thus less than half the value of -1.36 in the latter case

and c) the length of the standing eddy behind a normal plate with a non-oscillating wake is 17 times the height of the plate.

Rouse (33), 1961,. From the above measurements of the mean flow and turbulence characteristics, Rouse (33) evaluated the various terms involving turbulent fluctuations in the equations of motion.

Nagabhushanaiah (21), 1961, extended the work of Arie and Rouse (4) by evaluating the effect of the approach boundary layer

on the flow past a flat plate placed normal to a plane boundary. (It may be noticed that the work of Arie and Rouse corresponds to the case of zero thickness of boundary layer). He conducted experiments in a wind tunnel 1.83 m x 1.83 m in cross section and 20 meters long, using plates of height ranging from 1.25 cm to 30 cm, the tunnel floor serving as the plane boundary. The ratio of the boundary layer thickness to the height of plate, δ/h, was varied from 0.67 to 17.0 . (δ is the height from the wall at which the velocity is 99 percent of the free stream velocity). The drag force on the plate was obtained by pressure measurements and the data were not corrected for the blockage effect. The conclusions from his study were :

a) The length of the standing eddy behind a flat plate kept normal to a plane boundary is 12 times the height of the plate and is independent of δ/h in the range of $\frac{\delta}{h}$ 0.67 to 17; it may be mentioned that at δ/h equal to 0, the length of the standing eddy is reported as 17h by Arie and Rouse (4).

b) The resultant force on the plate acts at the mid-height of the element, while it acts at 0.45 h from the bottom in the case when δ/h equals zero.

c) The drag coefficient C_{D_1}, defined with respect to the free stream velocity, varies as shown in Fig. 2.2, showing a continual decrease from a value of 1.20 at δ/h equal to 0.67, with increase in δ/h.

Nash, Quincey and Callinan (22),1962, studied the effect of length of a tail plate on the flow past a model with a blunt

trailing edge and a sharp nose at subsonic and transonic flows. They found that the dimensionless pressure $\frac{p_d - p_o}{\rho U_o^2/2}$ increases with increase in length of the tail plate, for a given Mach number. With fairly large lengths of tailplate, the dimensionless pressure on the rear tends to approach that for a negative step.

Abbott and Kline (1), 1962 performed studies in open channels in which sudden expansion was provided on one side and also on both sides. Visual observation of the flow by introduction of dye, led them to classify the entire region of separation into three zones. The first zone, called the three-dimensional zone and located immediately downstream of the expansion, was characterised by one or more vortices rotating about an axis normal to the wall (and parallel to the floor). The adjacent vortices in the zone were found to rotate in opposite directions and were not of the same size always. The average number of vortices for an expansion on one side was three and they were two in number in case of an expansion on both sides.

The second zone called the two-dimensional zone is immediately adjacent to the first zone and contains the classical separation pattern. That is, the flow in the region close to the wall is in the upstream direction and in the region close to the main flow, the particles move in the downstream direction. The overall length of separation includes the above two zones and a third zone at the end of which some fluid near the wall tends to move into the upstream separated region.

The lengths of these different zones were determined for the case of the single backward step as well as the symmetrical

expansion and they were related empirically to the flow geometry.

Maskell (14), 1963 , performed a semi-theoretical analysis of the effects of blockage on the flow past bluff bodies in closed wind tunnels. It was pointed out by Maskell that the available corrections (25) are meant for application to flow past streamlined bodies like aerofoil sections. An analysis of the blockage effects on flow past bluff bodies was therefore, carried out and the results led him to conclude that the constraint of the tunnel walls can be interpreted as an effective increase in stream velocity. The correction proposed by Maskell is applicable to bluff bodies with fixed separation points (in the range of aspect ratio from one to infinity. For the case of a normal plate of any shape kept in midstream but without a tail plate), the correction can be written in the form ;

$$C_{D_c} = \frac{C_{D_1}}{1 + \epsilon\ C_{D_1}\ h/D} \qquad \ldots\ldots\ldots\ldots (2.2)$$

where C_{D_1} = Drag coefficient with respect to the free-stream velocity of a plate of area 'A_p' held in a tunnel of cross-sectional area 'A_t'

C_{D_c} = Drag coefficient with respect to the free-stream velocity, but corrected for blockage effect,

and $\epsilon = 1/C_{P_{bc}}$ .....(2.3)

where $C_{p_{bc}}$ = Base pressure corrected for blockage effect.

The value of ϵ was found on the basis of experimental results of various investigators. For the case of a two-dimensional normal

plate in midstream (but without a tail plate) ϵ was found to be 0.96, so that equation (2.2) can be written as follows, for this case ;

$$C_{D_c} = \frac{C_{D_1}}{1 + 0.96 \frac{C_{D_1} h}{D}} \qquad \ldots\ldots\ldots(2.4)$$

The applicability of the above equation to the case of a two-dimensional plate provided with a tail plate , however, requires verification.

Modi (16), 1964, conducted experiments in a wind tunnel with the object of studying the resistance characteristics of two-dimensional inclined plates kept on a plane boundary. His experiments revealed that for plates inclined between 30° and 90° to the upstream direction, the length of the standing eddy behind the plate is approximately equal to 12 times the projected height of the plate.

Mueller, Korst and Chow (20), 1964, carried out a semi-theoretical analysis of the characteristics of the redeveloping boundary layer downstream of the standing eddy behind a roughness element. A method of predicting the velocity distribution in the redeveloping boundary layer under zero pressure gradient was developed.

Plate (26), 1964, conducted an experimental investigation of the drag on a smooth boundary with a two-dimensional vertical roughness element immersed in the turbulent boundary layer on the boundary. The flow pattern for this case, originally presented by Plate, is illustrated in Fig . 2.3. The experimental

work for the study was carried out in a wind tunnel having a 1.83 m square test section 27 meters long, the floor of which was used as the plane boundary. The height of roughness elements was varied from 1.25 cm to 5 cm and the ratio δ/h was varied from approximately 2.5 to 12.0 (δ, the boundary layer thickness was defined as the distance from the wall at which the velocity is 99 percent of the free,-stream velocity). Experimental results have been presented concerning the pressure distribution on the vertical strip, and the variation of the friction coefficient for the plane boundary downstream of the roughness element. The main conclusions from his investigation are as follows :-

a) The drag coefficient C_{D_1} of the roughness element is related to δ/h by the equation,

$$C_{D_1} = 1.05\ (h/\delta)^{2/7} \qquad \ldots\ldots\ldots(2.5)$$

(The equation has been used to show the variation of C_{D_1} with δ/h on Fig. 2.2. The difference between Plate's and Nagabhushanaiah's results are obvious)

b) The negative friction in the standing eddy cancels approximately with the positive friction downstream of the re-attachment point over a distance of 35 times the height of the element. Further downstream of this point, the friction coefficient is approximately equal to that obtained at the same point by treating the boundary layer as an undisturbed one.

Summary : As a result of the above review the following comments can be made :

a) The flow past a roughness element placed in uniform flow without a tailplate differs from that past a plate in uniform flow with a tailplate; in the latter case the wake behind the element is of the non-oscillating type and this leads to a decrease in the drag coefficient,

b) The drag coefficient of a normal plate in a boundary layer decreases continually from a value of 1.38 at δ/h equal to 0; however, the difference between the findings of Plate (26) and Nagabhushanaiah (21) regarding this variation, suggests need for further study on the problem. Further, the use of the above methods does not lead to the prediction of resistance of a plate kept in a stream of finite depth; a method which could take this flow parameter into account would be useful in problems in hydraulics.

c) The length of the standing eddy behind a plate kept on the boundary is approximately 17 times the height when δ/h equals zero, but at values of δ/h greater than zero, the length is approximately 12 times the height of the element.

2.3 Studies on a Series of Roughness Elements :

Though the concept of Nikuradse's sandgrain roughness (combined with Colebrook-White transition function) has been known (38) to be valid for commercial pipe surfaces, extension of the concept to surfaces with artificial arrangements of roughness elements needs experimental study. One of the earliest attempts

at evaluating the effect of the roughness concentration on the resistance coefficient was made by Schlichting (38). He conducted experiments in a rectangular conduit under pressure, artificial roughness elements of different shapes being arranged at various concentrations on the bottom of the conduit. The values of K_s, the equivalent sand grain roughness, were determined by obtaining the velocity profile in the conduit and then applying the logarithmic velocity distribution equation. The above values of K_s for various roughness patterns have been listed by Schlichting (38).

Many other investigations concerning this problem have been carried out since then and almost without exception, these have been flume investigations involving measurements of total resistance. The studies directly concerning the problem under scrutiny are reviewed briefly.

Johnson (12), 1944, performed experiments with two-dimensional strips of some finite thickness placed on the bed of an open channel. For the roughness elements used, he found that the value of K_s/h is a maximum at a relative spacing L/h equal to 12. Also, the use of Bazin's data (28) along with the data collected by him indicated that for a given relative spacing, a strip dimension t/h between 1.25 and 4.0 may give the maximum value of K_s/h. (Here t is the thickness of the strip)

Powell (28), 1946, studied the variation of the resistance due to roughness elements similar to the ones used by Johnson. However, these strips were placed along the bed and up the side walls also. His studies confirmed the findings of Johnson that K_s/h attained a maximum value at approximately L/h equal to 12.0

Further, he found that the Chezy's coefficient 'C' is a function of the flow depth and the roughness geometry only at values of Froude number less than 1.69, but is a function of Froude number also at Froude number greater than 2.49; no data were collected in the range of Froude number from 1.69 to 2.49. (Chezy's coefficient 'C' is given by the equation $\overline{V} = C\sqrt{RS}$ where $\overline{V}$ is the Mean velocity of flow over the cross section of the channel, R the hydraulic radius and S the slope of the water surface).

Einstein and Banks (9), 1950, suggested the rational procedure of treating the total resistance of a composite bed as the sum of the individual resistances. The concept was verified in an open channel investigation by using different types of roughnesses and their combinations, namely blocks, blocks with offsets, and pegs. In the range of their experiments they found that the resistance of pegs could be predicted by using drag coefficient values for isolated cylinders at the appropriate Reynolds number. Further, the total resistance as measured in a case where all the above roughness elements were present on the bed, was approximately equal to the sum of the individual resistances, also found by experimentation. They found that the pattern of arrangement of the pegs, apart from the concentration of pegs would influence the resistance. However, Herbich and Shulits (11) and Morris (17) have expressed the opinion that the arrangement of the roughness elements is of very secondary importance. As mentioned earlier, the concept that the total resistance can be treated as the sum of the individual resistances would imply that there is little interference effect and this is questionable when extended to cover various types and concentration of rough-

..

nesses.

Robinson and Albertson (31), 1952, used short angle irons as discontinuous roughness elements on the bed of the flume, in their investigation . They used angle irons of length equal to four times the height and placed at a lateral spacing, (centre to centre) of six times the height and a spacing in the flow direction equal to ten times the height. They used geometrically similar patterns, with two heights of roughnesses, viz. 1.27 cm and 2.54 cm, and obtained the following relation between $C/\sqrt{g}$ and D/h on the basis of their experiments :

$$\frac{C}{\sqrt{g}} = 4.70 \log_{10} D/h + 1.31 \qquad \text{.....(2.6)}$$

Here, g is the acceleration due to gravity.

Morris (17) , 1955, analysed the data on rough and transition boundaries of conduits in a fashion much different from the conventional. He quoted instances in which the transition region on the plot of friction factor 'f' versus the conduit Reynolds number R_e yielded horizontal or rising curves, while the usually accepted function of Colebrook and White (38) shows a falling curve. Here

$$h_f = \frac{f L_c \bar{V}^2}{2 g D_c} \qquad \text{.....(2.7)}$$

and

$$R_e = \frac{\bar{V} D_c}{\nu} \qquad \text{.....(2.8)}$$

where D_c is the diameter of the conduit, h_f is the head loss in a length of conduit L_c and ν is the kinematic viscosity of the fluid. Even for cases where the usual falling characteristic is obtained, instances were cited in which the computed value of K_s was a function of R_e and pipe diameter. As such, Morris

concluded that the sandgrain concept was unsuitable in cases other than the uniform sand-coated surfaces.

Morris classified the flow past a boundary with roughness elements on it into three categories :-

a) Isolated roughness flow :- In this type of flow, the wake zone and vortex-generating zone at each element are completely developed and dissipated before the next element is reached. The total resistance could be calculated as the sum of the form drag on the roughness elements and the friction drag on the plane boundary between the elements. The equation for friction factor, given by Morris, is

$$f = f_s \left(1 + 67.2\, C_{D_1} \frac{p}{P} \cdot \frac{h}{L}\right) \qquad \ldots\ldots(2.9)$$

where f_s is friction factor for the plane boundary at the Reynolds number of the flow,

P is the total perimeter of channel

and p is the perimeter of roughness elements in a cross section.

b) Wake-interference type of flow :- In this case the roughness elements are at such a spacing that the separation zones and regions of vortex generation and dissipation behind each element are not fully developed before the next element is met. For this type of flow, different transition functions (between the smooth and rough boundaries on a plot of $1/\sqrt{f} - 2 \log_{10} D/L$ and $\frac{R_e\sqrt{f}}{D/L}$) were obtained for spot roughness, strip roughness and the corrugation

roughness. For the fully rough flow, he found that

$$1/\sqrt{f} = 2 \log_{10} \frac{D}{L} + 1.75 \qquad \text{.....(2.10)}$$

c) Quasi-smooth flow :- The roughness elements in this type of flow are to close that the flow essentially skims over the crests of the elements and stable vortices exist between the elements. The friction, factor for this type of flow, as given by Morris, is

$$f = f_s + \frac{\left(\frac{C_w u_h}{\bar{V}} \right)^3}{L/h,j} \qquad \text{.....(2.11)}$$

where 'u_h' is the velocity of crest level of element,

C_w is a constant usually taken as 0.5,

and 'j' is the width of the groove and should be used in the equation if 'j' is smaller than 'h' ; otherwise 'h' should be used.

If the width of the groove is smaller or equal to the height of the element, the flow was classified as quasi-smooth (18). The classification between the other two regimes of flow can be done with the help of Fig. 2.4, presented by Morris (18).

The datum for the measurementof depth of flow was taken as the top of the roughness element for all the three flow regimes. It was thought that any attempt at locating the datum so as to make a logarithmic velocity distribution fit the whole depth would be inaccurate, since a break in the velocity profile has been observed in many cases (Vide Fig. 2.5).

Koloseus (13), 1958, developed a criterion for instability of flow using the friction factor equation for a rough channel.

(It may be mentioned, that under the unstable condition, a disturbance of the free surface increases in magnitude as it moves downstream). The criterion based on Froude number, $\bar{V}/\sqrt{gD}$, and the friction factor 'f' could be approximated as follows :

$$\left.\begin{array}{l} \text{If } \dfrac{\bar{V}}{\sqrt{gD}} < 1.60 \text{ , flow is stable} \\ \text{If } \dfrac{\bar{V}}{\sqrt{gD}} > 1.60 \text{ , flow is unstable} \end{array}\right\} \quad \ldots\ldots\ldots(2.12)$$

For a bed with a diamond arrangement of cubes at two concentrations, different resistance relations were developed for the stable and the unstable flows, based on experimental data, the classification of flows being done with the help of the above criterion. The equations are of the form

$$\frac{1}{\sqrt{f}} = 2 \log_{10} \left(\frac{XD}{h}\right) \quad \text{for stable flow} \quad \ldots\ldots(2.13)$$

and

$$\frac{1}{\sqrt{f}} = Y \log_{10} \left(\frac{ZD/h}{\bar{V}/\sqrt{gD}}\right) \quad \text{for unstable flow} \quad \ldots\ldots\ldots(2.14)$$

where X, Y and Z are functions of the roughness concentration.

Sayre and Albertson (37), 1961, carried out experiments in a flume 2.4 metres wide with discontinuous angle iron roughness elements on the bed. The lateral and the longitudinal spacings of the elements were changed, keeping the size of the element constant at 15 cm (width) by 3.80 cm (height). Data on the the velocity distribution and flow resistance were collected under uniform flow conditions, and analysed . By plotting $C/\sqrt{g}$ against D/h for the data collected by Koloseus (for stable flows) Robinson, and Sayre and Albertson, they found that the resistance equation could be written as :

$$\frac{\bar{V}}{V_*} = 6.06 \log \frac{D}{K'_s} \qquad \text{.....(2.15)}$$

where K'_s is a roughness parameter and a function of the height, spacing and arrangement of the roughness elements and V_* is the shear velocity equal to $\sqrt{gDS}$.

The above equation yields a value of 0.38 for the Karman's coefficient, K, but analysis of velocity profiles indicated K to vary appreciably with the roughness concentration, as shown in Fig. 2.6; nevertheless, they contended that a value of 0.38 may be assumed for K for the wake-interference flows. Based on this value of K, they studied the variation of K'_s with the geometry of the roughness pattern for all the available data and found that depending on the arrangement and type of roughness elements, the maximum resistance is obtained at different concentrations.

In a discussion of the above paper, Harleman and Rumer (37) suggested that mere wind tunnel determination of the drag coefficient of the roughness elements should help in predicting the total resistance, since it is merely the sum of the form drag and skin friction. But Sayre and Albertson (37) felt that the absence of a fully developed boundary layer in a tunnel of small length could make it difficult to extend wind tunnel results to flume studies.

Rouse, Koloseus and Davidian (34), 1963, presented a stability criterion covering a higher range of 'f' than in the criterion given by Koloseus (13). Analysing data on flow over a diamond arrangement of cubes with the roughness concentration λ, varying from 1/512 to 1/8, they developed resistance equa-

tions for stable and unstable flows, namely,

$$\frac{1}{\sqrt{f}} = 2 \log_{10} \left(\frac{0.55\ D/h}{\lambda^{0.9}} \right) \text{ for stable flows} \qquad \ldots\ldots\ldots(2.16)$$

$$\text{and } \frac{1}{\sqrt{f}} = 2 \log_{10} \left(\frac{0.55\ D/h}{\lambda^{0.9} \left(\frac{Fr}{Fr\text{-}n} \right)^{2/3}} \right) \text{ for unstable flows} \qquad \ldots\ldots\ldots\ldots(2.17)$$

Where Fr is the actual Froude number of the flow and Fr-n the Froude number corresponding to neutral stability . λ is defined as the ratio of the area of the roughness elements perpendicular to the flow to the area of the bed.

It may be noticed that the equations are of a different form from the ones given by Koloseus(13); further, at higher concentrations, log K'_s/h would not show the same linear relation with log λ - which is implied in the above form of equations - as at lower concentrations. In fact, plots by Rouse (35) indicate a linear relation between log K'_s/h and log λ only upto λ = 0.15 . Thus, one would expect a change in Eqs. (2.16) and (2.17) at higher concentrations.

O'Loughlin and Macdonald (24), 1964, performed experiments in an open channel to study the effect of roughness concentration and type of pattern on the resistance coefficient. Uniform sand grains and cubes were used as the roughness elements Their results indicate that the shape of the roughness element and the arrangement pattern are not very important at low concentrations, but the resistance coefficient is significantly affected by these at concentrations above 0.10. Also in the case of the closely packed sand grains (λ was 0.64),the equivalent sand grain diameter was about 1.5 times the diameter of the sandgrains, while Nikuradse's value was equal to the sandgrain

diameter. Further, the transition function followed a similar variation as the Colebrook-White function for commercial pipes, rather than that for the uniform-sand-roughness, thus raising doubts about the equivalent sandgrain concept. Their studies also indicate departure from the linear relation between $1/\sqrt{f}$ and $\log_{10} D/h$ at values of $\frac{D}{H}$ less than 3.0 as shown in Fig.2.7 .

Adachi (3), 1962, carried out studies in an open channel with roughness elements of 5 mm x 5 mm x 6 mm on the bed. Using the resistance relation,

$$\frac{\bar{V}}{V*} = 5.75 \log D/K_s + 6.00 \qquad \text{.....(2.18)}$$

he studied the variation of K_s/h with the relative flow depth. The final empirical relation based on the above variation was checked using U.S.W.E.S. data.

Adachi (2) , 1964. made an experimental investigation of open channel flow with [illegible] strip roughness-es on the bed of the channel. He collected data on the velo-city distribution, resistance and the pressure distribu-tion around the roughness element at various spacings. The velocity profiles over the element and midway between the elements were different for large spacings, but tended to coalesce at L/h less than or equal to 10.0 (vide Fig. 2.8). Thus Adachi supposed that wake-interference flow would exist at L/h less than 10.0.

Based on the measured drag coefficients at various spacings and the estimated sheltering effects at these spacings, he classified the roughness pattern with L/h less than 8.0 as 'groove roughness' and those with L/h greater than 8.0, as 'ridge roughness'. In both cases, K_s was computed using the

logarithmic resistance equation with K equal to 0.4 and K_s/h was related to the parameter $R_{b/h}$ in the case of ridge roughness; a separate relation was obtained for the groove roughness. Here R_b is the hydraulic radius with respect to the bed.

Herbich and Shulits (11) 1964, experimented with large cubical roughnesses at small depths so that the boundary layer effects were inappreciable. The study was carried out with the intention of providing useful information for the flow in boulder streams. Their studies indicated that the orientation and the shape of the roughness element is not very important and the resistance coefficient is governed primarily by the concentration of roughness elements. Based on experimental data, they developed dimensional curves relating discharge to the roughness concentration, depth and slope.

Rouse (35), 1965, presented a critical study of the present state of knowledge of the resistance of rigid-bed open channels. From studies made at Iowa, he presented the variation of $K_{s/h}$ with the roughness concentration for a variety of shapes and arrangements. He also reported Roberson's experiments on measurement of drag on a single element kept on the floor of a wind tunnel. However, as reported by Rouse, the resistance in the flume at low concentrations was different from that obtained by computing the form resistance based on wind tunnel measurements and adding it to the skin friction of the plane boundary. But O'Loughlin (23) emphasised the inapplicability of a single law for the velocity distribution very close to the wall and in the outer region and contended that the use of such a simplified law

may be the reason for the departure between the computed and the observed resistance.

Summary : The above review of the existing work in the field brings out some points on which there is no general agreement or information is lacking. They are :

a) Velocity distribution with roughness elements on the bed:- The available data on velocity distribution indicate in some cases a break in the velocity profile, as pointed out by Morris (17). This would mean that different velocity distribution laws could be expected close to the wall and away from the wall as emphasised by O'Laughlin (23) . Further, the velocity distribution over the roughness element and that between the roughness elements are different at some roughness concentrations (2). Thus, it seems that the velocity profiles are not completely similar, i.e. definition of an average velocity distribution law over the whole length and depth may be difficult. Also, as found by Sayre and Albertson (37), the value of K found from velocity profiles could be quite different from that obtained through a plot of $\overline{V}/V^*$ and D/h, at some concentrations. Thus, any analysis of the problem of resistance of artificial roughness elements, which requires a knowledge of the velocity distribution would necessarily be approximate.

b) Value of Karman's coefficient K' :- The value of 'K' obtained from plots of $\overline{V}/V^*$ versus D/h ranges from 0.38 (Sayre-Albertson) to an extreme value of 0.49

(Robinson-Albertson), while a value of 0.40 for 'K' has been accepted normally in case of pipes (38). This large variation cannot be attributed to variations in the roughness concentration, since most investigators have covered approximately the same range of concentration and obtained the same value of 'K' for all concentrations used by them. However, since ℓ is defined as Ky for small distances 'y' from the wall (ℓ being the mixing length) one might expect 'K' to vary with the shape and concentrations of roughness elements.

An interesting deviation from the above mode of analysis in which an average value of 'K' was found by plotting V/V_* against log D/h, is that of Adachi (2); he treated K as constant at 0.4 and studied the variation of K_s for any pattern with the flow depth. Though the first approach is desirable from the point of view that K_s becomes a function of only the roughness pattern and geometry, there is no definite indication about either the constancy or otherwise of 'K_s' or 'K' and the second method appears equally acceptable.

c) Choice of datum : There appears to be no general agreement concerning the datum for depth measurement in a channel with artificial roughness elements on the bed. While Morris and Johnson have used the crest of the element as the datum, Sayre-Albertson, Powell and others have used the flume bottom as the datum, Adachi, and O'Loughlin and Macdonald have used a datum changing with the roughness concentration.

Apart from the qualitative acceptance that the datum should be the flume bottom at large spacings and should be at the crest of the roughness elements at very small spacings, no effort has been made to locate the datum suitably at all spacings for different types of roughnesses. As pointed out by Morris, selecting the datum to obtain a logarithmic fit for velocity distribution over the whole depth may not be justifiable.

d) Individual resistances : Apart from the works of Adachi and Roberson, there does not appear to be any effort made at measuring the individual resistances.

CHAPTER - III

ANALYTICAL CONSIDERATIONS

3.1 Preliminary Remarks :

With the results of the previous investigations as a guide, some of the fundamental aspects of the problem are considered in this chapter. The problem, as posed for investigation, requires two different aspects of study. Firstly, the average resistance of a roughness element placed on the boundary at various spacings- upto a spacing of infinity, which forms the limiting case of a single element - needs to be determined. Secondly, an estimate is to be made of the skin friction on the plane boundary between the roughness elements.

It is known that a body placed in a flowing fluid experiences a force in the direction of flow, usually termed 'Drag'. The total drag force exerted on the body at high Reynolds number can be split up into (a) frictional drag and (b) form drag. The frictional drag is the component in the flow direction of the tangential force due to the velocity gradient near the boundary and is proportional to the viscosity of the fluid. The form drag is the result of separation of flow which occurs in the case of bluff bodies even at moderate . Reynolds numbers; as a consequence of separation, the pressure at the rear of the body is less than the pressure at the front and the difference of pressure is equal to the form drag.

For a sharp-edged vertical plate kept in a fluid at Reynolds number exceeding approximately 10^3 , the entire drag is

the form drag. However, no theoretical method is available to estimate the form drag on a sharp-edged plate placed normal to a plane boundary at different spacings. As such, recourse has to be taken to experimental techniques to determine the form drag or the resistance of the roughness element described above. Further, the estimation of the frictional resistance on the plane boundary between the elements by theoretical methods would be complicated and would require simplifying assumptions, the validity of which would be questionable. Therefore, the problem will be approached in the following way: Wind tunnel studies for the required arrangement of roughness elements (including the case of a single element in the boundary layer) will be made to obtain the form drag on the roughness elements. The total resistance for any given roughness pattern on a plane boundary shall be obtained by open channel studies. A comparison of the two resistances would indicate the magnitude of the skin friction on the plane boundary.

The experimental programme for obtaining data on the above aspects of the problem has to be planned keeping the following points in mind :

3.2.1 Blockage Effect :

Most of the wind tunnel studies related to drag on bodies held in midstream have been conducted in streams which are very large in comparison to the size of the body and thus the stream could be treated as infinite . But, if tests are performed in a stream which is finite in size as compared to the size of the model, the results must be corrected in order to eliminate

the effect of boundary proximity on the drag coefficient.

When one compares the flow pattern past a body in an infinite stream with that past a body in a small wind tunnel, the following difference is obvious; the ceiling and the floor of the tunnel form limiting streamlines which are different in shape from those obtained at their location if the stream were infinite. The restraint exercised by the tunnel boundaries would also change the flow pattern close to the body from that in the infinite case. It is known that the drag force on the body is affected chiefly by the flow pattern close to the body. The change in flow pattern caused by the proximity of the tunnel boundaries, produces an acceleration of flow close to the body, which is more than that in the infinite case. Consequently, it has been found that there is an increase in the drag coefficient in the case of a body in a small wind tunnel and this value would not represent that for the infinite case. This is called the 'blockage effect' and values of C_D obtained by studies in small wind tunnels need to be corrected for this effect.

Methods of correcting for the blockage effect have been suggested by Pope (27), but it was found (30) that they could not be applied successfully to triangular elements. It is thus doubtful that the above corrections could be applied with confidence for various body shapes and at large blockage values. The correction proposed by Maskell (14) has been based on studies on bluff bodies kept in midstream, without a tailplate. It needs to be checked whether the correction is valid for the case of elements in midstream provided with a tailplate or those placed in a boundary layer. Further, most problems in hydraulics require

the estimation of drag force in finite streams; hence an effort will be made to obtain the drag coefficient at various contraction ratios for elements in midstream provided with a tailplate and then extrapolate it to the case of zero-contraction or the infinite case. This relation between the drag coefficient and the contraction ratio will be used to eliminate the effect of proximity of tunnel ceiling in case of a single element placed in a boundary layer. For elements in series placed on the boundary, no effort will be made to approach the infinite case, as the interest in this part of the study is mainly in open channel flows with finite contraction ratios.

3.2.2 Wave Resistance and Skin Friction in Open Channel Experiments with Roughness Elements :

Wave Resistance: The total resistance to flow in an open channel with artificial roughness elements on the bed is the sum of the effective frictional resistance on the plane boundary, the form resistance of the roughness elements and the resistance due to water surface waves. In a closed conduit like the wind tunnel, the third type of resistance is absent and the energy loss is only due to the first two types of resistances. It is well known(29) that the wave resistance in an open channel is a function of the Froude number of the flow. However, in an open channel with cubical roughnesses at various concentrations, Froude number is shown (13) to have no effect on the total resistance when the Froude number is less than 1.6, approximately. This indicates , therefore, that the wave resistance forms an insignificant component of the total resistance in the flow over artificial roughness elements at low Froude numbers. Since the

flume experiments for this investigation were conducted at Froude number less than about 0.4, one can assume with justification that the wave resistance forms an insignificant part of the total resistance in these runs.

Skin Friction of the Plane Boundary :- To separate the form resistance from the total resistance in the flume runs, therefore, one has to make either analytical estimations or reasonable assumptions of the skin friction of the plane boundary between the roughness elements; the latter course has been adopted in this study.

Sayre and Albertson (37) estimated the form resistance of the roughness elements used by them on the assumption of a uniform plane boundary friction along the length and a constant value of Manning's 'n' . Their analysis revealed that the form resistance is approximately 92 percent to 98 percer of the total resistance at most spacings, while at the lowest roughness concentration used by them, the form resistance was 86 percent of the total resistance. One might probably expect the percentage of form resistance to be higher in the case of continuous (two dimensional) roughness elements used in this study.

However, it must be emphasised that the assumption of a uniform skin friction on the plane boundary is a simplifying one. It is well known (26) that the friction would be negative on the boundary within the standing eddy, while positive friction would be experienced by the flow beyond the standing eddy. In the flow past a single two-dimensional element kept in a boundary layer, Plate (26) found that the positive and negative parts of

skin friction cancel out over a distance of 35 h downstream of the element. However, no such results are available in the case of roughness elements kept in series at various spacings.

In the present investigation, the maximum value of L/h used is 40, at which the percentage (out of the total resistance) of skin friction on the plane boundary would be higher than at other (smaller) spacings. But, even at this spacing, on the basis of the results of Plate (26) and Sayre and Albertson (37), one may assume the contribution of the plane boundary friction to the total resistance to be insignificant. Obviously at smaller spacings, this assumption would involve negligible error.

Therefore, the flume data can be analysed on the assumption that wave resistance and the plane boundary friction are negligible and that the total resistance is equal to the form resistance of the roughness elements.

3.2.3 Reynolds Number Effects :

The total resistance coefficient of a plane boundary with artificial roughness elements on it, is, in general, dependent on the Reynolds number and the roughness geometry. However, the form resistance coefficient of sharp-edged roughness elements is known (36) to be independent of the Reynolds number at $U_o h/\nu > 10^3$, approximately. This fact, coupled with the assumption that the plane boundary resistance is negligible, leads one to the conclusion that the resistance coefficient is independent of the Reynolds number $U_o h/\nu$, provided the value is larger than 10^3. Thus any difference in the Reynolds numbers in the flume and tunnel for a particular

roughness pattern is, therefore, immaterial - provided the value is more than 10^3 - so far as comparison of their resistance characteristics is concerned.

3.2.4 Choice of Velocity :

The drag force 'Fd' on a body of area, A, immersed in a fluid, is expressed (38) in the form ;

$$F_d = C_D A \rho V^2/2 \qquad \text{.....(3.1)}$$

where V is a characteristic velocity.

Thus, the value of C_D computed from measured drag force is dependent on the velocity which is chosen as characteristic. Drag coefficients of bodies completely immersed in a fluid have been invariably defined using the free-stream velocity. In the case of roughness elements placed on the boundaries of a conduit, Morris (17) has used the velocity at the crest level of the roughness element (without the presence of the element) and the values of C_D found for elements placed at the middle of streams of infinite extent to compute the resistance of the roughness element. However, because of the uncertainties associated with the prediction of velocity distribution in the flow over roughness elements, the use of this characteristic velocity may not be very desirable . In the case of two-dimensional elements placed on a plane boundary (including the case of normal plate in midstream) in the wind tunnel, the average velocity obtained by integration of the velocity distribution curve, over the whole depth at the centre line of width, V , is used in this investigation in preference to the free-stream velocity. Apart from the fact that this would take into account the velocity distribution in the

approach boundary layers on the floor and ceiling of the wind tunnel, the use of this velocity would make the comparison of the flume and wind tunnel data easier.

The pressure distribution around the element on the centre line of width and the average velocity over the vertical centre line were measured in the tunnel; in the flume runs, the average velocity over the cross section, $\bar{V}$, and the effective sum of the form resistance of the strip and the skin friction of the plane boundary, were measured. It has been shown in Chapter VI that this procedure enables an easy comparison of the resistances measured in the flume and in the tunnel.

3.2.5 Tunnel Length Required to Achieve Quasi-Uniform Flow Conditions :

It was surmised by Sayre and Albertson (37) that wind tunnel studies to evaluate the form resistance of a given roughness pattern studied in an open channel may be impracticable in view of the large length of tunnel required to achieve flow conditions similar to that in the flume. Since such a comparison is envisaged in this investigation, some aspects concerning the nature of flow over the roughness elements need to be studied before the comparison is attempted.

The flow in the case of an open channel with a smooth or rough boundary with small-sized roughness elements on the bed is taken to be established fully when the boundary layer meets the free surface. But very little information is available about the nature of the velocity distribution in open channels with large sized roughness elements, so that no accurate estimate can be made of the entrance length, beyond which the flow may be taken to be

established and uniform. The available data on the velocity distribution for open channel flow with large roughness elements (2,17) indicate considerable departure from the classic boundary layer velocity distribution; thus, extension of the results for the flow in open channels with smooth or rough boundaries with small-sized roughness elements to the present case is difficult. Hence an effort has been made to obtain quasi-uniform flow conditions in the tunnel, which indicate considerable similarity with the flow conditions obtained in the flume.

Firstly, an overlapping range of D/h in flume and tunnel runs is used to permit comparison with confidence. The variation of resistance and flow pattern in the initial length of the tunnel has also been studied to check whether quasi-uniform conditions are obtained at all in the tunnel. Also, the nature of the velocity profiles in the tunnel and the flume are examined to establish a similarity of flow pattern.

3.3 Dimensional Analysis :

As has been mentioned in the previous sections of the Chapter, a completely theoretical approach to the problem under investigation is not possible at the present state of knowledge. To facilitate a rational analysis of the experimental data, a dimensional analysis of the problem has been carried out in this section.

a) Resistance of a Single Element Placed on the Boundary :

The force F on a unit length of a two-dimensional normal plate kept on a boundary can be expressed by the following functional relationship :

$$F = \phi_1 (h, D, V, \delta, \rho, \mu) \quad \ldots\ldots\ldots(3.2)$$

where μ = Dynamic viscosity of the fluid.

This equation can be written in terms of dimensionless parameters by choosing V, h and ρ as repeating variables.

$$\text{i.e. } \frac{F}{\rho V^2 h^2} = \phi_2 (D/h, \delta/h, Vh\rho/\mu) \quad \ldots\ldots(3.3)$$

$$\text{i.e. } C_D = \phi_3 (D/h, \delta/h, Vh\rho/\mu) \quad \ldots\ldots(3.4)$$

But the drag coefficient of a sharp-edged element held in uniform flow region is independent of the Reynolds number at values of Reynolds number above 10^3, approximately (36). However, little information is available concerning the variation of C_D with $Vh\rho/\mu$ for elements placed in the boundary layer. Considering only the case of a turbulent boundary layer, if it is assumed that viscous effects are taken into account by the parameter δ/h, $Vh\rho/\mu$ may be omitted as insignificant and the above equation written as

$$C_D = \phi_4 (D/h, \delta/h) \quad \ldots\ldots\ldots(3.5)$$

It may be noticed that in the case of an element placed on a boundary in a stream of infinite extent,

$$C_D = \phi_5 (\delta/h) \quad \ldots\ldots\ldots(3.6)$$

Also for elements held in a region of zero velocity gradient, but with a tailplate,

$$C_D = \phi_6 (D/h) \quad \ldots\ldots\ldots(3.7)$$

It may be mentioned that the value of δ used throughout this investigation is the boundary layer thickness obtained at the element section before placing the element. Also the depth,

D, was always measured from the flume bottom or the tunnel floor as the case may be.

The functional relationships in equations (3.6) and (3.7) need to be determined by experimental methods.

b) Resistance of Elements in Series Placed on a Boundary :-

The average shear stress ' τ_o ' on the bed of a wide open channel with roughness elements on it can be written as ;

$$\tau_o = \phi_7 (h, L, D, \bar{V}, \rho, \mu, \Delta r_f) \quad \ldots\ldots\ldots(3.8)$$

where Δr_f is the difference in specific weights of flowing fluid and the fluid above it.

Choosing , $\bar{V}$, D and ρ as repeating variables, the above equation becomes ;

$$\frac{\tau_o}{\rho \bar{V}^2} = \phi_8 \left(h/D, L/D, \bar{V}D\rho/\mu, \bar{V}/\sqrt{\frac{\Delta r_f \, D}{\rho}}\right) \quad \ldots\ldots(3.9)$$

$$\text{i.e.} \quad \frac{\bar{V}}{V_*} = \phi_9 \left(D/h, L/h, \bar{V}D/\nu, \frac{\bar{V}}{\sqrt{gD}}\right) \quad \ldots\ldots\ldots(3.10)$$

$$\text{Since,} \quad V_* = \sqrt{\frac{\tau_o}{\rho}} \quad \ldots\ldots\ldots(3.11)$$

$$\text{and} \quad \frac{\Delta r_f}{\rho} = g \quad \ldots\ldots\ldots(3.12)$$

As mentioned earlier, Froude number may be left out from the analysis in the range of Froude numbers for which the experiments are planned. Further, based on the supposition that the skin friction of the plane boundary forms an insignificant part of the total resistance and also noting that the form resistance of sharp-edged roughness elements is independent of the Reynolds number at large values of Reynolds number, equation (3.10) can

be written as ;

$$\frac{\bar{V}}{V_*} = \phi_{10}\,(D/h,\ L/h) \qquad \ldots\ldots\ldots(3.13)$$

Considering the flow past a series of roughness elements on the floor of the tunnel, the drag force, F, per unit length of the element may be written as

$$F = \phi_{11}\,(h, L, D, V, \rho, \mu) \qquad \ldots\ldots\ldots(3.14)$$

which reduces to

$$C_D = \phi_{12}\,(D/h,\ L/h,\ Vh\rho/\mu) \qquad \ldots\ldots(3.15)$$

On the basis of the arguments presented earlier $Vh\rho/\mu$ may be omitted from the analysis and the equation (3.15) becomes

$$C_D = \phi_{13}\,(D/h,\ L/h) \qquad \ldots\ldots\ldots(3.16)$$

3.4 Concluding Remarks :

An analytical study of the problem posed for investigation reveals that it is not possible to solve it by a completely theoretical method and the problem requires an experimental study. In the range of variables contemplated during experimentation, the assumption of negligible wave resistance and skin friction on the plane boundary in case of open channels with artificial roughness elements, appears logical and justified by data from previous studies. The assumption that the form resistance of the roughness element is independent of the Reynolds number in the range of variables likely to be encountered, also seems to be justifiable. Equations (3.13) and (3.16) which are based on the above premises serve as a basis for the analysis of experimental

data on a series of roughnesses. Experimental data concerning the resistance of a single element can be analysed on the basis of equations (3.6) and (3.7).

-:o:-

CHAPTER - IV

EXPERIMENTAL EQUIPMENT AND PROCEDURE

4.1 Preliminary Remarks :

The experimental work for this investigation was carried out in the Hydraulics Laboratory of the University of Roorkee. The work was planned and carried out in such a way as to provide detailed information on mean flow patterns and pressure distribution on single elements, as well as on elements in series kept on a plane boundary. The experimental work comprised of three parts, namely, studies in a flume with water, studies in a 32.4 cm x 32.4 cm open circuit wind tunnel and lastly those in a 81 cm x 114 cm closed circuit wind tunnel. The details of the above equipment, their calibration and the experimental procedure adopted, are described in this Chapter .

4.2 Open Channel Investigations :

Equipment :- The open channel experiments were conducted in a 47.2 cm wide, 60 cm deep and 11 metres long tilting flume, in which water was re-circulated through an overhead tank arrangement. (Vide Fig. 4.1). The flume was provided with glass side walls and a wooden false bottom which was levelled carefully. At the entrance to the flume, a honey-comb wall of small-sized bricks was constructed to reduce the disturbance in the approaching flow. Flow straighteners in the form of a number of vertical metallic plates about 20 cms long were placed just downstream of the baffle to yield flow which was essentially parallel to the side walls. A movable carriage with a point gauge (the point gauge arrangement had a least count of 0.01 cm) was mounted on

brass rails at the top of the flume. The brass rail was maintained parallel to the bed. An adjustable gate at the downstream end of the flume enabled adjustment of the depth of flow in the flume.

For the measurement of discharge, a rectangular sharp-crested weir was installed in a settling tank downstream of the flume. The weir was first calibrated volumetrically over the entire range of discharges for which studies were intended. The velocity distribution in the flume during a run was measured by a calibrated Prandtl tube and an inclined manometer. The average value of Manning's 'n' for the bed without roughness elements was found to be 0.0135 approximately.

The roughness elements used were angle iron strips of negligible thickness, which were formed out of galvanised iron sheets and could be nailed to the flume bottom. Two different heights of element, viz 2 cm and 4 cm, were used in this part of the study and in all cases, the elements spanned over the entire width of the flume; the elements were not fixed on the sidewalls. Two different types of roughness patterns were formed using these elements.

a) Elements of a particular height were placed at regular intervals on the flume bottom.

b) 4 cm elements were placed at a spacing of 80 cms on the flume bottom; at a certain fixed distance downstream of each of these elements, another roughness element (usually of 2 cm height) was placed to form a second series of roughness elements on the bed. The relative position of the second set of elements

with respect to the first was varied. The above procedure was also followed in the case of 4 cm elements placed at a spacing of 160 cms.

Table 4.1 summarises the details of the various roughness patterns used in this part of the study.

Experimental Procedure : The experimental work was carried out at two different slopes, namely 7.5×10^{-4} and 2.875×10^{-3}. These slopes were given to the rails with the help of a Surveyor's level and point gauge. Studies on all the roughness patterns were first conducted at one slope and then the slope changed and studies repeated for all the roughness patterns at this slope. The following procedure was employed in experimentation.

After adjusting or checking the slope, as the case may be, the required roughness pattern was placed on the flume bottom. A certain discharge was then allowed into the flume and uniform flow established by adjusting the tailgate. It was found that the initial three metres and the last metre length of the flume were affected slightly by the disturbances at the entry and backwater effect; hence only the other 7 metre length of the flume was used for checking uniform flow and also measurement of depth. Further, the discharge was so adjusted that uniform flow was obtained at approximately the pre-determined depth. Three to four different depths of flow in the range from 10 cms to 33 cms were used for each roughness pattern at a particular slope. Also, for most runs, after establishment of uniform flow, centre line velocity profiles were taken at two or three typical sections in the latter half of the length of the flume. The average depth

TABLE - 4.1

Details of Roughness Patterns used in Flume Studies

a) Roughness elements of one height

b) Roughness elements of different heights

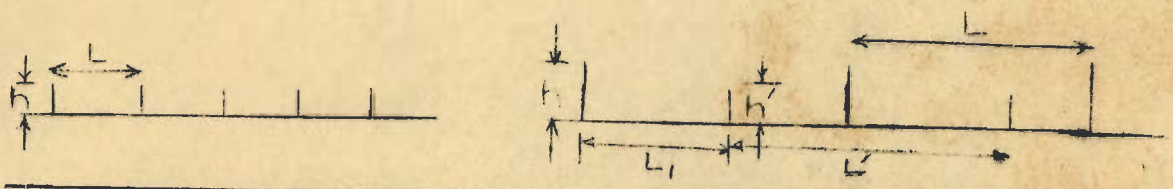

Notation	cm h	cm L	cm h'	cm L'	cm L_1
A_1	4.0	160.0	-	-	-
A	"	80.0	-	-	-
A_2	"	40.0	-	-	-
A_3	"	20.0	-	-	-
A_4	"	10.0	-	-	-
A_5	"	30.0	-	-	-
A_6	"	60.0	-	-	-
A_7	"	15.0	-	-	-
P	2.0	80.0	-	-	-
P_1	"	40.0	-	-	-
P_3	"	20.0	-	-	-
APX	4.0	80.0	2.0	80.0	40.0
APY	"	"	"	"	60.0
APZ	"	"	"	"	20.0
AP_1Z	"	"	"	40.0	"
AAU	4.0	80.0	4.0	80.0	10.0
A_1P_2W	4.0	160.0	2.0	160.0	80.0
A_1P_2X	"	"	"	"	40.0
A_1P_2T	"	"	"	"	120.0
A_1PX	"	"	"	80.0	40.0

of flow, the discharge and the temperature of water were noted for each run. The experiments were repeated for other roughness patterns on the same slope and then at a second slope for all the roughness patterns.

4.3 Open-Circuit Wind Tunnel Studies :

Instruments : The open-circuit tunnel in which the measurement of pressure distribution around the roughness elements was carried out (See Fig. 4.2) had a test section 31.8 cm x 31.8 cm at the upstream end, increasing to 33 cm x 33 cm at the downstream end of its 2.75 metre length. The top and bottom of the test section were built out of wood and the sides out of perspex sheet. A separation -free entrance 1.22 metres in length was provided upstream of the test section. The area of the inlet of the entrance cone was 9 times that of the test section and a grid designed on the basis of Baines-Peterson's analysis (5) was provided at the inlet to control the turbulence intensity in the test section. However, because of lack of instruments, the intensity of turbulence was not measured. A sand-paper roughness strip was provided on the floor of the tunnel at the entrance to the test section to ensure a turbulent boundary layer along the floor of the tunnel for its whole length.

The diffuser downstream of the test section was 0.915 metre long, square in cross section and the area of the exit end of the diffuser was 2.3 times that of the test section. A suction fan was placed in a straight uniform duct downstream of the diffuser to suck the air into the test section and discharge it back to the atmosphere. The fan was connected to a dimmerstat and a voltage stabiliser for controlling the speed. The maximum

velocity of air in the test section without any roughness element in it was about 13 metres per second.

A calibrated Prandtl tube (outer diameter = 0.30 cm) and a total head tube (outer diameter = 0.07 cm), which could be moved along the centre line of the test section were used for the measurement of point velocities in the tunnel. An inclined manometer of adjustable inclination with methyl alcohol as the indicating fluid was used for pressure measurements. The manometer had twenty tubes taking off from a tank of large capacity, so that connections could be made simultaneously to a large number of pressure tappings. A vernier scale with a movable hair and mirror arrangement- which enabled elimination of parallax error - and which could read upto 0.01 cm of liquid along the inclined length was fitted into this manometer. A quadrantal ring graduated from 0° to 90° was fitted to the manometer and was used to determine the inclination of the manometer; preliminary checks on the inclination by other methods indicated the above method to be accurate (Photograph 1 shows the manometer).

The average velocity of flow along the vertical centre line of width was obtained by noting the difference of pressure between two fixed points in the entrance cone; this difference of pressure was calibrated against the above velocity by running velocity traverses at various sections along the length.

The roughness elements used were made of wood and spanned the entire width of the tunnel. Most of the elements used were about 0.3 cm thick with a sharp bevelled edge at the top. Use of this type of roughness element necessarily meant that the pressure tubings would cause some obstruction to the flow.

To check the degree of disturbance caused by these, a few box-type roughness elements (with pressure tubings hidden inside) with a sharp bevelled edge at the top were also tested. These were assumed to represent sharp-edged elements of negligible thickness and the results of drag measured on these were compared with those on the elements mentioned earlier; it was found thatt the differences were very small and insignificant. It may be mentioned that measurements made on an angle iron strip also gave essentially the same drag as on the other strips under the same conditions. Hence, the wooden strips of 0.3 cm thickness were used in a majority of cases, though a few runs - particularly many of those with roughness elements in midstream - were conducted with the box-type roughness elements. The height of roughness elements used in this tunnel varied from 1 cm to 8 cm. In all cases, copper tubes of inside diameter 0.15 cm spaced at approximately 0.4 to 0.5 cm were provided on both faces of the roughness element for pressure measurement. The pressure holes were staggered along the width, but they were placed very close to the centre line, so that they were well within the central core, where there was no transverse velocity gradient. Connections from the pressure points to the manometer were made through plastic tubes.

Flow Characteristics : Velocity profiles taken across the width at a section approximately midway in the length of test section, as well as visual observation of the flow with the help of thin threads suspended into the flow indicated the flow to be straight and symmetrical. Also, one run in which the pressures were measured on the centre line of a roughness element

and some distance away from the centre line but within the central core, showed no appreciable difference between the two. Thus, the staggered pressure holes could be expected to give the pressure distribution on the centre line of the roughness.

A number of measurements were made for the variation of static pressure in the tunnel for flow without any roughness elements. The data collected during the measurement of boundary layer thickness, calibration of the velocity gauge in the entrance cone were also analysed along with the above measurements. Fig. 4.3 shows the plot of the dimensionless static pressure versus x (distance from the upstream end of the test section) with all the data plotted. It was seen that the effect of variation of velocity was insignificant and thus an average line has been drawn. This shows that the pressure is approximately constant in the initial 1.50 metres, but beyond this there is a gradual reduction, until at the downstream end of the test section the pressure is approximately 5 percent less than that at the upstream end. However, it was assumed that this small pressure gradient would not have a marked influence on the results and no efforts were made to correct for this pressure gradient.

Velocity profiles in the vertical were taken with the help of the total head tube and the Prandtl tube at various stations along the length of the tunnel to determine the boundary layer growth along the floor of the tunnel. The range of velocities at which the measurements were made was from 6.80 m/s to 12.5 m/s. (It may be mentioned, however, that with roughness elements in the tunnel, the maximum velocity was only about 10 to 11 m/s). Fig. 4.4 shows a typical velocity profile in the vertical in the tunnel and Fig. 4.5 shows the variation of δ (the

boundary layer thickness on the floor) with x. It may be noticed that the variation of δ with velocity, for a given value of x, is small and not consistent. Further, the boundary layer thickness computed with the equation

$$\delta/x = \frac{0.377}{(U_o x/\nu)^{1/5}}$$, using the beginning of the test section as origin, is slightly larger than the observed thicknesses. It is supposed that this difference is a result of the presence of the small pressure gradient, since the above equation is valid in the case of zero pressure gradient. Despite the slight scatter of points on Fig. 4.5, an average line showing the variation of δ with x in the range of velocities used has been drawn. Using the values of δ given by this line, Fig. 4.6 has been prepared to study the velocity distribution law in the boundary layer in the tunnel. The data indicate that $u/U_o = (y/\delta)^{1/8}$, while velocity distribution is usually expected to follow the 1/7th power law at these Reynolds numbers. (Here u is the velocity at a height y from the floor). However, data at small values of y/δ indicate deviation from the proposed law, as can be seen on Fig. 4.6.

Experiments on Single Element Kept in Midstream : Experiments were carried out to study the variation of C_D with D/h for the case of δ/h equal to 0 in the following way. An aluminium plate 0.6 cm thick, but chamfered to give a line contact with the normal plate was placed behind a normal plate kept at the middle of depth of the tunnel. The normal plate was placed at about a metre from the upstream end and the length of the tailplate was

kept at 10 times the total height of the normal plate, as suggested by Arie and Rouse (4). (Fig. 4.7 and Photograph 2 show the placement of the element in midstream). It may be seen that this arrangement represents the case of a normal plate kept on a plane boundary, but at zero thickness of boundary layer. The procedure for measurement was as follows : After steady flow conditions were established, the pressures around the normal plate were read on the manometer and the average flow velocity obtained by pressure measurement at the two points in the entrance cone, as mentioned earlier. The ambient pressure was measured by a Prandtl tube held fairly well upstream of the plate. In the initial runs, the pressure distribution around both the top and bottom half of the normal plate was measured and these indicated a symmetry about the centre line . Hence, in later runs, the measurements were made on either the top half or bottom half only. The measurements on each height of plate were made at three to four air velocities, the variation of velocity being effected through the dimmerstat. The temperature of air was noted in all cases.

Experiments on Single Element Placed in a Boundary Layer : To study the effect of submergence of the element in a boundary layer, the roughness elements were fixed on the wooden floor of the tunnel (which served as the plane boundary, in all cases), perpendicular to the direction of flow. Elements of height ranging from 1 cm to 4 cm were placed at various sections along the length of the tunnel to get the maximum possible rangeof δ/h ; the range of δ/h used in these studies is from 0.195 to 4.35.

The pressure distribution around the element, the average velocity etc., were measured as described in the former case. For each position of any element, the measurements were made at three to four different velocities.

Experiments with Elements of one Height Kept in Series on a Boundary :- The form resistance of a roughness element when kept in series on a plane boundary was studied by placing roughness elements of a particular height on the tunnel floor at various spacings. Three different heights of elements and a number of spacings were used. The first element was kept at approximately 25 cm from the upstream end of the test section in all cases. For the roughness element of height 4 cm., the pressure distribution around all the elements in the series were measured at spacings of 20, 30, 40 and 60 cm . At a spacing of 80 cm , only four elements could be placed on the tunnel floor and measurements were made on the central two only. From these studies, the distance beyond which the drag coefficient of the element attains an approximately constant value was found out by analysis of the data . For other heights of elements and other spacings, the pressure measurements were made only on the element representative of a series of large number of elements. It may however be mentioned that for elements of 6 cm height, at the largest spacing, the number of elements that could be placed in the tunnel may not be adequate to obtain truly representative conditions. The pressures were measured in this case on the last but one element in the series.

The pressure measurements were made at three or four different velocities in all cases. Also, velocity profiles at one or two sections - close to the element on which the pressures were measured - were taken at one velocity for all spacings with roughness elements of height 2 cm and 4 cm.

Experiments with Combination of Elements of Different Heights :

This phase of experimentation was conducted with a view to study the effect of placing a small roughness element downstream of a larger one, on the drag coefficients of both the roughness elements. Two series of tests were carried out in this phase:

a) A roughness element of 2 cm height was kept at various distances downstream of an element of 4 cm height, both being on the floor. The 4 cm element was kept at a section where the boundary layer thickness was 1.12 cm and only the position of the 2 cm element was changed. The pressure distribution around both the elements was measured at three different velocities.

b) 4 cm elements were kept in series on the floor at a spacing of 80 cm and a series of 2 cm or 4 cm elements also at a spacing of 80 cm were superposed on this at different locations, as shown in Fig. 4.8. In both these series - called the 'primary' and the 'secondary' series for convenience - only a maximum of four elements could be placed in the length available. Hence, without consideration to the attainment of a constant C_D value, the pressure measurements were made on the last but one element in the series, at three different velocities.

4.4 Studies in Closed-Circuit Wind Tunnel :

For the cases of a normal plate in midstream (with a tailplate), and a series of roughness elements of one height placed on the floor, a few runs were conducted in a closed-dircuit wind tunnel. The tunnel had a uniform test section 81 cm deep, 114 cm wide and 3.05 m long. The floor and ceiling were built out of wood, and perspex windows were provided on the sides. The maximum velocity that could be obtained in the test section without any roughness elements in it was 38.0 m/sec. The difference in pressure between two points in the entrance cone was calibrated against the average velocity along the vertical centre line and this pressure difference was used to calculate the velocity diring the runs subsequently. For the purpose of calibration of the above set up, velocity profiles were taken with a Prandtl tube at four average velocities, but only at one section on the centre line of the tunnel.

Three different heights of plates were tested for their drag coefficient, when placed in midstream (with a tailplate), in the same manner as in the open-circuit tunnel studies. Also, the drag coefficient of a representative element in the downstream part of the test section, was measured for the case of elements of one height placed at various spacings on the floor. The height of elements used was 3 cm.

Tables 4.2 and 4.3 summarise the range of variables in the data collected in the flume and the tunnels.

TABLE 4.2

Range of Variables for Studies on Single Element

cm h	cm D	cm δ	m/s V
1.0 to 14.0	32.4 to 81.0	0 to 4.35	6.80 to 35.0

TABLE - 4.3

Range of Variables for Studies on Elements of one Height Kept in Series.

cm h	cm L	cm D	m/s V	$S \times 10^3$
2.0 to 6.0	5.0 to 160.0	10.0 to 81.0	0.12 to 35.0	0.75 to 2.875

CHAPTER - V

ANALYSIS OF DATA - I

RESISTANCE OF A SINGLE ELEMENT

5.1 Preliminary Remarks :

The data collected concerning the pressure distribution around a single element kept on a plane boundary are analysed in this chapter. The data for the case when δ/h is equal to zero have been analysed first in order to evaluate the effect of contraction of the stream on the drag coefficient. These results have been used later to obtain the effect of the presence of the boundary layer alone on the resistance. The data presented by Plate (26) have been used in the above analysis; the analysis presented by him has been also critically examined in this chapter.

5.2 Elements Held in Midstream (With a Tailplate):

The flow past a normal plate, with a symmetrical tailplate, held in the centre of the tunnel is a limiting case of flow past a plate kept on a plane boundary - namely, with zero thickness of the approach boundary layer - as mentioned earlier. For this type of flow and with a stream which is infinite in extent in comparison to the plate height, the drag coefficient of the plate has been found to be 1.38 (4). This result is useful in the case of atmospheric flow over fences and buildings - the height of obstacle being insignificant in comparison to the flow depth - though the effect of the approach boundary layer needs to be evaluated for a complete solution.

However, the value of C_D found by Arie and Rouse (4) is not directly applicable to problems in which the stream must necessarily be treated as finite; flow over an isolated roughness on a channel bottom, flow around spurs are examples of this category. The analysis in this Chapter is aimed at extending the results of Arie and Rouse (4) to various contraction ratios.

Pressure Distribution : The pressures measured on the two faces of a roughness element placed as described above indicated that the pressure over the downstream face was constant for a given velocity , h and D.(For any particular set of the above values, the pressure at any point on the downstream face varied by less than 3 percent from the mean pressure on the downstream face). Advantage is taken of this fact in plotting the pressure distribution diagrams for the normal plates; Fig.5.1 shows a plot of y/h vs $\frac{p_u - p_d}{\rho V^2/2}$ for two different heights of plates. Here p_d is the constant pressure on the downstream face and p_u the pressure on the upstream face at a distance y from the plane boundary (the tail plate). This manner of plotting was adopted to avoid the distortion that would be introduced into the conventional form of pressure distribution diagram, namely, $\frac{p-p_o}{\rho V^2/2}$ vs y/h , due to the possible errors in measurement of p_o, the ambient pressure. Nevertheless, the characteristics of the variation of upstream pressure are still reflected in Fig. 5.1 , because the downstream pressure is constant. It should be noticed that the average abcissa for the plotted curves yields the form drag coefficient for the plate. Figure 5.1 shows that the drag coefficient varies with the para-

meter h/D and also in the range of velocities studied (6.8 to 12.0 m/s), the pressure distribution is independent of the velocity. It may be supposed, therefore, that C_D is independent of Vh/ν, provided the ratio h/D is kept constant.

A study of the variation of the average pressures on the upstream and downstream faces with change in h/D has been made and the results shown in Fig. 5.2. Since, in some cases, the value of p_o could not be measured accurately, Fig. 4.3 was used to determine p_o upstream of the element section. Using this value of p_o, the value of $p_d - p_o / \rho V^2/2$ was computed for each velocity, for a given element. The variation of $\frac{p_d - p_o}{\rho V^2/2}$ with velocity, for any given element, was small (of the order of 5 to 6 percent from a mean value) and insignificant; thus an average value of $\frac{p_d - p_o}{\rho V^2/2}$ was used for each value of h/D. The average value of C_D for each value of h/D was found by plotting pressure distribution diagrams in the form of Fig. 5.1, for each velocity. An average value of C_D was used for each value of h/D, since the average value indicated variations less than 2 to 3 percent from the actual values at various velocities. The value of $\frac{\bar{p}_u - p_o}{\rho V^2/2}$ where $\bar{p}_u$ is the average pressure over the height on the upstream face, was found as the difference between the above values of C_D and $\frac{p_d - p_o}{\rho V^2/2}$. The pressures so computed for the data collected in the open-circuit tunnel have been plotted on Fig. 5.2. data collected in the closed-circuit tunnel have not been used in this figure, since the value of p_o was not measured in this case. The plot indicates that the

pressure on the downstream face decreases much faster than that on the upstream face with increase in the value of h/D. In fact, upto a value of h/D equal to 0.18, the value of $\frac{\bar{p}_u - p_o}{\rho V^2/2}$ remains approximately constant at the value of + 0.81 found by Arie and Rouse (4) for h/D equal to zero; on the other hand, the value of $\frac{p_d - p_o}{\rho V^2/2}$ decreases continually with increase in h/D from a value of - 0.57 at h/D equal to zero.

Drag Coefficient :

a) Verification of Maskell's Equation : As mentioned in section 2.2, according to Maskell, the blockage effect can be corrected by Eq. 2.2 namely,

$$C_{D_c} = \frac{C_{D_1}}{1 + \epsilon C_{D_1} \, h/D}$$

Since the value of ϵ for the case of a two-dimensional normal plate (without a tail plate) was found by Maskell to be 0.96 the same value was used in the above equation to compute C_{D_c} for normal plates provided with a tailplate. For the data collected during the present investigation, C_{D_1} was first determined from the measured pressure distribution and the values of C_{D_c} computed from Eq. 2.2 using these values of C_{D_1}, are shown in the following Table.

It is seen from this table that C_{D_c} increases (more or less) continually with increase in h/D. If the above equation with ϵ equal to 0.96 were to hold good at all the blockage values tested, C_{D_c} would have attained a constant value of 1.38, given by Arie and Rouse (4) for the case when h/D equals zero.

TABLE 5.1

Variation of C_{D_c} with h/D (ϵ = 0.96)

h/D	C_{D_1}	C_{D_c}
0.037	1.50	1.42
0.0617	1.56	1.43
0.065	1.555	1.42
0.1235	1.90	1.55
0.154	2.18	1.65
0.173	2.26	1.64
0.185	2.40	1.69
0.247	2.96	1.74

The fact that C_{D_c} increases with increase in h/D suggests either that the actual value of ϵ may be different from the assumed value of 0.96, or Eq.(2.2)in its present form is inadequate for large blockage values. To check the former, the value of ϵ was computed from the value of $\frac{p_d - p_o}{\rho V^2/2}$ found by Arie and Rouse (4) for the case of h/D equal to zero. The value of ϵ so computed was 1.755. Using this value of ϵ and Eq. (2.2) C_{D_c} values were recomputed for all the data and the results are shown in Table 5.2 .

TABLE - 5.2

Variation of C_{D_c} with h/D (ϵ = 1.755)

h/D	C_{D_1}	C_{D_c}
0.037	1.50	1.37
0.0617	1.56	1.34
0.065	1.555	1.32
0.1235	1.90	1.35
0.154	2.18	1.37
0.173	2.26	1.34
0.185	2.40	1.35
0.247	2.96	1.30

It is seen from the above table that for all runs, the value of C_{D_c} computed with ϵ equal to 1.755 is close to the value of 1.38 given by Arie and Rouse for the infinite-stream case (4). It may, therefore, be concluded that Eq. (2.2) given by Maskell can be used to correct for blockage effect in the present case also, but with a value of ϵ equal to 1.755. An alternative correction based on experimental data has also been suggested in the following section.

b) Variation of C_D with h/D : The average abcissa on Fig. 5.1, as mentioned earlier, is the form drag coefficient of the normal plate and in the case of these sharp-edged plates, it becomes the total drag coefficient itself. As shown in Chapter III, the drag coefficient of the plate in this case should be a function of h/D only. The value of C_D which is an average of

the values obtained at different velocities, has been used in the analysis. The results have been shown in Fig. 5.3, where $\log_{10} C_D$ has been plotted against $\log_{10} (1-h/D)$, the latter parameter being chosen to enable extrapolation to the case when h/D equals zero. The plotted points include data collected in the open-circuit and closed-circuit tunnels during this study and also that of Arie and Rouse (4). It is seen from the plot that extrapolation of the straight line, fitting the author's data to the limit h/D equal to zero yields a value of C_D, identical with that obtained by Arie and Rouse (4) for a normal plate. The equation of the line fitting all the points can, therefore, be expressed as ;

$$C_D = 1.38 (1 - h/D)^{-2.85} \qquad .....(5.1)$$

The nature of this variation between C_D and h/D has been checked for plates of other inclinations[10] namely, 45^o and 135^o - and these results are also shown on Fig.5.3. It is seen from these that Eq. (5.1) can be written in the form

$$C_{D_o} / C_D = (1 - h/D)^{2.85} \qquad .....(5.2)$$

Where C_{D_o} = Drag coefficient for the plate of given inclination kept in an infinite stream i.e. at h/D equal to zero.

Equation 5.2 can probably be used for plates of all inclinations for correcting the data collected in a small tunnel for the blockage effect and also for predicting the drag coefficient at any value of h/D from that measured at a particular value of h/D. The above equation has been obtained

on the basis of studies on two-dimensional sharp-edged plates of inclination varying from 45° to 135° and of negligible thickness; the modification or the application of this equation for other body shapes and strips of finite thickness needs further study.

Since Figs. 5.2 and 5.3 show that the average pressures on the upstream and downstream faces, as well as the drag coefficient, are unique functions of h/D, one would expect a relation between C_D and the value of $\frac{p_d - p_o}{\rho V^2/2}$. The relation obtained on the basis of measurements is shown in Fig. 5.4, and it is seen that C_D increases linearly with decrease in $\frac{p_d - p_o}{\rho V^2/2}$.

5.3 Elements Placed in a Boundary Layer :

The analysis presented in the previous paragraphs pertains to a limiting case - namely when δ is zero - of the general problem of resistance of an element kept in a boundary layer. As shown by dimensional analysis, the drag coefficient of a normal plate set on a plane boundary is a function of the parameters δ/h and h/D. One would also expect that the pressure distribution around the element in the case of a plate held in uniform flow and that in a boundary layer would be different. Hence the pressure distribution around the element was studied first and the analysis is presented below.

Pressure Distribution :- As in the case of plates held in uniform flow region, the pressure over the downstream face was constant along the height in this case also for given values of δ, h, D and V. As such, the pressure distribution has been

plotted in the convenient form of y/h vs $\frac{p_u - p_d}{\rho V^2/2}$ for four different values of δ/h ranging from 0.195 to 2.18 in Fig. 5.5. The characteristic shape of this diagram has been reported earlier by Nagabhushanaiah (21) and Plate (26). The difference in the nature of pressure distribution for plates in the boundary layer and for those in uniform flow is probably due to the difference in the flow conditions obtained immediately upstream of the element. For a plate in a boundary layer a standing eddy forms upstream of the element because of separation of the boundary layer on the wall in frontof the element. However, in case of a plate held in uniform flow region, the separation of flow takes place only at the sharp edges of the element. Hence, the pressure distribution on the upstream face may be expected to be different in the two cases and the difference in the shape of the pressure distribution diagrams may be attributed to the above phenomenon. It was also found by a study of all the pressure distribution diagrams that the maximum value of $\frac{p_u - p_d}{\rho V^2/2}$ occurs at 0.60 h to 0.65 h from the bottom; however, it was found by Plate (26) that this value occurs at 0.52 h to 0.62 h from the bottom. Further, the ratio of the maximum value of $\frac{p_u - p_d}{\rho V^2/2}$ to the average value of $\frac{p_u - p_d}{\rho V^2/2}$ (which is equal to C_D) did not show any systematic variation with δ/h. It can also be noticed that $\frac{p_u - p_d}{\rho V^2/2}$ tends to be approximately constant over the height at larger values of δ/h.

Figure 5.5 shows data plotted at three different velocities. As mentioned earlier, an average value of δ, in this range of velocities, was taken from Fig. 4.5 and used in the analysis. The data on Fig. 5.5 at different velocities, for a given value of δ/h and D/h, indicate that the pressure distribution is independent of the Reynolds number Vh/ν. One may, therefore, suppose that the viscous influence is taken into account by the parameter δ/h and the effect of Reynolds number, if any, is insignificant.

The variation of the average pressure on the upstream and downstream faces with change in δ/h has been shown in Fig. 5.6. The plot shows the average values of $\frac{\bar{p}_u - p_o}{\rho V^2/2}$ and $\frac{p_d - p_o}{\rho V^2/2}$ computed in the same way as for elements in midstream - plotted against δ/h, for a plate of height 2 cms. The value corresponding to δ/h equal to zero, for this height of element, was taken from the runs with the plate in midstream. It is seen from the plotted data that the non-dimensional pressure on the upstream face decreases with increase in δ/h, while the non-dimensional pressure on the downstream face increases with increase in δ/h; however, at values of δ/h greater than 0.5, the variation of the pressures with δ/h is very gradual.

The above variation is typical of that obtained for elements of other heights also, though a different set of lines was obtained (not shown here) for the 4 cm element. An attempt was made at applying the blockage correction, namely Eq.(5.2), as a velocity correction as shown below to obtain a unique relation between δ/h and the average values of $\frac{p_d - p_o}{\rho V^2/2}$ and

$\frac{\bar{p}_u - p_o}{\rho V^2/2}$;

i.e. $\frac{C_{D_o}}{C_D} = (1 - h/D)^{2.85}$ can be written as

$$C_D = \frac{F}{h \rho V^2/2} = C_{D_o} (1-h/D)^{-2.85} \quad \ldots\ldots(5.3)$$

By using a corrected velocity V_c given by

$$V_c^2 = V^2 (1-h/D)^{-2.85} \quad \ldots\ldots\ldots\ldots(5.4)$$

the computed drag coefficient with respect to V_c for the same measured force F, would be C_{D_o}. It was therefore hoped that by non-dimensionalising the pressures $p_d - p_o$ and $\bar{p}_u - p_o$ using $\rho V_c^2/2$, one would get a unique set of lines on Fig. 5.6 for data with different values of h/D. However, plots of $\frac{p_d - p_o}{\rho V_c^2/2}$ and $(\bar{p}_u - p_o)^{1/} \rho V_c^2/2$ against δ/h (not shown here) still yielded different lines for different values of h/D, though the resultant value $\frac{\bar{p}_u - p_d}{\rho V_c^2/2}$ appeared to be uniquely defined by δ/h alone. Hence, it may be concluded that Eq. 5.2 may be used for correcting the resultant pressure or the drag coefficient - as has been shown in the following section - but the correction may not be valid for the pressure distribution on the two faces independently.

Variation of Drag Coefficient : The functional relationship obtained in Chapter III showed that

$$C_D = \phi_4(h/D, \delta/h)$$

for plates kept normal to a plane boundary. The values of C_D were computed from the pressure distribution diagrams with a view to find the function, which describes the variation indicated by the above equation. The values of C_D were computed at

various velocities for a given position of element (or δ/h) and the variation with velocity was found to be invariably less than about 5 percent from the mean value and even this slight variation with velocity was insignificant; hence the mean of the C_D values at the various velocities was used in the analysis. Fig. 5.7 shows the variation of C_D with δ/h for two different heights of plates, the values of C_D at δ/h equal to zero being taken from the studies for the midstream case. The figure shows that C_D decreases with increase in δ/h ; further different curves are obtained for the two heights of plates, indicating the effect of the parameter h/D on the drag coefficient. An attempt was, therefore, made to correct the data for the blockage effect and study the variation of C_{D_o} (the drag coefficient of the plate corresponding to an infinite stream, but placed in a boundary layer) with δ/h. Such a procedure is based on the assumption that the effects of contraction of the stream (due to placement of the element) and presence of the boundary layer on the drag coefficient of the element are independent of eachother and can be evaluated separately. The data analysed justify this assumption.

Figure 5.8 is a plot of C_{D_o} vs δ/h and the plotted data include those collected by the author and Modi (16) in the open-circuit tunnel using elements 1 cm to 8 cm in height. The data collected by Plate (26) with elements of height ranging from 2.5 cm to 5 cm and placed on the floor of a 1.83 metre high tunnel are also used. The values of drag coefficient listed by Plate (26) are based on the free-stream velocity and these were first corrected to obtain C_D based on the average velocity

in the vertical centre line, which is used in these studies; this drag coefficient was corrected for the blockage effect using Eq.5.2 to get C_{D_o} as was done for the author's and Modi's data also. It may however be mentioned that the velocity distribution in the boundary layer in the tunnel used by Plate (26) followed the 1/7th power law, while for the other data, the velocity distribution followed the 1/8th power law; it is assumed that the effect of this change in velocity distribution for a given value of δ/h, is insignificant and the various sets of data have been analysed together. The value of C_{D_o} equal to 1.38 at δ/h, equal to zero given by Arie and Rouse (4) forms a limiting point on Fig. 5.8. It is seen from the figure that data from various sources follow a single trend as a result of the blockage correction applied through Eq. 5.2. This may, therefore, be supposed to indicate the reliability of Eq. 5.2 and also justify the assumption that the effects of blockage and boundary layer submergence are independent and can be evaluated separately.

Figure 5.8 shows that C_{D_o} decreases continually from a value of 1.38 at δ/h equal to zero with increase in δ/h, reaching a value of 0.575 at δ/h equal to 10; the decrease however is more rapid at small values of δ/h and very gradual at higher values of δ/h.

The data of Nagabhushanaiah (21) indicated much lower values of drag coefficient than those of Plate (26) as shown in Fig. 2.2. On correction of the data for the blockage effect, the data collected by Nagabhushanaiah would yield considerably smaller values than those indicated on Fig. 2.2, because the elements used by him were of large height. Hence these points

would fall much below the line drawn on Fig. 5.8 based on the data of Plate (26), Modi (16) and the author; however, no explanation can be offered for this difference.

The following procedure may be used to evaluate the drag coefficient for a given case on the basis of Fig. 5.8 and Eq. 5.2 :

a) In the case of atmospheric flow over an obstacle on ground and similar to the element used in these studies, one might make the approximation that the free-stream velocity and the average velocity in the vertical are not appreciably different. Further, since the stream is infinite, C_{D_o} can be read from Fig. 5.8 for known δ/h value and used directly along with the free-stream velocity to estimate the drag force.

b) In the case of an element in a boundary layer, but in a finite stream, C_{D_o} is obtained from Fig. 5.8 for the known value of δ/h . The actual drag coefficient corresponding to the given value of h/D can be obtained using Eq. 5.2. The drag force can be estimated using the above value of C_D and the average velocity along the vertical.

Interpretation of Plate's Equation :- The equation given by Plate (26) for the drag coefficient of a plate kept in a boundary layer is

$$C_{D_1} = 1.05\ (h/\delta.)^{2/7} \qquad \ldots\ldots\ldots(2.5)$$

where C_{D_1} is the drag coefficient with respect to the free-stream velocity U_o. The data used in developing the above equation were not corrected for the blockage effect, but the

effect is not serious in the above set of runs since their h/D values are quite small. Using the observed 1/7th power law of velocity distribution, one can write the above equation as follows:

$$C_{D_1} = \frac{F}{h \rho V_o^2/2} = 1.05 (h/\delta)^{2/7} \quad \ldots\ldots$$

$$= 1.05 (u_{h/U_o})^2 \quad \ldots\ldots\ldots(5.5)$$

where u_h is the velocity at the crest level of the element without the element in position. Hence C_D' the drag coefficient of the element with respect to the crest-level velocity can be written as ;

$$C_D' = \frac{F}{h \rho u_h^2/2} = 1.05 \quad \ldots\ldots\ldots\ldots(5.6)$$

However, Eq. (2.5) has been obtained based on data in the range of δ/h from approximately 2 to 12. But for δ/h values between zero and one, the velocity at the crest of the element is equal to the free-stream velocity itself; as such C_D' - which would be equal to C_{D_1} in this range - would not be a constant at least in the range of δ/h from zero to one. In fact at δ/h equal to zero, C_D' would have a value of 1.38, the value given by Arie and Rouse (4). Therefore, to study the variation of C_D' in the range of δ/h from 0 to 12, the following procedure is employed :

The drag doefficient C_{D_o} computed in these studies could also be treated as the drag coefficient C_{D_1} (with respect to the free-stream velocity) in the case of an infinite stream with a finite thickness of boundary layer. Using these values of C_{D_o} - obtained with the help of observed C_D values and Eq. 5.2 - the values of C_D' were computed for the data collected by

Plate (26), Modi (16) and the author, using the appropriate velocity distribution law. Figure 5.9 shows the variation of C_D' with δ/h for the various sets of data. Despite some scatter, the data indicate a decrease in C_D' with increase in δ/h from 0 to 1 and an increase in C_D' thereafter with increase in δ/h, reaching a constant value at higher values of δ/h.

Relation between $\frac{p_d - p_o}{\rho V^2/2}$ and C_D : The equation given by Plate (26) relating the drag coefficient of a plate kept in a boundary layer to the dimensionless parameter for pressure on the rear is

$$C_{D_1} = 1.65 \frac{p_d - p_o}{\rho U_o^2/2} \qquad \text{.....(5.7)}$$

Since Eq. 5.7 is based on data not corrected for blockage effect, the unique relationship between C_{D_1} and $\frac{p_d - p_o}{\rho U_o^2/2}$ would imply that the relation accounts for the blockage effect as well as submergence in the boundary layer; however, as mentioned earlier, the former effect is relatively less important in the above data owing to the small values of h/D.

The above equation was derived using data with a limited range of C_{D_1} and is valid with an accuracy of $\pm$ 10 percent for the above data (26). In order to extend the above form of equation to a wider range of drag coefficient, a plot was made (See Fig. 5.10) between the drag coefficient C_D and the dimensionless pressure $\frac{p_d - p_o}{\rho V^2/2}$ using the data collected by Plate (26), Modi (16) and the author. It should be noticed that a definite variation between these two parameters

if any, would include the combined effect of the presence of the boundary layer and the contraction of the stream caused by the element itself.

Equation 5.7 can be modified to suit the new parameters, as ;

$$C_{D_1} = \frac{F}{h\rho V^2/2} \left(\frac{V^2}{U_o^2} \right) = 1.65 \frac{p_d - p_o}{\rho V^2/2} \left(\frac{V^2}{U_o^2} \right) \quad \ldots\ldots\ldots(5.8)$$

$$\text{i.e.} \quad C_D = 1.65 \frac{p_d - p_o}{\rho V^2/2} \quad \ldots\ldots\ldots(5.9)$$

Equation 5.9 has been represented on Fig. 5.10, along with the plotted data. The data indicate considerable departure from the relation proposed by Plate (26), namely, Eq. 5.9, at large values of C_D. In the absence of any certainty that a relation including the boundary layer and the contraction effects exists between the two parameters, no effort is made to draw an average curve fitting all the data on Fig. 5.10.

5.4 Application of Results to Flume Studies :

For fully developed turbulent flow in an open channel, one can use Fig. 5.8 and Eq. 5.2 in the following way to predict the resistance of a vertical strip placed on the bed. Since the depth of flow is equal to δ in this case, one can find C_{D_o} from Fig. 5.8 for the known value of δ/h. The above value of C_{D_o} and the known value of h/D can be substituted in Eq. 5.2 to get the actual drag coefficient C_D. The variation of C_D with D/h, obtained by such a procedure, is shown in Fig. 5.11. The resistance of an infinitesimal length of strip δx at the centre of width can be found as .

$$F_{\delta x} = C_D . \delta x . h . \rho V^2/2 \quad \ldots\ldots(5.10)$$

using the above drag coefficient and the average velocity along the centre line of width of the channel.

The results of measurements made by Adachi (2) on a two-dimensional strip of thickness 6.4 mm and height 5 mm and kept on the bed of a 20 cm wide flume are also shown in Fig. 5.11. It is seen that there is a considerable difference between Adachi's curve obtained by direct measurements and the curve obtained by the author in Fig. 5.11 by the above indirect procedure. The curve presented by Adachi (2) predicts a higher value of C_D than that obtained by the author's curve; on the other hand, because of the influence of thickness on C_D (26), one would expect Adachi's curve to fall below that proposed by the author. One plausible explanation for this anomaly may be that Adachi has used the average velocity over the whole width - inspite of the pressures being measured only on the centre line - and not the average velocity along the centre line as used by the author. In a flume of small width, as used by Adachi (2), the values of drag coefficient computed using these two different characteristic velocities would be considerably different. Obviously, using the average centre line velocity along with the observed centre line pressures for Adachi's data would shift the curve predicted by him considerably downwards on Fig. 5.11.

Two check runs were conducted in the flume with water to verify the applicability of the author's curve (Fig. 5.11) to open channels. Uniform flow was first established in the flume (with no roughness element in it) and the average velocity along the centre line of width was found by running a velocity traverse at a pre-determined location in the downstream half of

the flume. A 4 cm high two-dimensional sharp-edged roughness element with pressure points on it was then placed on the bed at the section where the velocity profile was taken. The pressures on the two faces of the element were measured using an inclined manometer and the drag coefficient computed with respect to the average velocity obtained by the velocity profile already taken. The results of these two runs are also plotted on Fig. 5.11 and it is seen that the points fall well above the curve predicted from the wind tunnel studies, but close to the curve proposed by Adachi (2).

One of the main reasons for the difference in behaviour between the wind tunnel and flume data appears to be the change in the shape of the top boundary. In the wind tunnel, the top was smooth and parallel to the floor, while in the flume runs, a significant dip in water surface immediately downstream of the element was noticed. It is supposed that this decrease in depth just downstream of the element, resulting in higher acceleration of the flow, might lead to a larger drag coefficient. However, it was noticed during both the runs that the increase in depth upstream of the element, after placement of the element, is appreciable; in such a case, the use of the original flow depth and velocity (before placing the element) in the analysis may be unrealistic.

A second point of difference between the flow in the flume and that in the tunnel is in regard to the values of δ/D in the two cases. The data on Figs. 5.3 and 5.8 cover a range of δ/D from 1/16 to 1/3 , while the value of δ/D for fully

developed turbulent flow in an open channel is 1.0. It was assumed that the use of the average velocity in the vertical, in preference to the free-stream velocity, would implicity take into account the effect (if any) of variations of δ/D. In view of the difference noticed in the behaviour of the tunnel and flume data, the effect of variations of δ/D may need to be studied in detail. One may also consider the possibility of treating δ/D as approximately equal to 0.8 in an open channel, while using Fig. 5.8, since it has been noticed (7) that the maximum velocity usually occurs at approximately 0.05D to 0.25 D from the water surface; such a procedure would shift the predicted line, shown in Fig. 5.11, higher.

In view of the uncertainties mentioned in the foregoing paragraphs, the predicted variation in Fig. 5.11 may not prove reliable for determination of resistance of a single element on the bed of an open channel. However, it is hoped that it could be used to determine the resistance of a right-angled spur on the sides of a channel.

-:o:-

CHAPTER - VI

ANALYSIS OF DATA - II

RESISTANCE OF ELEMENTS IN SERIES

6.1 Preliminary Remarks :

An analysis of the several aspects concerning the resistance of a plane boundary with elements kept in series on it is presented in this chapter. Despite the fact that the approach suggested by Morris (17) is a fairly generalised one which is valid for all types of roughness elements, very little effort has been made in the past to verify it for the type of elements used in this study. Hence, firstly, the available flume data on this type of elements have been used to verify the reliability of the above method for this type of roughness elements. The data indicate that the above approach is not completely satisfactory over a wide range of variables and the necessity of a more reliable method for this type of elements is therefore realised

It has been emphasised earlier that a knowledge of the individual resistance effects is essential in understanding the mechanism of resistance to flow over artificial roughness elements. Hence, further analysis presented in this chapter, based on flume and wind tunnel data, is aimed at providing information on the form resistance of the roughness elements, the skin friction on the plane boundary and velocity distribution in this type of flow. The analysis has been performed on the basis of certain premises, which are justified by past studies or by data collected during the present study.

6.2 Verification of Morris's Method (17):

Though several investigations concerning the resistance of artificial roughness elements have been conducted, the approach suggested by Morris(17) is the only one of a general nature with applicability to a variety of roughness shapes and patterns. Further, very little work has been reported concerning the resistance of two-dimensional roughness elements of negligible thickness. As such, the data collected during this investigation along with those of Sayre and Albertson (37) and Basha (6) have been used to verify the curves proposed by Morris, only. The following steps were followed in computing the required parameters for all the flume runs (computations were made choosing the top of element as datum in accordance with the approach followed by Morris).

a) From the plot of h/D vs D/L with $C_{D_1}\ p/P$ as third parameter (18), shown in Fig. 2.4, the type of flow- isolated roughness flow or wake-interference flow - was determined. Since all the runs were with L/h greater than 1.0, no run was of the quasi-smooth type (18). The value of C_{D_1} used was 1.90 for all the runs as recommended by Morris (18) and p/P was equal to unity in all the runs except those of Sayre - Albertson (37).

b) For the wake interference type of flow, the friction factor was computed as

$$\bar{V}/V_* = \sqrt{8/f} \qquad \text{.....(6.1)}$$

where $V_* = \sqrt{gR_bS}$ .....(6.2)

R_b being the hydraulic radius with respect to the bed computed as suggested by Einstein (8).

A plot of the parameters $1/\sqrt{f} - 2\log_{10} D/L$ and $\sqrt{32}\ \frac{V_* L}{\nu}$ is made using all the data and the data are compared with the predicted line (by Morris) in Fig.6.1.

c) For the isolated-roughness flow, the value of f_s, (the smooth-boundary friction coefficient) was determined first by using the diagram relating f_s to the flow Reynolds number (7); the predicted friction factor for bed with roughness elements was then computed using Eq. 2.2 namely ;

$$f = f_s \left(1 + 67.2\, C_{D_1} \cdot P/P \cdot h/L\right)$$

The predicted friction factor has been plotted against the actually observed friction factor in Fig. 6.2.

These two diagrams reveal that the prediction of resistance by Morris's method is not of a desirable degree of accuracy. Figure 6.1 shows a reasonable scatter of points on both sides of the predicted curve, except for Sayre-Albertson's data; these indicate a much lower resistance than that predicted by the curve proposed by Morris. But, in case of the isolated-roughness flow, there is a considerable difference between the observed and predicted resistances, as can be seen from Fig.6.2. The plotted data indicate that, in general, Eq. 2.2 overpredicts the resistance when L/h is less than approximately 10 and underpredicts the resistance when L/h is greater than 10 approximately. However, the agreement is quite good for the Sayre-Albertson data on discontinuous roughness elements. The following comments concerning Morris's method bring out the

inherent limitations of the method :

a) The criterion for prediction of the type of flow (Fig. 2.4) is arbitrary and in many instances, the type of flow predicted is different from that which can be physically visualised. For example, some of the runs for the two-dimensional strips with L/h equal to 7.5 and 5.0 fall under the category of isolated-roughness flow when this criterion is used. One would normally expect that wake-intereference would prevail for this type of roughness elements, even at L/h equal to 10. Morris himself, recently (19) has commented that wake-intereference type of flow persists at larger spacings than predicted, with certain types of roughness elements. Therefore, an analysis was made by assuming that wake-interference flow exists at a relative spacing L/h less than 10 and the actual resistance compared with the resistance predicted by treating the flow as of wake-interference type. However, the agreement was not satisfactory (not shown here) and this , therefore, raises doubts about the accuracy of the resistance curves proposed by Morris, for this type of roughness elements, in the above range of L/h.

b) Any number of roughness patterns can be arranged with a given value of L/h, p/P and a particular type of roughness element. But, in all these cases, the resistance coefficient predicted by this method would be the same at a given Reynolds number. However, the

investigations of O'Loughlin and Macdonald (24) and Einstein and Banks (9) reveal that apart from the roughness concentration, the arrangement of the roughness elements has some influence on the resistance coefficient, particularly at large concentrations.

c) The drag coefficient used for the computation of the form drag (in isolated-roughness flow) and for the classification of flow (Fig. 2.4) is that which is valid for an element held in an infinite stream without a tail plate; for example, the drag coefficient recommended for use for elements used in this study is 1.90. Also, the velocity used in the computation of form drag is that at the crest level of the elements (17) . Assumption of a value of C_D equal to 1.90 (for the elements used in this study) fails to take cognizance of the effect of placing the element on a boundary and also of the interference effect when elements are placed in series. It may be emphasised that when an element is placed on a boundary with zero thickness of the approach boundary layer, the drag coefficient would be 1.38 (4). In case of elements placed in series at very large spacings, the effect of the boundary layer would be appreciable and a value of C_D' (with respect to the velocity at the crest level) of approximately 1.05 is more realistic than a value of 1.90, as can be seen from Fig. 5.9. Also at smaller spacings , even of the order of L/h equal to 20 , at which Fig. 2.4 predicts isolated-roughness flow almost

invariably - the interference effect would be very important as shown later. Further, in view of the uncertainties regarding the velocity distribution over an artificially roughened bed, the use of the velocity at the crest level of elements would introduce a certain degree of approximation. In fact, it is felt that the variations between the observed and predicted resistances for the isolated-roughness flow, noted earlier, may be primarily due to the departures of the actual drag coefficient and the crest-level velocity from the assumed values.

It is, therefore, concluded that the method proposed by Morris (17) despite its generality of application, is inadequate over a wide range of roughness concentrations and patterns. A logical approach involving study of the variation of drag coefficient with spacing based on wind tunnel experiments and its application to the flume experiments with two-dimensional roughness elements has been suggested in the following sections as an alternative to the method proposed by Morris.

6.3 Wind Tunnel Experiments :

The data collected on the pressure distribution around roughness elements kept in series on the floor have been analysed in this section of the chapter. From a study of the variation of C_D for different elements along the length of the tunnel, the length required for the attainment of an approximately constant value of C_D is determined. The pressure distribution diagrams of elements representative of those in a series of infinite number of

elements and their characteristics are studied next; these pressure distribution diagrams are then made use of to study the variation of C_D with the spacing parameter L/h and D/h.

Variation of C_D along the Length : The drag coefficient of every element in an infinite series of elements placed on a boundary would be obviously the same for all elements. However, in experimenting with a small length of tunnel - about 3 metres long as in the present case - one has to ascertain whether a fairly constant value of C_D along the length is attained and, if so, after what distance from the upstream end or from the first element. For this purpose the data on pressure distribution around the element collected for a number of spacings were analysed. With elements of 4 cm height, pressure measurements had been made on practically all the elements kept on the tunnel floor at spacings of 60 cm., 40 cms., 30 cm and 20 cms. Also, with an element of 4 cm height at 80 cm. and a 2 cm element at 80 cm. spacing, measurements were made on the central two in a series of four. All these measurements were performed in the open-circuit tunnel with the first element being placed at approximately 25 cm. from the upstream end of the test section. From the observed pressures the form drag and the average drag coefficient C_D of all the elements was computed. The variation of C_D of the elements along the length at various spacings is shown in Figs. 6.3 a and 6.3 b and also Table 6.1.

TABLE 6.1

Variation of C_D along the Length

Height of element cm.	Spacing cm.	Total no. of elements in tunnel	Position of element in series	Average C_D
			2nd from upstream	1.17
4	80	4	3rd from upstream	1.22
			2nd from upstream	1.07
2	80	4	3rd from upstream	1.02

It can be seen (from Table 6.1 and Fig. 6.3) that, while at L/h values of 20 and 40 the drag coefficient on the second and third elements is approximately the same, there is considerable variation of C_D along the length for some distance from the upstream end at the smaller spacings. The variation, however, is not completely erratic; a close examination shows that the drag coefficient on the second element in the series is much smaller than that on the first and in many cases even negative. The drag coefficient of the third element again shows a substantial increase over that of the second, though this value is less than that of the first. This manner of variation continues along the length with the difference in drag coefficient between successive elements decreasing in the downstream direction.

It is felt that changes in the extent and nature of the separation zones behind the roughness elements are responsible for this manner of variation along the length. However, it is seen from Fig. 6.3, that in the cases of L/h equal to 5, 7.5 and 10, an approximately constant value of C_D appears to have been obtained in the downstream end of the tunnel. In the case of roughness pattern with L/h equal to 15, this constancy could not be obtained because of the impossibility of placing larger number of elements at this spacing in the short length of test section available. Nevertheless, from the variations shown in Fig. 6.3 and Table 6.1, one may suppose that an established pattern of separation zones leading to an approximately constant value of C_D along the length is obtained at all the spacings after a distance of approximately 40 to 50 h from the first element.

The attainment of a constant value of C_D was also checked for a roughness pattern comprising of 3 cm elements at a spacing of 15 cm. in the closed circuit tunnel. The measured values of C_D on the 16th, 17th and 18th elements in a series of 21 elements were 0.149, 0.143 and 0.154 respectively; the variation is insignificant considering the probable accuracy of measurement and one may assume therefore, that a constant value of C_D is obtained after an initial length of 50 h, as mentioned before.

Pressure Distribution-Elements in Series : Figures 6.4a to 6.4f show the pressure distribution on a representative element - decided from the criterion mentioned in the previous paragraphs - for L/h ranging from 2.5 to 40. For all the

spacings except L/h equal to 2.5, the pressure on the downstream face was constant over the height for a given value of h and D at a particular velocity. For elements spaced at L equal to 2.5 h, there was a slight variation of pressure on the rear over the height, though not always consistent. However, in all cases a constant pressure has been assumed on the downstream face, an average value being taken in case of elements at L/h equal to 2.5 . The pressure distribution diagrams have been prepared showing the variation between y/h and $\frac{p_u - p_d}{\rho V^2/2}$, the same parameters used for single elements.

It is seen from the above diagrams that the dimensionless pressure distribution around the element is practically independent of the velocity at all spacings. This is consistent with the established concept (36) that the dimensionless pressure distribution and the drag coefficient for a sharp-edged element are independent of the Reynolds number, for Reynolds number values exceeding 10^3 . However, the scatter of points on Fig. 6.4 with change in velocity is slightly more than that on Figs. 5.1 and 5.5, probably because of larger fluctuations of pressure in case of elements in series. Also, since except in one or two cases, the slight variation with change of velocity was inconsistent, it is concluded that the dimensionless pressure distribution is independent of the velocity changes and hence average lines have been drawn.

A study of all the pressure distribution diagrams indicates that the shape of these curves for L/h values of 20 and 40 is approximately the same as that for a single element

kept in a boundary layer. This similarity probably indicates that there is no pronounced wake-interference and the flow is akin to the isolated-roughness type of flow mentioned by Morris (17). At L/h values of 15 and 10, the value of $\frac{p_u - p_d}{\rho V^2/2}$ is approximately constant over the entire height of the element, except for a small region near the crest. At L/h values between 2.5 and 7.5, a pronounced decrease in $\frac{p_u - p_d}{\rho V^2/2}$ near the centre of height of the element is noticed. The differences in the shape of the pressure distribution diagrams with variation in L/h are the probable result of the changes in the character of the separation zone downstream of the previous element.

Variation of C_D with h/L and $\bar{D}$/h : The drag coefficient of a representative element in the series was computed at all the velocities at various spacings by integration of the pressure distribution diagrams. In case of some runs (for example L/h equal to 15 and h equal to 4 cm.) adequate number of elements could not be placed in the tunnel to obtain conditions representing a series of large number of elements. The drag coefficient of an element in a series of infinite number of elements was then estimated from Fig. 6.3. With elements of 6 cm height kept in series, measurements were made on the last but one element in the series and this was assumed to be the representative element; in view of the small number of elements at large spacing using this height of element, this may be an approximation at large L/h values. In all cases, the computed value of C_D showed no significant dependence on the velocity and

average values have been used in the analysis.

By dimensional analysis it has been shown in Chapter III that

$$C_D = \phi \ (h/L \ , \ D/h)$$

The data plotted on Fig. 6.5 indicate that the use of D/h as a third parameter systematises the scatter of points on a plot of C_D vs h/L. For a given value of D/h, C_D continually decreases with increase in h/L, and C_D decreases with increase in D/h for a given value of h/L.

Assuming that in the flow over a series of large roughness elements, the boundary layer effects are inappreciable, the values of C_D found for a single element kept in midstream (and with a tailplate) are also plotted on Fig. 6.5 as those corresponding to h/L equal to zero. It can be seen that the curves relating h/L to C_D at different values of D/h can be extrapolated smoothly to the limit h/L equal to zero. Obviously if the boundary layer effects are significant, the drag coefficient corresponding to h/L equal to zero would need to be determined at the given value of D/h (equal to δ/h) from Fig. 5.8 and Eq. 5.2 as described before. However, values so computed for h/L equal to zero were less than the observed C_D values for finite spacings of the order of 15 h. But the study of the variation of C_D along the length had shown that C_D attained a constant value after a comparatively short initial length and it may, therefore, be supposed that the boundary layer effects on C_D are inappreciable in these cases. Hence all the curves on Fig. 6.5 have been extended to the C_D value for an element in midstream, which is also free from

boundary layer effects. However, because of the short length of tunnel section, it was not possible to verify the trend of curves shown in the region h/L equal to 0 to 0.025. It remains to be checked whether at extremely large spacings, the element can be treated as isolated and immersed in a boundary layer and C_D estimated from Fig. 5.8 and Eq. 5.2 rather than from the extrapolation shown in Fig. 6.5. However, Adachi's experiments (2) on two-dimensional strips of finite thickness indicate that C_D increases continually with increase in L/h upto L/h equal to 160, at a given value of D/h; beyond L/h equal to 160, his data indicate that the strips could be treated as isolated-roughnesses.

A comparison between Fig. 6.5 and a similar plot prepared by Adachi (2) for two-dimensional strips of finite thickness revealed that at given values of D/h and L/h, the drag coefficients in Fig. 6.5 are higher. It is felt that this tendency reflects the effect of thickness of the strip on the drag coefficient.

Variation of C_{D_o} with h/L : The variation in C_D with variations in D/h at a given value of h/L shows the effect of the proximity of the top boundary on the flow. An effort was made to study the applicability of the blockage correction, namely Eq. 5.2, to eliminate the contraction effect for elements in series. Should the correction be valid for elements in serie a unique relation would be obtained between C_{D_o} - the supposed value for an infinite stream - and h/L. However, Fig. 6.6 shows that even on correction of the drag coefficient values through

Eq. 5.2, data with different values of D/h show different relations on the plot of drag coefficient versus h/L. It must be noticed that Eq. 5.2 affords a means of correcting for the variations in flow pattern (and consequently change in C_D) due to contraction in case of flow past a single element; apparently, in the flow over a series of roughness elements, the changes in flow pattern (and thus in C_D) due to changes in h/D are a function of h/L also. As such, it appears that Eq. 5.2 would be inapplicable to compute CD_o values (for the infinite stream case) for elements in series.

6.4 Combined Analysis of Wind Tunnel and Flume Data :

In this section an analysis of the resistance characteristics of roughness elements kept in series is presented. Wind tunnel and flume data have been used to evolve a relationship between the drag coefficient of the roughness element and the parameters L/h and D/h. In such an analysis of the two sets of data together, one must give due consideration to the various points enumerated below, someof which were discussed in Chapter III. A critical examination of all these aspects has been presented, as a result of which the combined analysis is justified.

a) Wave resistance in flume experiments.

b) Skin friction of the plane boundary.

c) Reynolds number effects.

d) Similarity of flow pattern in the flume and tunnel.

e) Choice of velocity.

It was shown in Chapter III that the wave resistance and the skin friction on the plane boundary would form insigni-

ficant contributions to the total resistance in the range of experiments carried out during this investigation. Further, it was emphasised that the Reynolds Number could be omitted from the analysis, provided the Reynolds number exceeded 10^3. The Reynolds number $\bar{V}h/\nu$ in flume runs ranged from 3.5×10^3 to 2×10^4, while for the wind tunnel data the range of the Reynolds number Vh/ν was from approximately 10^4 to 5.2×10^4. Hence, the flume data have been analysed on the assumption that the measured total resistance is equal to the form resistance of the strips. Also the Reynolds number has been omitted from the analysis for tunnel as well as flume data.

d) Similarity of Flow Patterns : While the three aspects examined earlier permit a combined analysis of the wind tunnel and flume data, further justification was sought by comparing the flow patterns in the two cases. Firstly, it was noticed in all the flume runs that the water surface was fairly smooth and plane, corresponding to the shape of the tunnel ceiling in the wind tunnel studies. Only at L/h equal to 40 and 20, a slight dip in the water surface immediately downstream of the roughness element was noticed at the smaller depths. However, this dip was much less significant than that observed in the flow over a single element; as such, the bottom and top boundaries (or the water surface) can be assumed to be plane and parallel to each other in the tunnel as well as in the flume.

The data concerning the velocity distribution in the flow over roughness elements are also used to compare the nature of the flow in the flume and the tunnel. In all cases

except one, only one or two velocity profiles were taken for each pattern at typical sections. In one particular run in the tunnel with L/h equal to 40 and h equal to 2 cms, a number of velocity profiles were taken along the length and the results are shown in Fig. 6.7. In the available length of test section four elements could be placed at the above spacing and velocity profiles taken over the first three elements and also midway between two consecutive elements are shown . It is seen from the figure that an average velocity profile can be drawn through the data at the sections between elements. However, the three profiles taken over the elements are different from one another, particularly in the region close to the element. Further though the mean velocity of flow was constant while the various profiles were taken, it may be seen from Fig. 6.7 that integration of these three profiles would lead to different discharge rates. Since the streamlines over the roughness elements would have considerable curvature, it is felt that an ordinary Prandtl tube without any attachment to enable placing it in the streamline direction would be inadequate to obtain accurate velocity distribution data. Apparently, the difference in the discharges that would be obtained by integration of the profiles shows that the curvature of the streamlines over the three elements (on which velocity profiles were taken) was varying . However, it is surprising that the data collected at three different sections midway between elements appear to define a single curve, since one expects a representative profile to be obtained only after some length. In fact, after a certain initial length, one can expect the velocity distribution at corresponding sections to be

identical. But data on Fig. 6.7 indicate that a single velocity distribution law may be inadequate to describe the velocity profile over the element and that between the elements, particularly at large spacings. The differences in the character of the velocity profiles over the element and between elements have been emphasised by Adachi (2) also.

In view of the possible inaccuracies in the velocity measurements with Prandtl tube in strongly curved flows, the limited number of profiles taken and also the differences in the profile over the element and that between elements, no effort is made at proposing a velocity distribution law for this type of roughness elements. Nevertheless, the data have been used in a qualitative way, namely to compare the nature of velocity profiles obtained in the flume and tunnel experiments. Figures 6.8a to 6.8 e show plots of $\log_{10} y$ versus u obtained from measurements in the flume as well as in the tunnel. The velocity profiles in the tunnel were taken close to the element supposed to be representative on the basis of Fig. 6.3. The data plotted in Fig.6.8 indicate firstly that there are considerable differences in the velocity distribution over element and between the elements at large spacings ; at small spacings, it may be seen that there is a tendency for the two profiles to merge together. It may also be noticed that the nature of the profiles in the tunnel and in the flume are similar. In both cases, at most spacings, there is a definite break in the velocity profile as also reported by Morris (17); at L/h less than 5, data appear to follow a single line while at higher spacings the break may be noticed. It may also be

mentioned that negative velocities were noticed immediately downstream of the elements and near the bed at some spacings, in the tunnel as well as in the flume, but they were not measured.

Hence it may be concluded from a study of Fig. 6.8 that the flow patterns obtained in the tunnel and flume at corresponding sections are similar; the results of an attempt at a quantitative comparison are discussed later.

e) Choice of Velocity : As mentioned earlier, the drag coefficient determined in the wind tunnel is defined with respect to the average velocity in the vertical centre line. In case of a channel of width B, considering a two-dimensional strip, one can write the force ΔF_B as

$$\Delta F_B = C_D \Delta x \cdot h \cdot \rho V^2/2 \qquad \ldots\ldots(6.3)$$

where ΔF_B is the force on a width Δx of the roughness element and V the average velocity along the vertical at the centre of Δx.

The total force F_B can be written as

$$F_B = \int_0^B C_D \Delta x \, h \, \rho V^2/2 \qquad \ldots\ldots\ldots(6.4)$$

Assuming C_D to be only a function of the roughness geometry and the parameter D/h, the force F_B corresponding to a given value of D/h becomes

$$F_B = \frac{C_D h}{2} \int_0^B V^2 \Delta x \qquad \ldots\ldots\ldots(6.5)$$

The integral in Eq. 6.5 may be written as $\overline{V}^2 B \beta$ where $\overline{V}$ is the mean velocity of flow over the channel cross section and β is the momentum correction factor for the velocity

distribution across the width. Equation 6.5 may therefore, be written as

$$F_B = \beta C_D \rho h B \bar{V}^2/2 \qquad \text{.....(6.6)}$$

The value of β is usually only slightly greater than unity and β is assumed to be unity in this case considering that the error introduced by such a step would be negligible. Hence Eq. 6.6 becomes,

$$F_B = C_D \rho h B \bar{V}^2/2 \qquad \text{.....(6.7)}$$

Equation (6.7) was used to calculate C_D for the flume data while C_D for the wind tunnel data were computed on the basis of centre line velocities and pressure measurements as mentioned earlier.

The critical examination of the several aspects mentioned in the foregoing paragraphs reveals that a combined analysis of the flume and wind tunnel data is justified. Such an analysis has been presented below and the values of C_D in case of flume runs, for this purpose, were computed as described below :

The average shear stress on the bed can be written as ;

$$\tau_o = \gamma R_b S \qquad \text{.....(6.8)}$$

This shear can be equated to the form resistance of the roughness strips, since the other types of resistance are assumed to be negligible.

$$\text{i.e. } \gamma R_b S = \left\{ C_D (h.1) \rho \bar{V}^2/2 \right\} \frac{1}{L} \qquad \text{.....(6.9)}$$

The values of C_D were computed for the various flume runs through Eq. 6.9.

Variation of C_D : On the basis of dimensional analysis presented earlier, the drag coefficient of a roughness element

in series can be written as

$$C_D = \phi \ (L/h, D/h)$$

By similarity with the semi-logarithmic equation for friction in pipes, plots of $1/\sqrt{C_D}$ vs $\log_{10} D/h$ were prepared for various values of L/h. A number of other forms were tried, but the above form appeared to yield the most encouraging form of relationship. Figures 6.9a to 6.9h are plots of $1/\sqrt{C_D}$ vs $\log_{10} D/h$ for different L/h values based on all the flume and wind tunnel data. The wind tunnel data plotted on this figure are the values of C_D for the representative element in the series as determined from Fig. 6.3.

For one run with L/h equal to 20 and h equal to 4 cms, the pressure distribution on the element was measured at the centre line of the flume. This measurement was performed on an element in the downstream half of the flume. A velocity profile was taken upstream of this element along the centre line of the flume and the drag coefficient computed with respect to the average velocity in this vertical has been plotted on Fig. 6.9g . For the same run, the value of C_D computed on the basis of the water surface slope and the average velocity over the whole section (i.e. using Eq. 6.9) has also been plotted on Fig. 6.9g . There is an appreciable difference between the two computed values and also the value of C_D computed from the measured pressures in the flume shows departure from the trend of the other flume and wind tunnel points on Fig. 6.9 g. On examination it was found that the average velocity in the vertical obtained by the pitot tube traverse was higher than that theoretically computed by assuming

an appropriate velocity distribution along the width. Further, the ratio of the average velocity along the vertical centre line to the average velocity over the whole cross section in this case was found to be about 1.24 and much higher than that observed in the case without any roughness elements on the bed. Thus, it is felt that the velocity measurements with an ordinary Prandtl tube in the case with large roughness elements are not very accurate and thus the departure seen on Fig. 6.9 g is understandable. In fact by using a corrected velocity (based on equations of velocity distribution across the width and also by application of the same ratio between centre line velocity and average velocity, as observed in the case with no roughness elements, to the present run) the C_D value from the observed pressures came out to be 1.66 and thus very close to the value of 1.69 computed from the water surface slope and average velocity over the whole cross section.

It can be seen from Fig. 6.9 that at any given spacing, flume and wind tunnel data follow an identical trend and the data together indicate a linear relationship between $1/\sqrt{C_D}$ and $\log_{10} D/h$ at all values of L/h. This identity of behaviour may be supposed to prove the validity of the premises stated earlier in justification of a combined analysis of flume and wind tunnel data. It may also be observed that for a given value of L/h, flume data at different slopes tend to fall on a single line showing that within this range of slopes, the water surface slope has no effect on the relationship.

The relationship between $1/\sqrt{C_D}$ and D/h can be written in the general form ;

$$1/\sqrt{C_D} = C_1 \log_{10} D/h + C_2 \qquad .....(6.10)$$

where C_1 and C_2 are functions of L/h.

From Fig.6.9, the values of C_1 and C_2 at various values of L/h were computed on the basis of the mean lines drawn through the plotted points. The variation of C_1 and C_2 with L/h is shown in Figs. 6.10 and 6.11 ; it can be seen that C_1 decreases with increase in L/h, whereas C_2 increases with increase in L/h. Use of Figs. 6.10 and 6.11 along with Eqs. 6.8, 6.9 and 6.10 would enable solution of the problem of resistance of roughness elements of the type used in this study. The extension of the approach to larger spacings than those used in the present study, where the skin friction of the plane boundary may become important, needs further research.

The only other set of data (apart from those collected during this study) on two-dimensional strips of negligible thickness are those of Basha (6). In analysing his data, Basha found that the resistance coefficient is significantly affected by variations in the water surface slope, though the variation was not consistent at all spacings. Nevertheless, it is seen from Fig. 6.12 that the lines predicted by using Fig. 6.10 and 6.11 and Eq. 6.10 represent the average lines for Basha's data, though the scatter of points is quite large. Experiments over a wider range of slopes than that covered in the present study need to be carried out to ascertain whether the water surface slope has a significant effect on the resistance coefficient or not, for this type of roughness element.

6.5 Comparison with Conventional Equation :

The conventional analysis of data on artificial roughness elements has been based invariably on some form of the equation ;

$$\bar{V}/V_* = 2.30/K \log_{10} D/h + B_1 \quad \text{.....(6.11)}$$

while B_1 is a constant dependent on the type and arrangement of the roughness elements, the value of K has been found to vary from 0.38 to 0.40 in a majority of cases. Expressing 2.30/K as A_1, Eq. 6.11 can be modified to ;

$$\bar{V}/V_* = A_1 \log_{10} D/h + B_1 \quad \text{.....(6.12)}$$

But Eq. 6.9 can be written as

$$\bar{V}/V_* = \sqrt{\frac{2}{h/L}} \sqrt{1/C_D} \quad \text{.....(6.13)}$$

Combining Eqs. 6.12 and 6.13 ;

$$1/\sqrt{C_D} = A_1 \sqrt{\frac{h/L}{2}} \log_{10} D/h + B_1 \sqrt{\frac{h/L}{2}} \quad \text{.....(6.14)}$$

Comparing this with Eq. 6.10,

$$C_1 = A_1 \sqrt{\frac{h/L}{2}} \quad \text{.....(6.15)}$$

Figure 6.13 shows a plot of L/h vs C_1 computed from Fig. 6.9. Assuming a constant value of A_1 as done by most investigators, one can draw a line of slope -1/2 relating C_1 and L/h on Fig. 6.13. The value of A_1 equal to 6.06, as given by Sayre and Albertson (37) has been used in drawing such a straight line on Fig. 6.13. The data indicate close agreement with the above line at L/h values greater than 5. At L/h values less than 5, the plotted data indicate C_1 values higher than those predicted by the linear relationship. It is felt that the reason for this difference lies in the shift of

datum that would be required at smaller values of L/h. It should be noticed that a shift in the datum upward would mean smaller computed values of $\Delta\overline{V}/V_*$ (difference in $\overline{V}/V_*$ values at two values of D/h) thus leading to smaller computed values of C_1. Apparently, Eq. 6.12 with a constant value of A_1 can be used with the flume bottom as datum at L/h values higher than 5; at L/h values below 5, a correction for the datum would be required . However, in using Eq. 6.10, one need not apply corrections for shift in the datum as it is implicit in the values of C_1 and C_2.

6.6 Variation of u/V_* with $\log_{10} y$:

For a given value of D/h and L/h, it is seen that $1/\sqrt{C_D}$ is constant; in other words $\overline{V}/V_*$ is constant. Thus in the conventional equation for resistance

$$\overline{V}/V_* = \frac{2.30}{K} \log_{10} D/K_s + \text{constant} \qquad .....(6.16)$$

K_s, the equivalent sandgrain roughness would be a constant for given values of D, h and L. An effort was thus made to study the variation of u/V_* with $\log_{10} y$ on the basis of the following equation ;

$$u/V_* = \frac{2.30}{K} \log_{10} y/K_s + \text{constant} \qquad .....(6.17)$$

One would expect that for any two runs with the same values of D , h and L, a unique relation would be obtained between u/V_* and $\log_{10} y$. A set of two runs with L equal 10 cm and h equal to 4 cm. - one from the wind tunnel and one from the flume - with approximately the same values of D was chosen and the velocity distribution data plotted in the form u/V_* vs $\log_{10} y$ on Fig. 6.14. For this purpose, in the wind tunnel data

V_* was computed from the known values of C_D, while for the flume data V_* equals $\sqrt{gR_b S}$. It is seen from Fig. 6.14 that there is an appreciable difference between the trend of the wind tunnel and the flume data. Though a large number of profiles were not available to make any general conclusions, it appears that the length after which C_D for the element remains constant is not adequate to achieve a representative velocity distribution. It is also possible that the parameter C_D is not so sensitive as the velocity distribution to the variations of flow pattern which may exist in the initial length. However, lack of certainty regarding the accuracy of velocities measured with Prandtl tube in strongly curved flows and the absence of velocity data in the region of reverse flows make it difficult to conduct a more thorough analysis of this aspect of the problem, at present.

-:o:-

CHAPTER - VII

ANALYSIS OF DATA - III

COMBINATION OF ELEMENTS OF DIFFERENT HEIGHTS

7.1 Preliminary Remarks :

In this Chapter, the experimental results on the resistance of elements in the case when elements of different height are placed together on the floor are analysed. The results on the resistance of a small roughness element kept down stream of a large one are analysed first; the combined effect of two roughness series on the total resistance is studied later.

7.2 Small Roughness Element Placed Downstream of a Large One (Both on the Floor):

The data on the resistance of a small roughness element placed in the wake of a large one were collected with the intention of providing information for the estimation of wind forces on smaller structures in the wake of large ones. As already described, a 4 cm high strip was placed at the section where δ is equal to 1.12 cm and the position of the 2 cm strip downstream of the former was varied; for each position of the smaller element, the drag force was measured on both the elements. The variation of drag coefficient (average of the values at different velocities) of both the elements with change in position of the smaller element is shown in Fig. 7.1. The diagram has not been prepared in dimensionless form since only one set of heights of elements was used. Further, the results

should be treated as purely qualitative as the values of C_D are not corrected for the blockage effect. Nevertheless, the following features may be noticed by a study of Fig. 7.1.

a) The drag coefficient of the 4 cm element is unaffected by its proximity to the smaller one and its value is approximately the same as that for a 4 cm element kept at the same section (δ equal to 1.12 cm) with the small element removed.

b) Within a distance of approximately 11 times the height of the large element, the drag coefficient of the 2 cm element is either negative or zero; the maximum negative value occurs at a distance of approximately 7.5 times the height of the large element.

c) Beyond a distance of 11 times the height of the large element, C_D for the small element is positive and Fig. 7.1 shows an increase in C_D with increase in distance between the two elements; but the increase in C_D occurs at a decreasing rate and a tendency for C_D to reach a maximum value at a distance of roughly 50 times the height of the large element is noticed. With further increase in the distance between the two elements, one may expect C_D of the smaller element to decrease, because of the increasing thickness of the redeveloping boundary layer downstream of the large element. However, data were not collected in this range, because of the limitation of the available length of test section of the tunnel.

7.3 Combination of Roughness Series :

Studies concerning the resistance of a roughness pattern in which one series of roughness elements is combined with a second series were performed with the object of providing some basic information concerning the sheltering effect in a bed with various sizes of roughness elements. The experiments were performed in the open-circuit wind tunnel as well as in the flume and the analyses of the data are presented below:

Wind Tunnel Studies : Experiments on this aspect of the study were conducted in the open-circuit tunnel. A series of 4 cm elements was placed at 80 cm spacing to form the 'primary series'; 2 cm elements were fixed at a certain distance L_1 downstream of each of the 4 cm elements to form the 'secondary series'. Different values of L_1 were used and the drag coefficients measured on the third element in the primary as well as the secondary series in most cases and these were assumed to be representative values. The secondary series was also formed by using another set of 4 cm elements . In this case also L_1 was varied and C_D found in the same way as for the former.

Figures 7.2 a and 7.2b show the variation of C_D of elements in the primary and secondary series, with L_1, for both sets of runs described earlier. The values of C_D (average of values at different velocities) are uncorrected for blockage effect and since the height of elements was not varied by a sufficient range, the curves have been plotted in dimensional form; further the total number of elements in the tunnel may not

be adequate to obtain a constant value of C_D along the length for each series; as such, the results are qualitative. In Fig. 7.2b, the maximum value of L_1 upto which the pressures were actually measured. was 40 cm ; obviously, beyond L_1 equal to 40 cm., the curves would be a mirror image of the curves upto L_1 equal to 40 cm..

It is seen from Fig. 7.2 that an element of the secondary series, if placed within 6h to 7h from an element of height 'h' in the primary series, experiences a negative drag force. Beyond this distance, the element in the secondary series has a positive drag coefficient. As contrasted to the case of only two elements placed on a boundary where the drag coefficient of the large element remained approximately constant, C_D of the element in the primary series is significantly affected by changes in L_1. This is understandable since, with elements in series, the flow conditions both upstream and downstream of the element in the primary series are affected by changes in L_1.

Flume Experiments :- The total resistance due to the combination of two roughness series was measured in the flume for the various patterns listed in Table 4.1 , of Chapter IV. The data are analysed in such a way that the change in resistance of the primary series due to the introduction of the secondary series is reflected. In other words, the 'effective' C_D of an element in the primary series is calculated from Eq. 6.9 from the measured values of $\overline{V}$, S and D when the two roughness series are kept on the bed. This amounts to ascribing the total resistance only to the elements in the primary series. Since the actual resistance of the primary series alone is known from

Figs. 6.10 and 6.11 and Eq. 6.10, the change in resistance due to the introduction of the secondary series may be calculated easily.

For the purpose of computing the change in resistance the following procedure was adopted. The computed values of $1/\sqrt{C_D}$ (where C_D is the 'effective ' drag coefficient of the element in the primary series) and $\log_{10} D/h$ were plotted and a straight line yielding the same value of C_1 as that for the primary series alone (obtained from Fig. 6.10) was fitted through the plotted points. The value of C_2 was then found from these lines. The change in the value of C_2 from that for the primary series alone reflects the effect of introduction of the secondary series.

Figures 7.3a to 7.3 i show plots of $1/\sqrt{C_D}$ versus $\log_{10} D/h$ for the different patterns tested . It is seen that the line fitted by assigning the same value of C_1 as for the primary series alone represents the average line for the plotted points in almost all cases, thus justifying the choice of C_1.

On the above figures are also plotted the values of the 'Effective' drag coefficient for the tunnel data computed from the easily derivable relation.

$$C_D \, h/L \, \rho \, V^2/2 = C_{D_p} \, h/L \, \rho \, V^2/2 + NC_{D_s} \, \rho \, V^2/2 \, h'/L \quad \ldots.(7.1)$$

where h' = Height of element in the secondary series

C_{D_p} = Drag coefficient of an element in the primary series

C_{D_s} = Drag coefficient of an element in the secondary series.

N = Number of elements in the secondary series in a length L.

In calculating C_D , consideration was also given to the sign of the drag coefficients C_{D_s} and C_{D_p} . It is seen that in all cases , the tunnel data so computed fall well below the lines drawn on Fig. 7.3. The fact that the values of C_{D_p} and C_{D_s} found in the tunnel may not be truly representative of elements in a series of large number of elements, could be one possible reason for the difference in the trend of the flume and tunnel data on Fig. 7.3; however, no complete explanation can be offered with the limited data available.

For the purpose of computing the value of C_2 in Eq.6.10 the lines drawn on Fig. 7.3 were used despite the departure of the tunnel data from this line. The above values of C_2 are plotted against L_1 for both sets - namely primary series with L/h equal to 20 and L/h equal to 40 - on Figs. 7.4a and 7.4b . In the case of the primary series with L/h equal to 40, it is seen that the introduction of the secondary series leads to an increase in resistance for all the values of L_1 tried; however, it remains to be seen whether the above behaviour is true when the secondary element is kept very close to the primary element. In the case of the primary series with L/h equal to 20, it can be seen from Fig. 7.4 b that introduction of the secondary series causes a decrease in resistance in all cases except when the secondary element is exactly midway between the primary elements.

-:o:-

CHAPTER - VIII

CONCLUSIONS

Additional data on the form resistance of two-dimensional roughness elements of negligible thickness have been made available as a result of this study. The various aspects of the problem studied include the effects of the boundary layer and the proximity of boundaries on the drag coefficient of a single roughness element. In case of roughness elements in series, the effects of variation of relative roughness height and relative spacing on the resistance coefficient were studied. Some experimental results concerning the resistance variations due to introduction of a small roughness element downstream of a large one have also been reported. The main conclusions, as a result of the analysis of experimental data, are as follows :-

1) The drag coefficient C_D of an inclined plate (provided with a symmetrical tailplate) held in uniform flow increases with increase in h/D. This increase in C_D can be attributed primarily to the decrease in the dimensionless pressure on the downstream face with increase in h/D. The equation

$$C_{D_o} / C_D = (1 - h/D)^{2.85}$$

can be used to find the drag coefficient C_{D_o} of a plate kept on a boundary but in an infinite stream.

2) The correction for blockage suggested by Maskell (14) for two-dimensional normal plates without a tailplate, with $\epsilon = 0.96$ is inapplicable in the case of an element

with a tailplate. However, the adoption of a value of ϵ equal to 1.755, based on the studies of Arie and Rouse (4), yields a blockage correction which is suited for the case of a normal plate provided with a tail plate.

3) The drag coefficient C_{D_o} of a single normal plate in a boundary layer decreases continually with increase in δ/h as shown in Fig. 5.8. Use of this figure along with the equation $C_{D_o}/C_D = (1-h/D)^{2.85}$ enables the estimation of the drag coefficient of an element in a boundary layer, but in a finite stream. Application of this procedure to the case of a roughness element on the bed of an open channel, however, indicates quantitative differences between the observed and predicted C_D values.

4) The drag coefficient with respect to the velocity at the crest level of a single element in the boundary layer (but in an infinite stream) C'_D is found to be approximately constant at high values of δ/h; at lower values of δ/h, C'_D is a function of δ/h as shown in Fig. 5.9.

5) The application of the method suggested by Morris (17) to estimate the resistance of a series of elements of the type used in this study reveals that the method is not reliable over a wide range of relative spacings. In general, for the isolated-roughness flow at L/h less than 10, the method overpredicts the resistance and it underpredicts the resistance at L/h greater than 10;

for the wake-interference flow, however, the agreement is fair.

6) For roughness elements in series, the drag coefficient of all elements in the series, beyond an initial length of 50 times the height of the element, is approximately constant.

7) The total resistance of a plane boundary with roughness elements having L/h ranging from 2.5 to 40.0 and at low Froude numbers may be estimated on the assumption that the total resistance is equal to the form resistance of the roughness elements. The empirical equation ;

$$1/\sqrt{C_D} = C_1 \log_{10} D/h + C_2$$

based on flume and tunnel data, enables determination of the total resistance of the bed; Figs. 6.10 and 6.11 show the variation of C_1 and C_2 with L/h.

8) A comparison of the above equation with the conventional resistance equation ;

$$\bar{V}/V_* = 6.06 \log_{10} D/h + \text{constant},$$

indicates that the datum may be set at the flume bottom for L/h ranging from 5 to 40 and above for this type of roughness elements; at L/h less than 5, the datum needs to be set at a higher level in using the conventional equation.

9) The drag coefficient of a small element (2 cm. high) kept downstream of a 4 cm high element is negative

when it is kept within about 11 times the height of the large element. Beyond this distance, C_D of the small element is positive and increases with increase in distance from the large element and appears to reach a maximum value when kept at approximately 50 h away from the large element. The drag coefficient of the large element, however, is unaffected by the proximity of the small element.

10) With 4 cm elements kept at a spacing of 80 cm., introduction of a smaller element of 2 cm height at any fixed point downstream of the large element leads to a decrease in resistance in most cases. However, with 4 cm elements at a spacing of 160 cm, introduction of the smaller element causes an increase in resistance in most cases.

-:o:-

REFERENCES

1. Abbott. D.E. and S.J.Kline 'Experimental Investigation of Subsonic Turbulent Flow over Single and Double Backward Facing Steps'. Jnl.of Basic Engg., Trans. A.S.M.E. Vol.84, Sept., 1962, pp. 317-325.
2. Adachi, S. 'On the Artificial Strip Roughness'. Bulletin No. 69, Disaster Prevention Research Institute, Kyoto University, March 1964.
3. Adachi, S. 'Experimental Study on the Artificial Spot Roughness' (In Japanese) Report of the Disaster Prevention Research Institute, Kyoto University, 1962.
4. Arie M. and H. Rouse, 'Experiments on Two-dimensional Flow over a Normal Wall', Jnl of Fluid Mechanics, Vol.I, Part 2, July 1956, pp. 129-141.
5. Baines, W.D. and E.G.Peterson, 'An Investigation of flow through Screens' Trans. ASME, Vol.73, 1951, pp.467-480.
6. Basha M.A., 'Resistance Characteristics of Artificially Roughened Open Channels in Relation to those of Alluvial Channels'. M.E. Dissertation, University of Roorkee, May, 1961.
7. Chow, V.T., 'Open Channel Hydraulics', McGraw Hill Book Company, Inc., 1959, pp. 110-113, p. 24, p. 10.
8. Einstein H.A., 'Formulas for Bed-Load Transportation', Trans. A.S.C.E. Vol. 107, 1942, pp. 561-597.
9. Einstein H.A. and R.B. Banks, 'Fluid Resistance of Composite Roughness', Trans. A.G.U., Vol. 31, No. 4, Aug.,1950 pp. 603-610.

10. Garde, R.J., K.G. Ranga Raju and P.N. Modi, 'Drag Coefficients of Inclined Plates Fixed at the Boundary- An Experimental Investigation', International Symposium on High-Velocity Flows, Indian Institute of Science, Bangalore, Jan., 1967.

11. Herbich J.B. and S. Shulits 'Large -Scale Roughness in Open-Channel Flow', Proc. A.S.C.E., Jnl, of Hyd. Div., Nov., 1964, pp. 203-230.

12. Johnson J.W., 'Rectangular Artificial Roughness in Open Channels'., Trans. A.G.U. Vol. 25, Part VI, 1944, pp. 906-914.

13. Koloseus, H.J., 'The Effect of Free-Surface Instability on Channel Resistance' Ph.D.Dissertation, State University of Iowa, Aug., 1958.

14. Maskell, E.C., 'A Theory for the Blockage Effects on Bluff Bodies and Stalled Wings in a Closed Wind Tunnel ' R.and M. No. 3400, A.R.C., Nov., 1963.

15. Meyer-Peter and Mueller , 'Formulas for Bed-Load Transport' 2nd Meeting of.I.A.H.R., Stockholm, Sweden, 1948, pp.39-64.

16. Modi, P.N. 'Study of Two-Dimensional Flow Past a Plate Set at an Inclination in Contact with a Plane Boundary' M.E. Dissertation, University of Roorkee, 1965.

17. Morris, H.M., 'Flow in Rough Conduits ' Trans. A.S.C.E., Vol. 120, 1955, pp. 373-410.

18. Morris H.M., 'Applied Hydraulics in Engineering' Ronald Press Company, New York, 1963.

19. Morris, H.M. (Personal Communication to the Author), 1966.

20. Mueller, T.J., H.H.Korst and W.L. Chow 'On the Separation, Re-Attachement and Redevelopment of Incompressible Turbulent Shear Flow' Jnl. ofBasic Engg,, Trans. A.S.M.E., Vol.86 June 1964, pp. 221-226.

21. Nagabhushanaiah, H.S., 'Separation Flow Downstream of a Plate Set Normal to a Plane Boundary' Ph.D., Dissertation, Colorado State University, Fort Collins, 1962.

22. Nash, J.F., V.G.Quincey and J.Callinan, 'Experiments on Two Dimensional Base Flow at Subsonic and Transonic Speeds' National Physical Lab., A.R.C., 25070, F.M.3356, Perf. 2226, P.A. 955.

23. O'Loughlin E.M., Discussion of'Critical Analysis of Open Channel Resistance' Proc. A.S.C.E., Jnl of HydlDiv. March, 1966, pp. 393-395.

24. O'Loughlin, E.M. and E.G. Macdonald,'Some Roughness Concentration Effects on Boundary Resistance' La Houille Blanche, No. 7/1964, pp. 773-784.

25. Pankhurst R.C., and D.W.Holder ,'Wind Tunnel Technique' Sir Issac Pitman and Sons, London, 1948, pp.327-349.

26. Plate E.J., 'The Drag on a Smooth Flat Plate With a Fence immersed in its Turbulent Boundary Layer' Presented at the Fluids Engg. Conference, Philadelphia, A.S.M.E., May, 1964.

27. Pope, A. ' Wind Tunnel Testing',John Wiley and Sons, 1954, p. 291.

28. Powell, R.W., 'Flow in a Channel of Definite Roughness' Trans. A.S.C.E., Vol. 111, 1946, pp. 531-566.

29. Prandtl, L. and O.G. Tietjens,'Applied Hydro and Aero-mechanics' Dover Publications, Inc., New York, 1957, p. 103.

30. Ranga Raju, K.G., 'Pressure Distribution on Triangular Elements', M.E. Dissertation, University of Roorkee, 1963.

31. Robinson, A.R., and M.L. Albertson, 'Artificial Roughness Standard for Open Channels', Trans. A.G.U., Vol.33,No.6, Dec., 1952, pp. 881-888.

32. Roshko, A., 'On the Wake and Drag of Bluff Bodies', Jnl. of Aero Sciences, Feb., 1955.

33. Rouse, H., 'Energy Transformation in Zones of Separation' I.A.H.R., Ninth Convention, Sept.,1961, pp.1291-1302.

34. Rouse, H., H.J.Koloseus and J.Davidian,'The Role of the Froude number in Open-Channel Resistance', Jnl. of Hydraulic Research, I.A.H.R., Vol.1, 1963, pp.14-19.

35. Rouse, H., 'Critical Analysis of Open Channel Resistance' Proc. A.S.C.E., Jnl. of Hyd. Div., July 1965, pp. 1-25.

36. Rouse, H., 'Fluid Mechanics for Hydraulic Engineers', Dover Publications, Inc., New York, 1961, p. 217, p.228.

37. Sayre W.W., and M.L.Albertson, 'Roughness Spacing in Rigid Open Channels', Trans. A.S.C.E., Vol. 128, 1963,pp.343-427.

38. Schlichting, H., 'Boundary Layer Theory' Pergamon Press Ltd., 1955, p. 396, p.425,p.423-424,p.397,p.15.

39. Tsubaki, T., 'On the Sediment Transportation with Sand Ripples', (In Japanese), Proc. J.S.C.E., Aug., 1955.

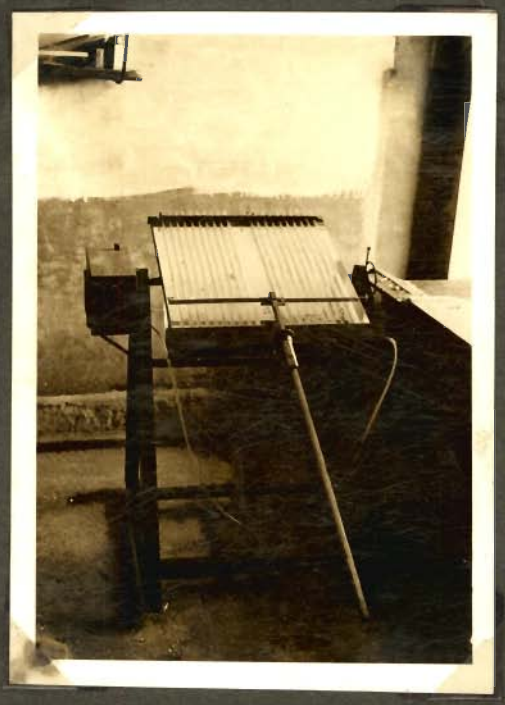

PHOTOGRAPH 1

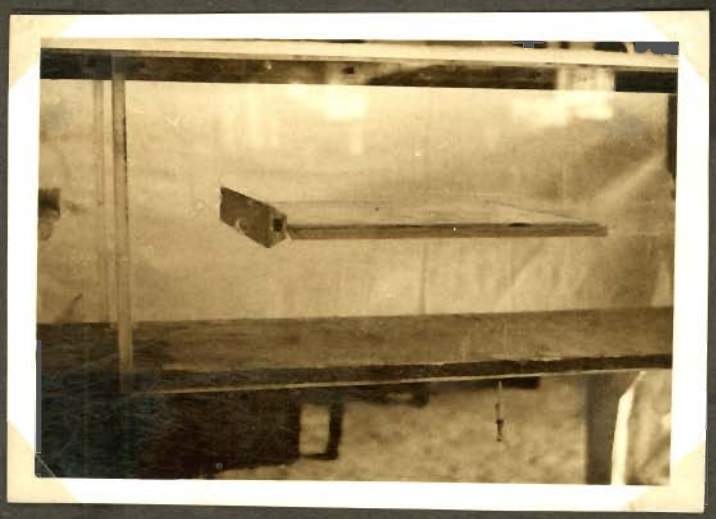

PHOTOGRAPH 2

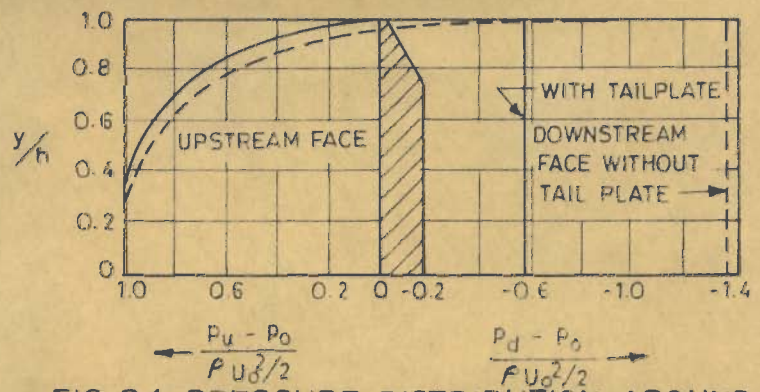

FIG. 2.1_PRESSURE DISTRIBUTION AROUND ELEMENTS IN MIDSTREAM (REF.4)

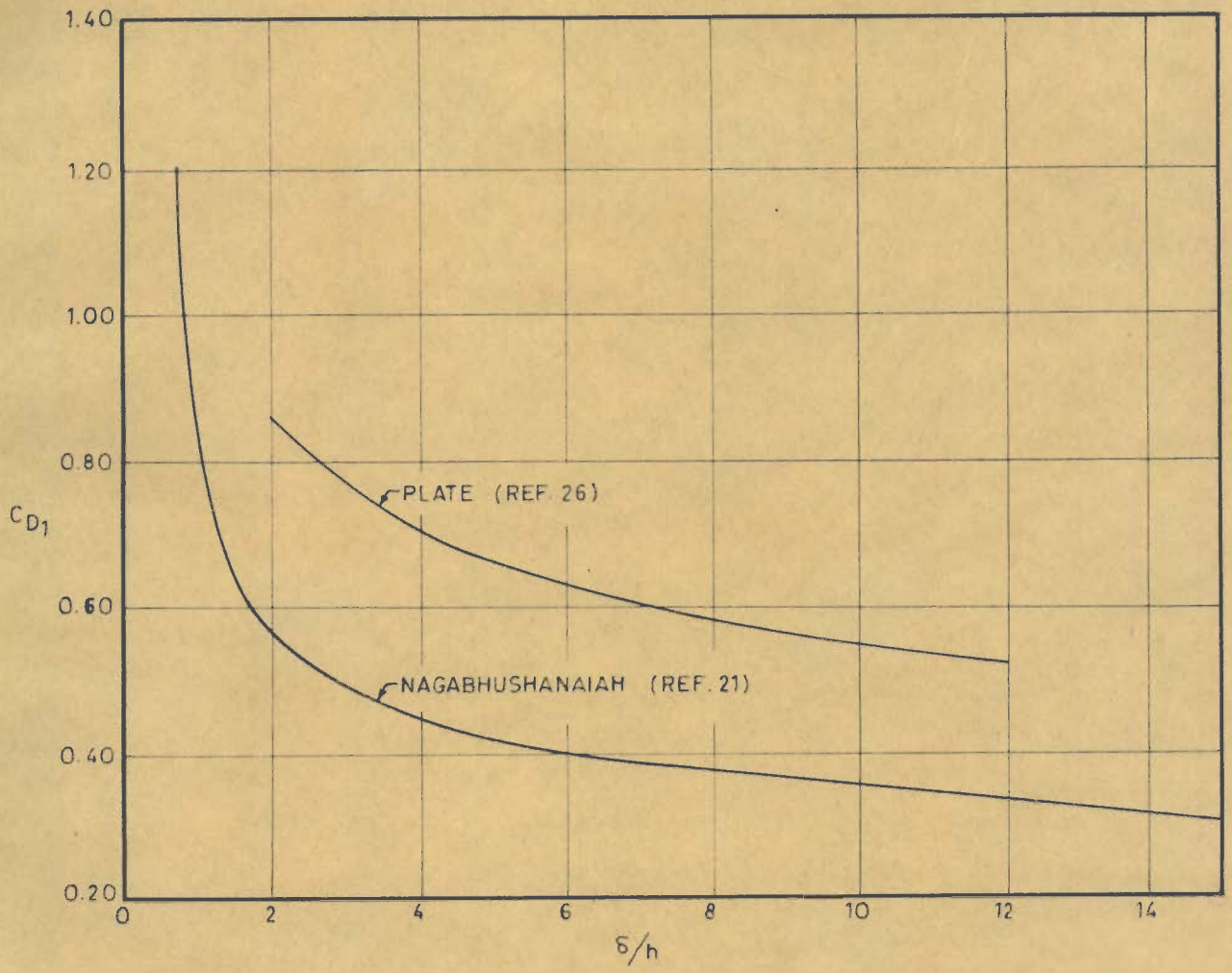

FIG. 2.2_VARIATION OF C_{D_1} WITH δ/h FOR NORMAL PLATES

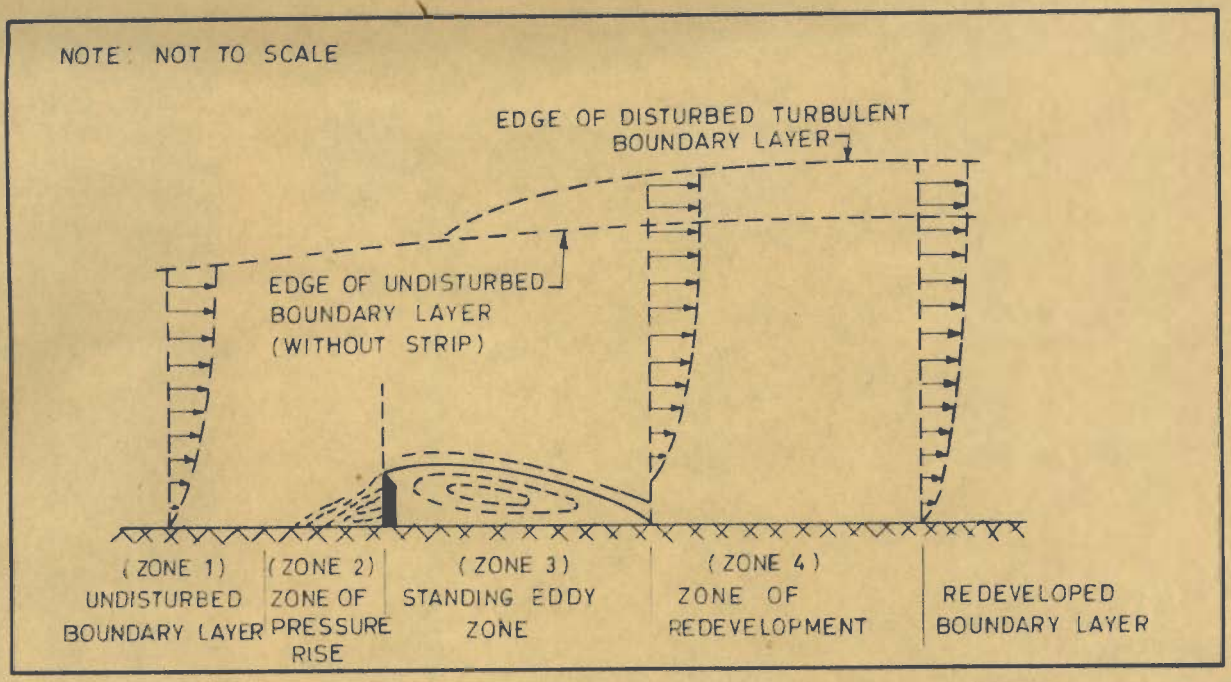

FIG.2.3_DIFFERENT ZONES OF FLOW FOR THE CASE OF A NORMAL PLATE IN A TURBULENT BOUNDARY LAYER (REF. 26)

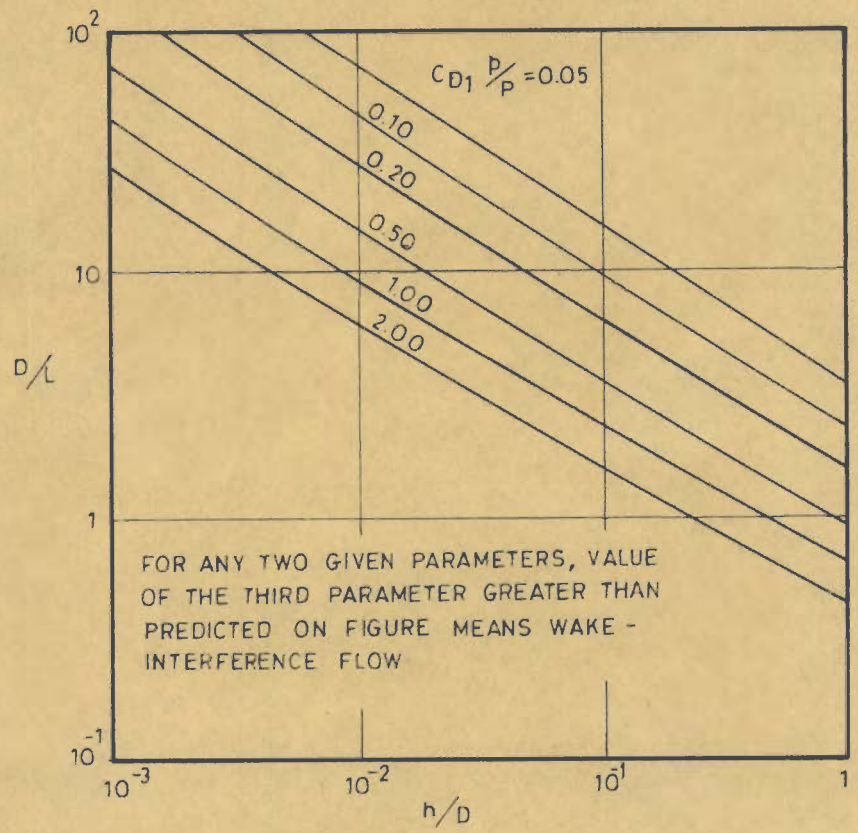

FIG.2.4_CRITERION FOR PREDICTION OF TYPE OF FLOW PROPOSED BY MORRIS (REF. 17)

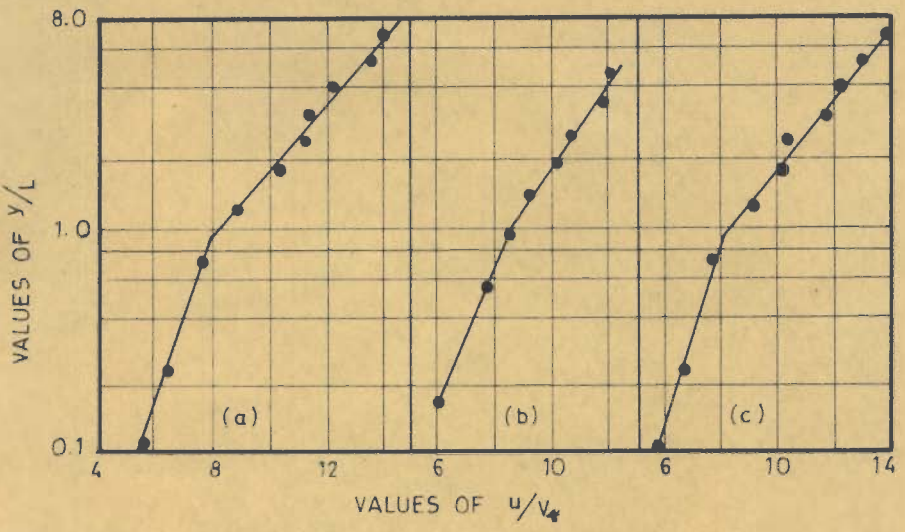

FIG. 2.5_TYPICAL VELOCITY PROFILES IN CORRUGATED METAL PIPES (REF. 17)

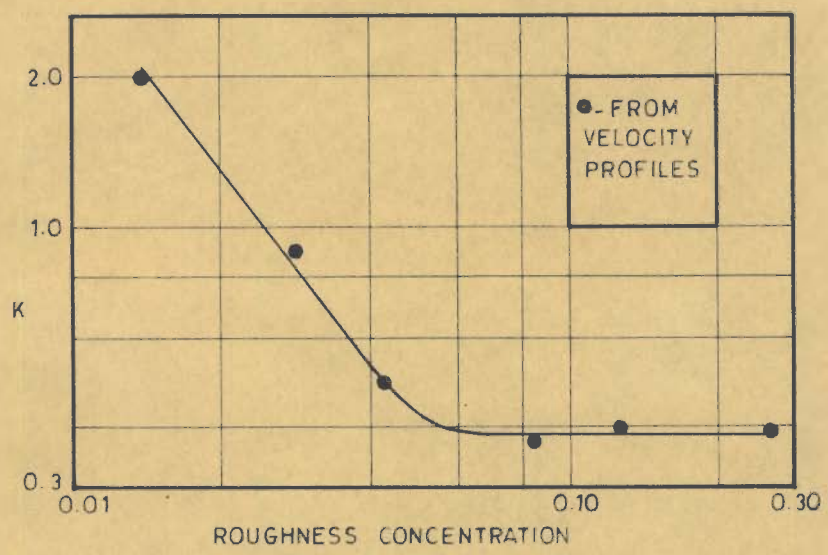

FIG. 2.6_VARIATION OF K WITH ROUGHNESS CONCENTRATION FOR STRIP ROUGHNESSES (REF. 37)

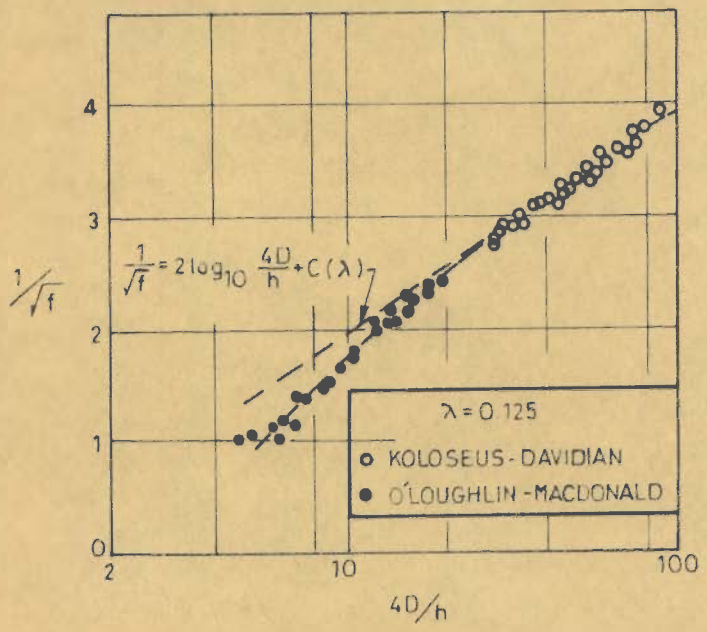

FIG. 2.7 RELATION BETWEEN $1/\sqrt{f}$ AND $4D/h$ AT SMALL VALUES OF D/h - CUBICAL ROUGHNESSES (REF. 24)

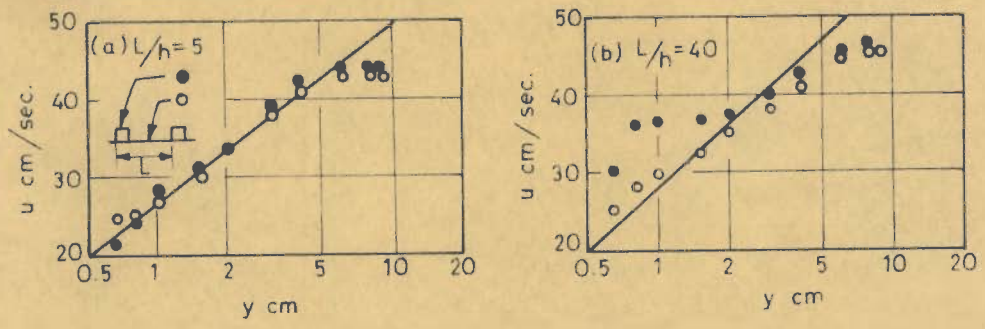

FIG. 2.8 - TYPICAL VELOCITY PROFILES WITH STRIP ROUGHNESSES (REF. 2)

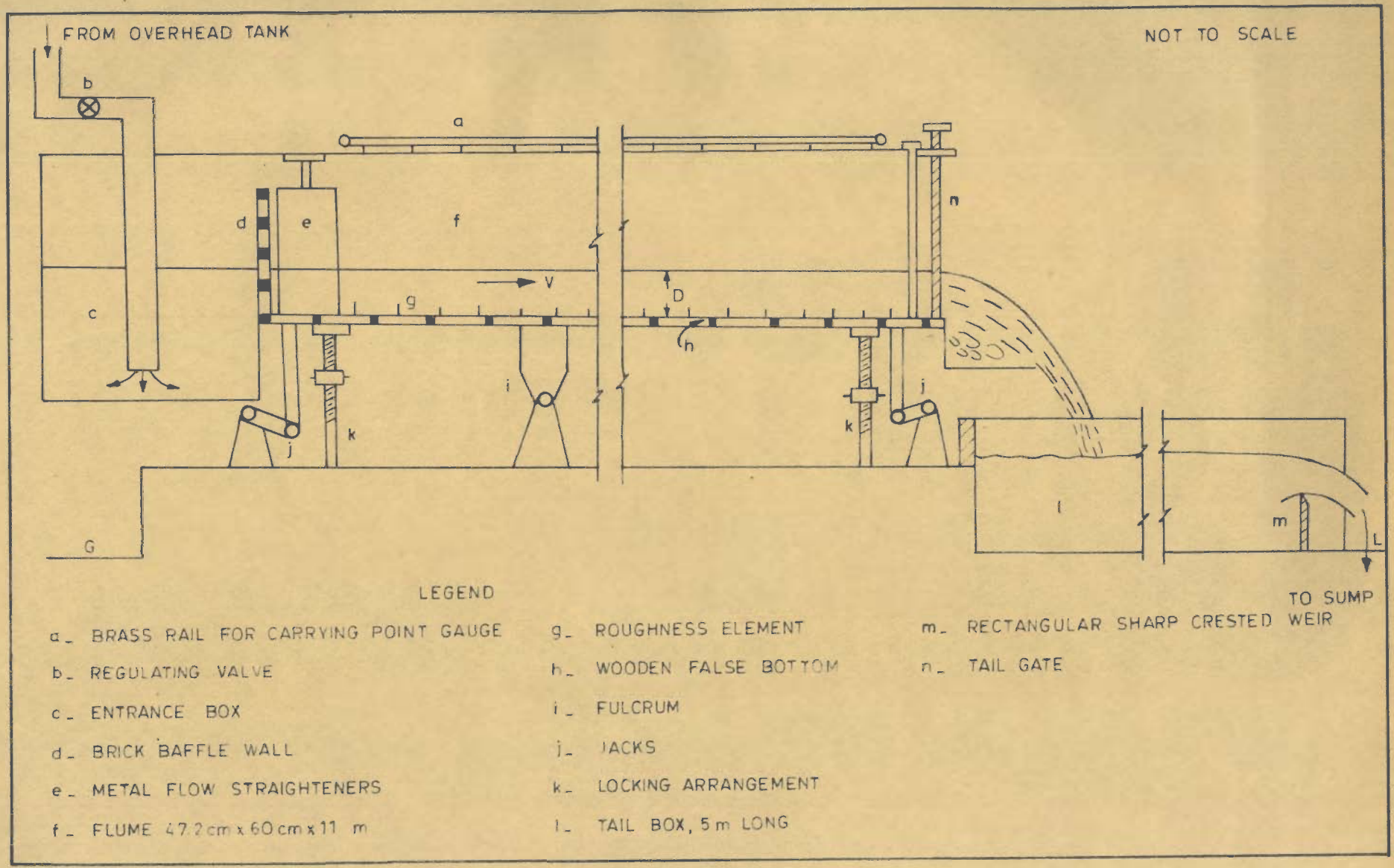

FIG. 4.1_ SCHEMATIC DIAGRAM OF THE FLUME

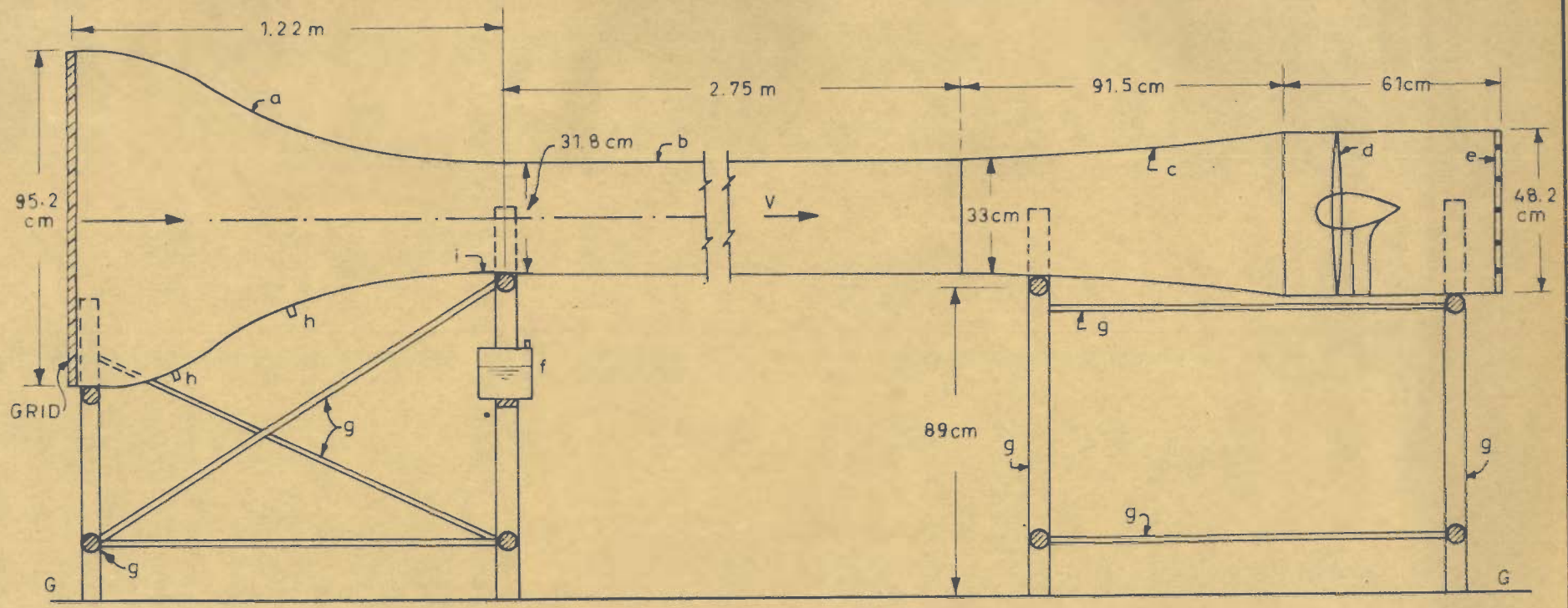

FIG.4.2_SCHEMATIC DIAGRAM OF OPEN-CIRCUIT WIND TUNNEL

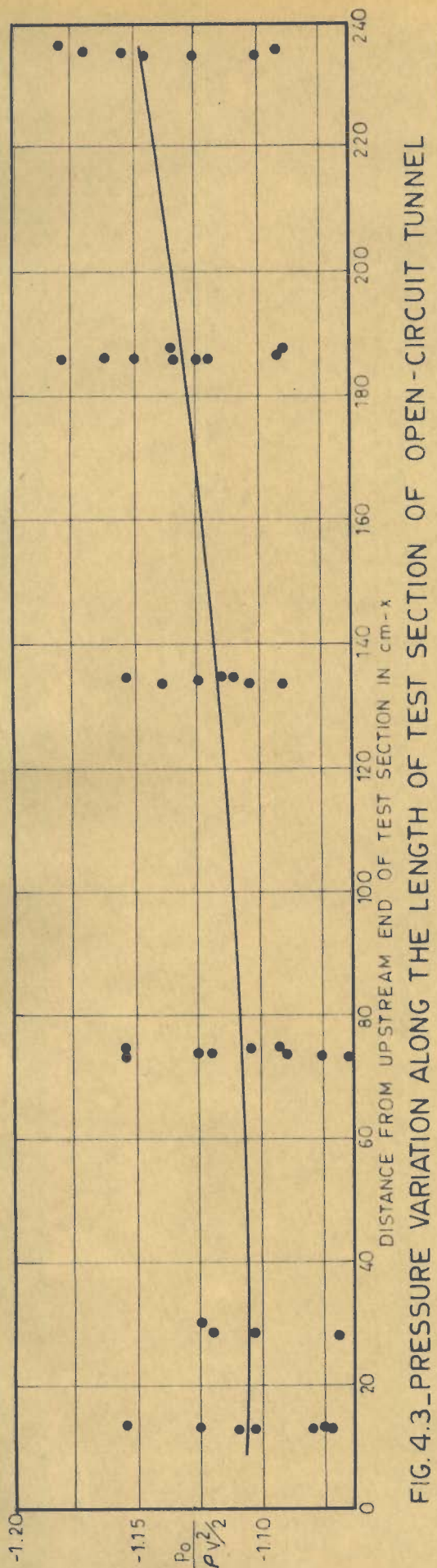

FIG. 4.3_PRESSURE VARIATION ALONG THE LENGTH OF TEST SECTION OF OPEN-CIRCUIT TUNNEL

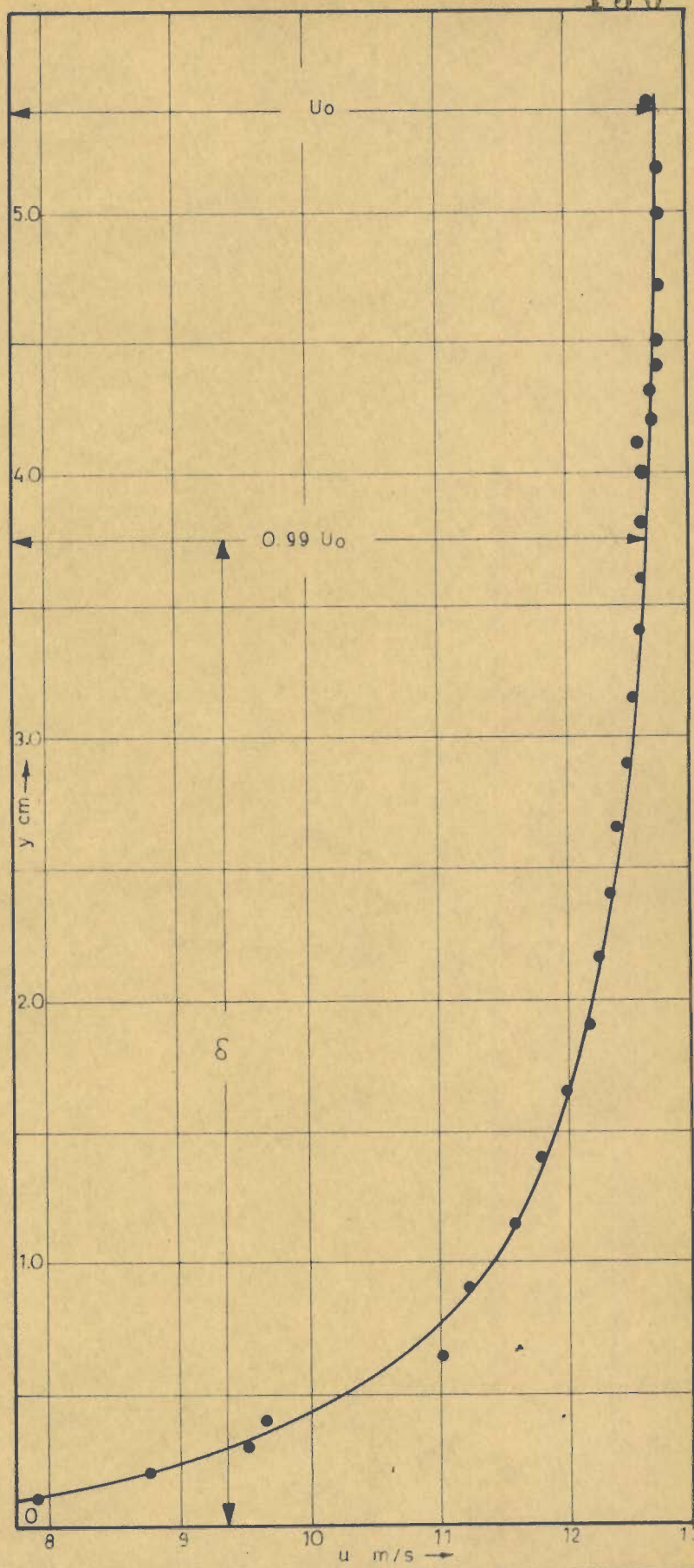

FIG. 4.4_TYPICAL VELOCITY PROFILE IN BOUNDARY LAYER OF OPEN-CIRCUIT TUNNEL

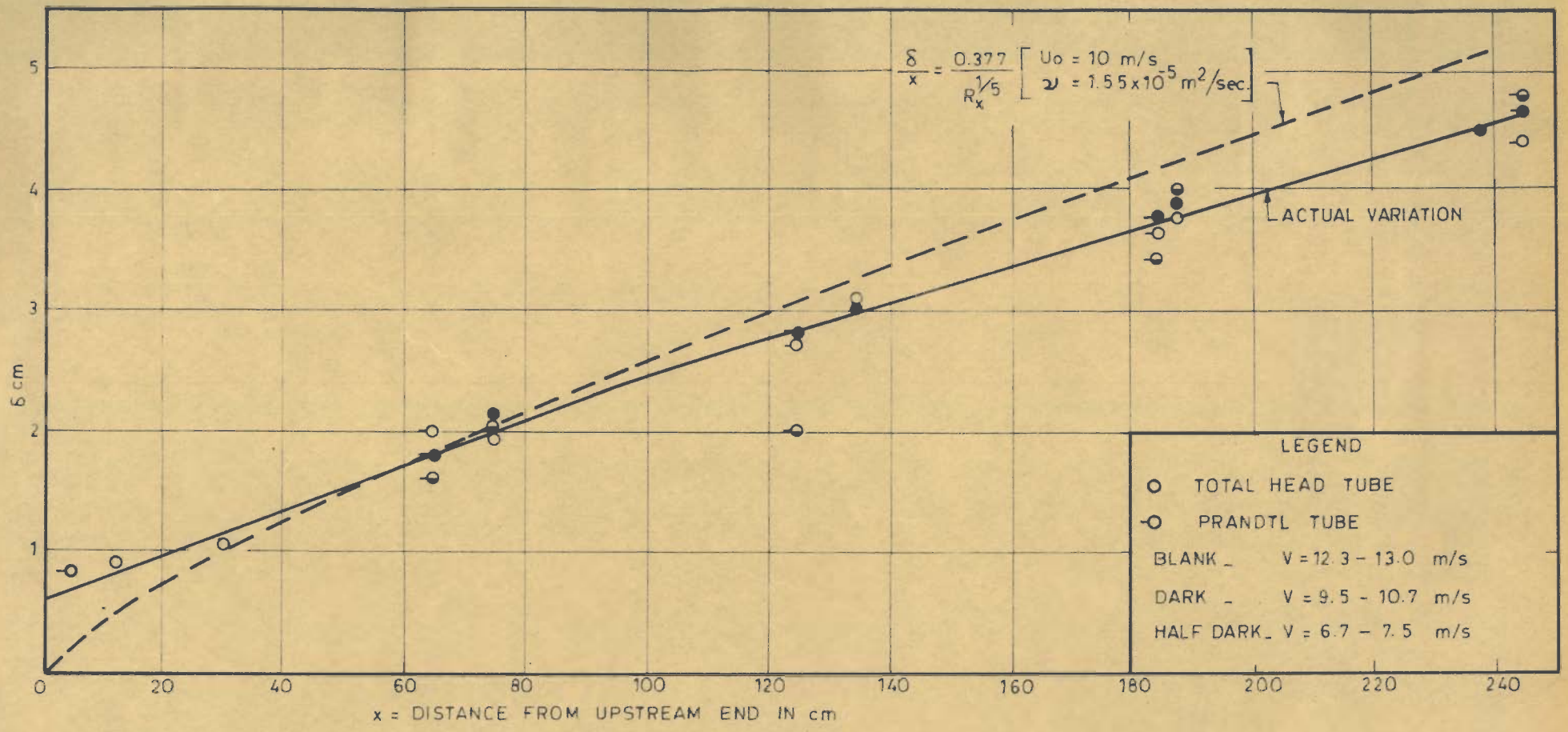

FIG. 4.5_VARIATION OF δ ALONG LENGTH OF TEST SECTION OF OPEN-CIRCUIT TUNNEL

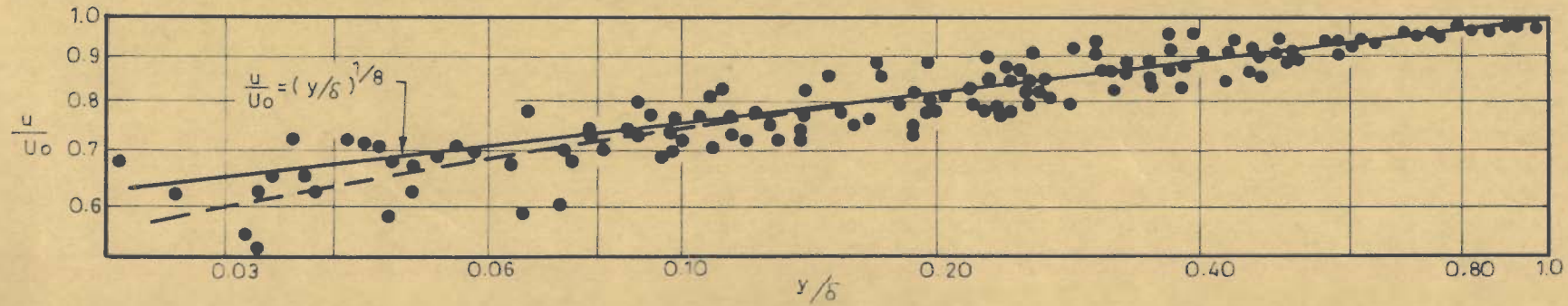

FIG. 4.6_VELOCITY DISTRIBUTION IN BOUNDARY LAYER IN OPEN-CIRCUIT TUNNEL

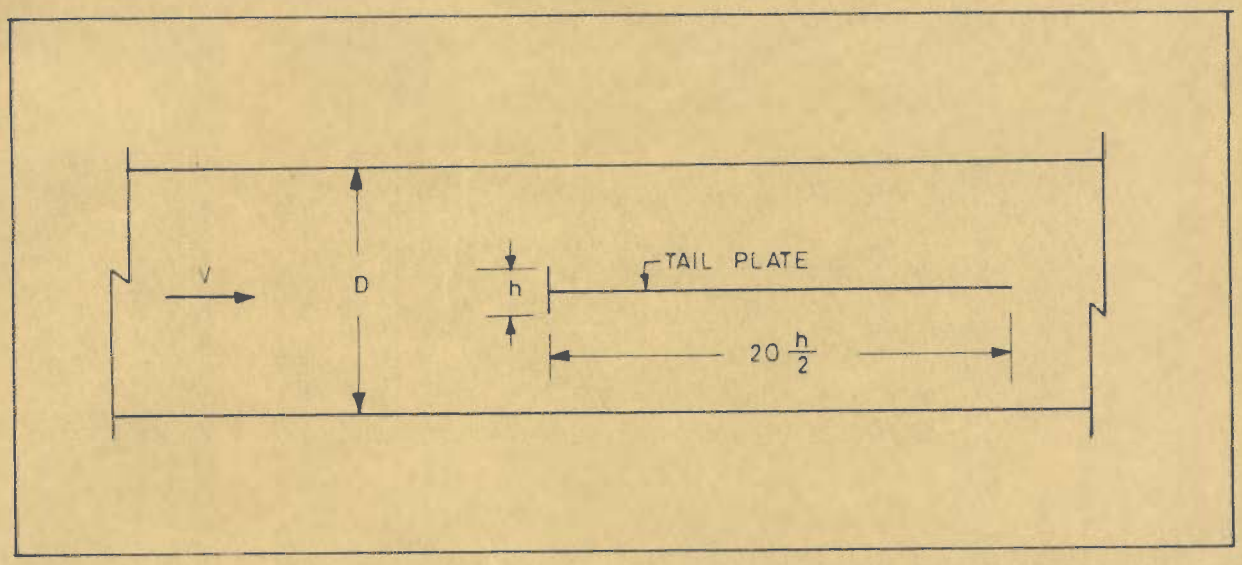

FIG 4.7 DIAGRAM SHOWING PLACEMENT OF ELEMENT IN MIDSTREAM

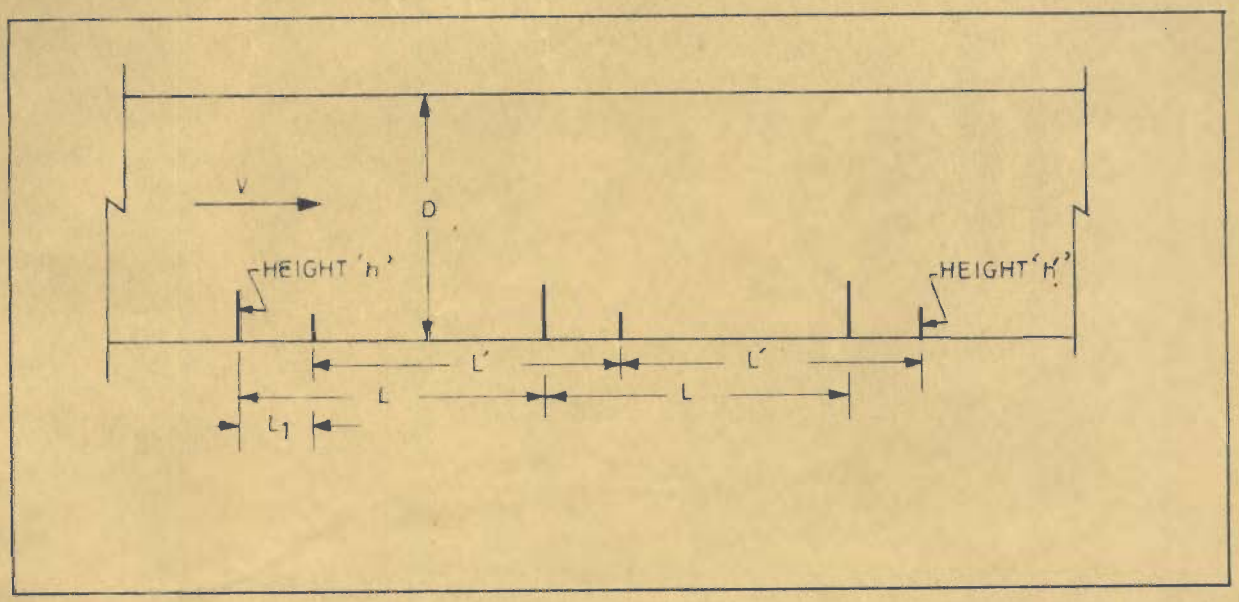

FIG 4.8 DIAGRAM SHOWING COMBINATION OF TWO ROUGHNESS SERIES

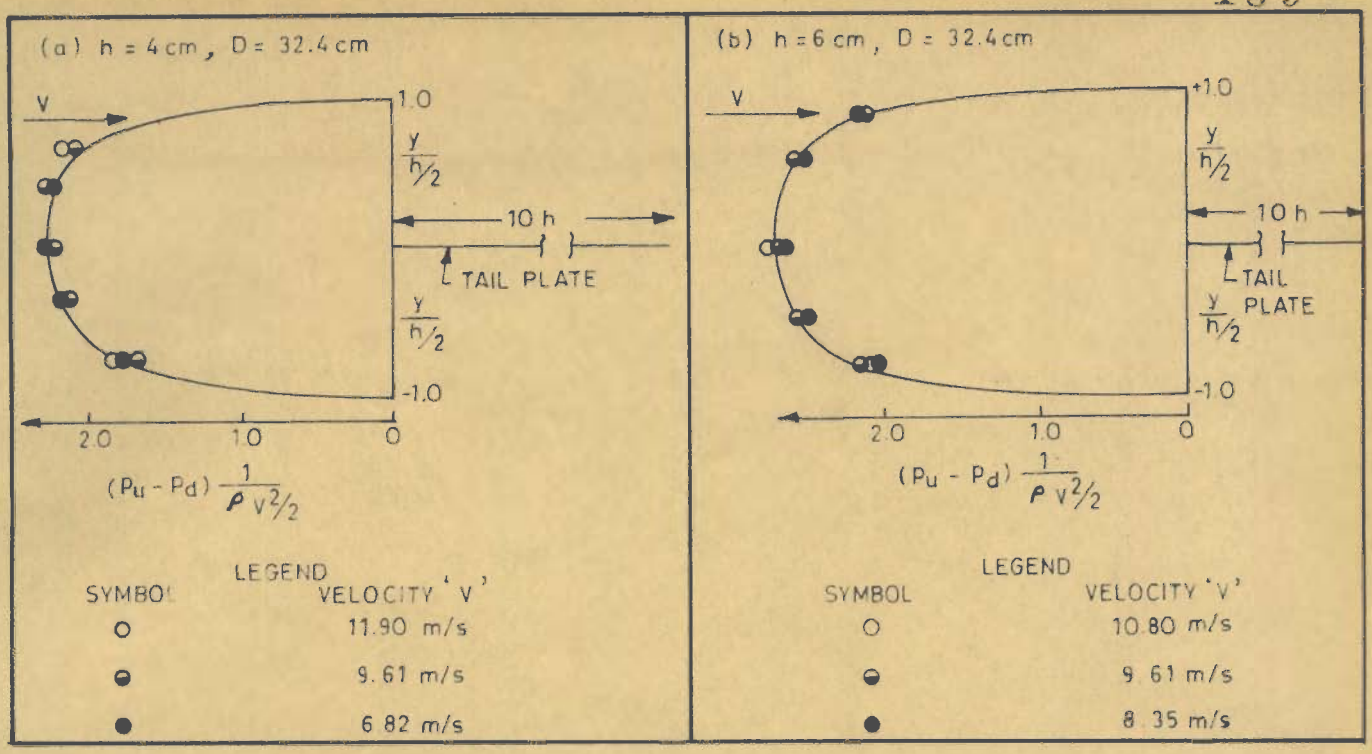

FIG. 5.1_PRESSURE DISTRIBUTION AROUND ELEMENTS IN UNIFORM FLOW

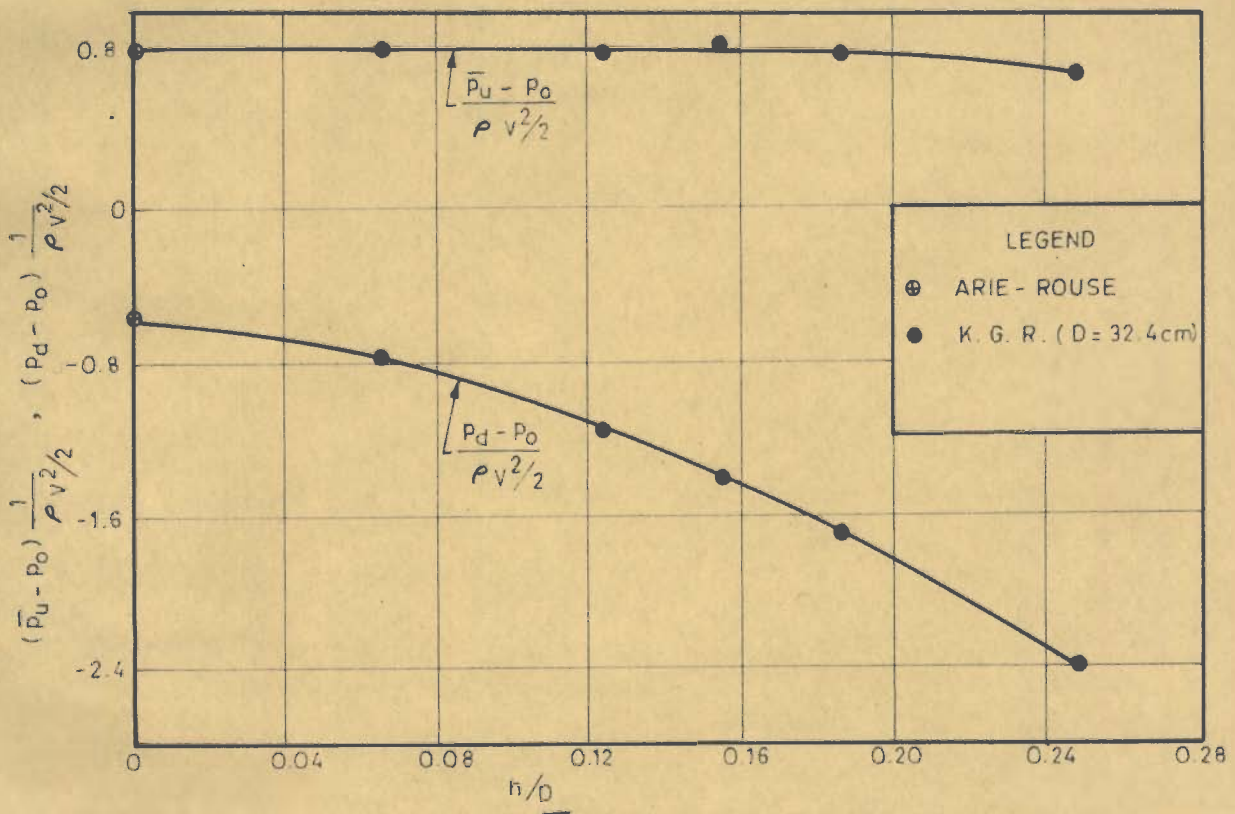

FIG. 5.2_VARIATION OF $\frac{(\bar{P}_u - P_o)}{\rho V^2/2}$ AND $\frac{(P_d - P_o)}{\rho V^2/2}$ WITH h/D FOR ELEMENTS IN UNIFORM FLOW

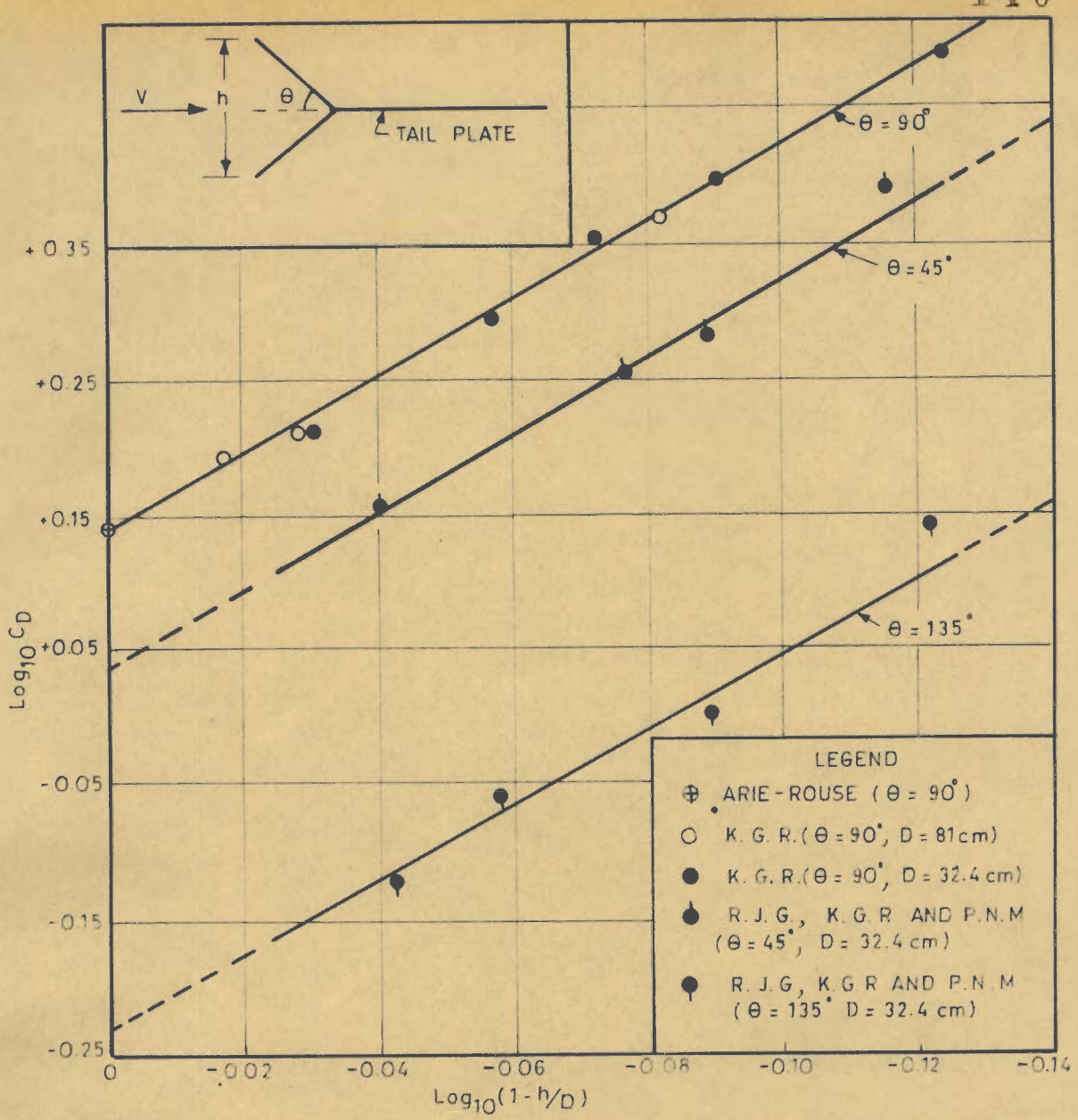

FIG.5.3_VARIATION OF C_D WITH $(1-h/D)$ FOR ELEMENTS IN UNIFORM FLOW

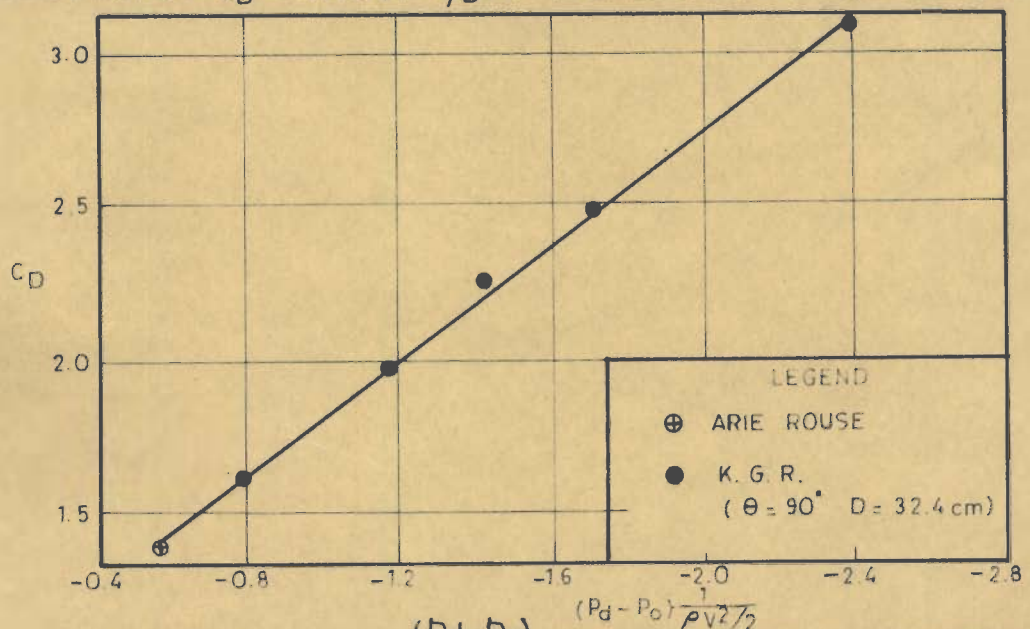

FIG.5.4_VARIATION OF C_D WITH $\frac{(P_d - P_o)}{\rho V^2/2}$ FOR ELEMENTS IN UNIFORM FLOW

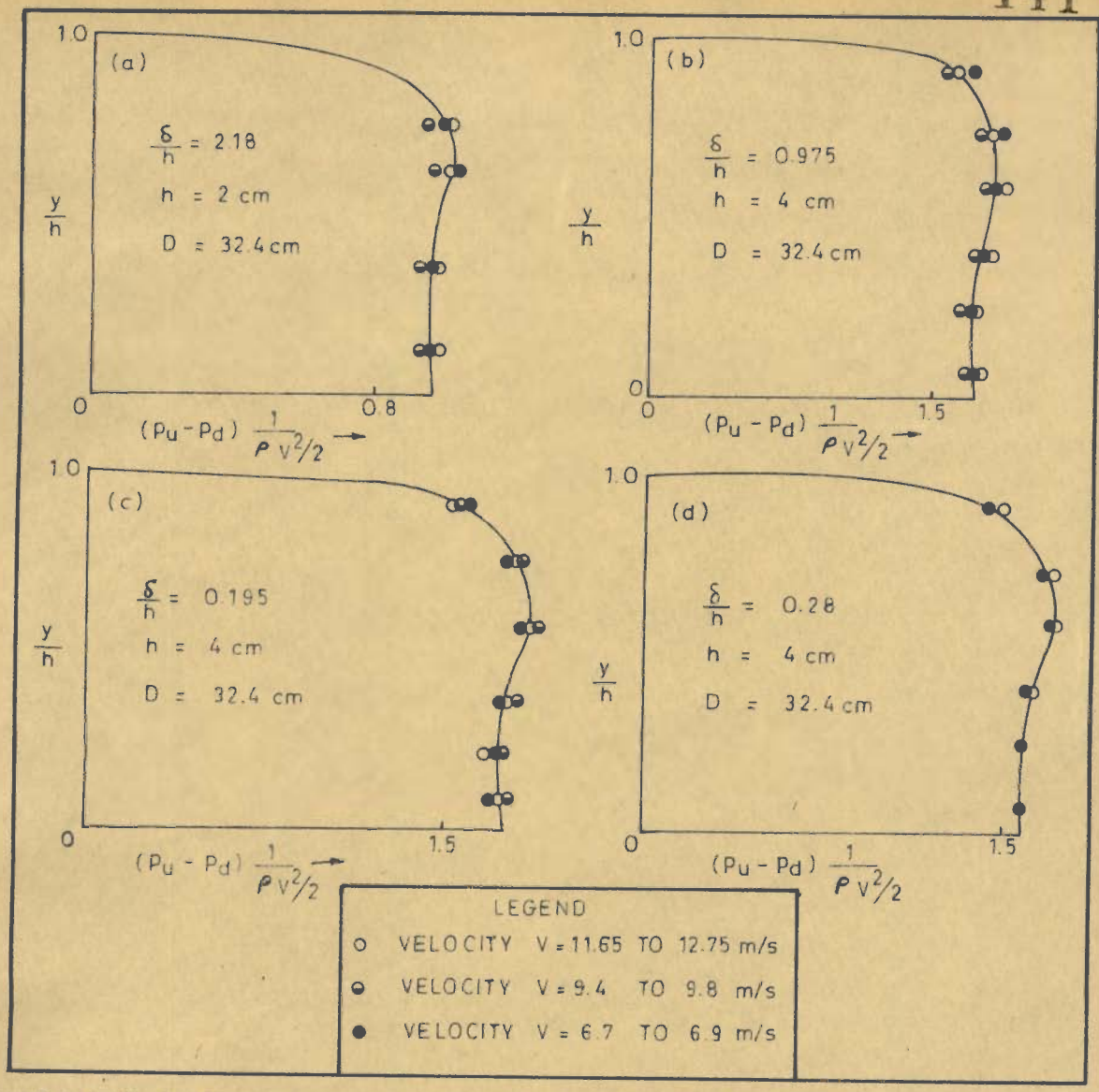

FIG.5.5_PRESSURE DISTRIBUTION AROUND ELEMENTS IN BOUNDARY LAYER

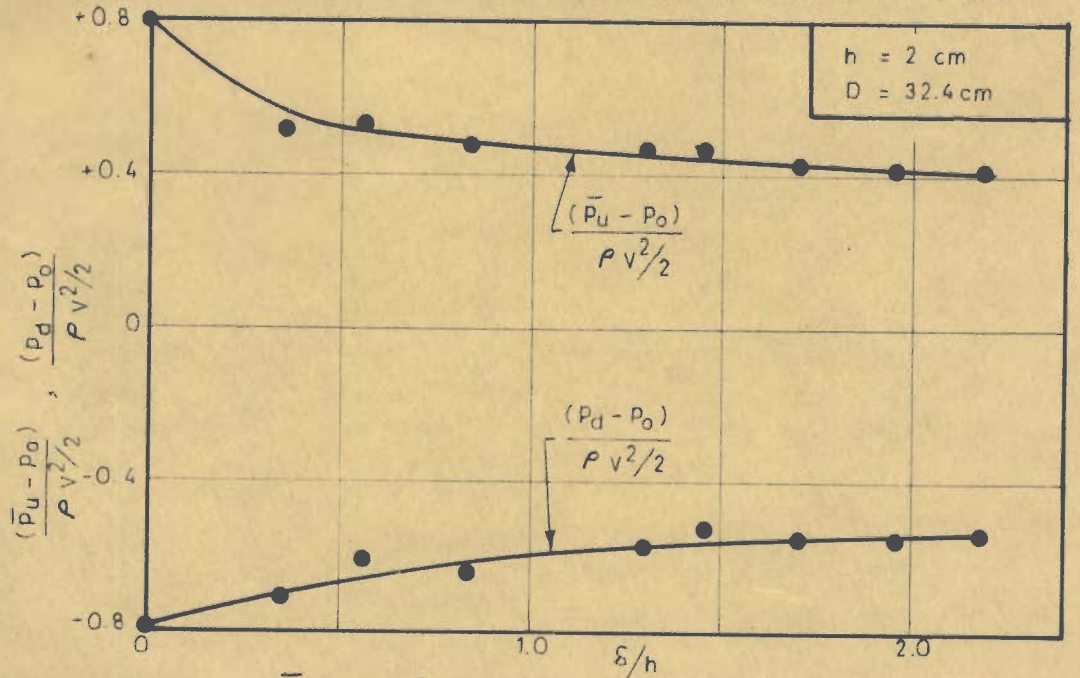

FIG.5.6_VARIATION OF $(\bar{P}u-Po)\frac{1}{\rho V^2/2}$ AND $(Pd-Po)\frac{1}{\rho V^2/2}$ WITH δ/h

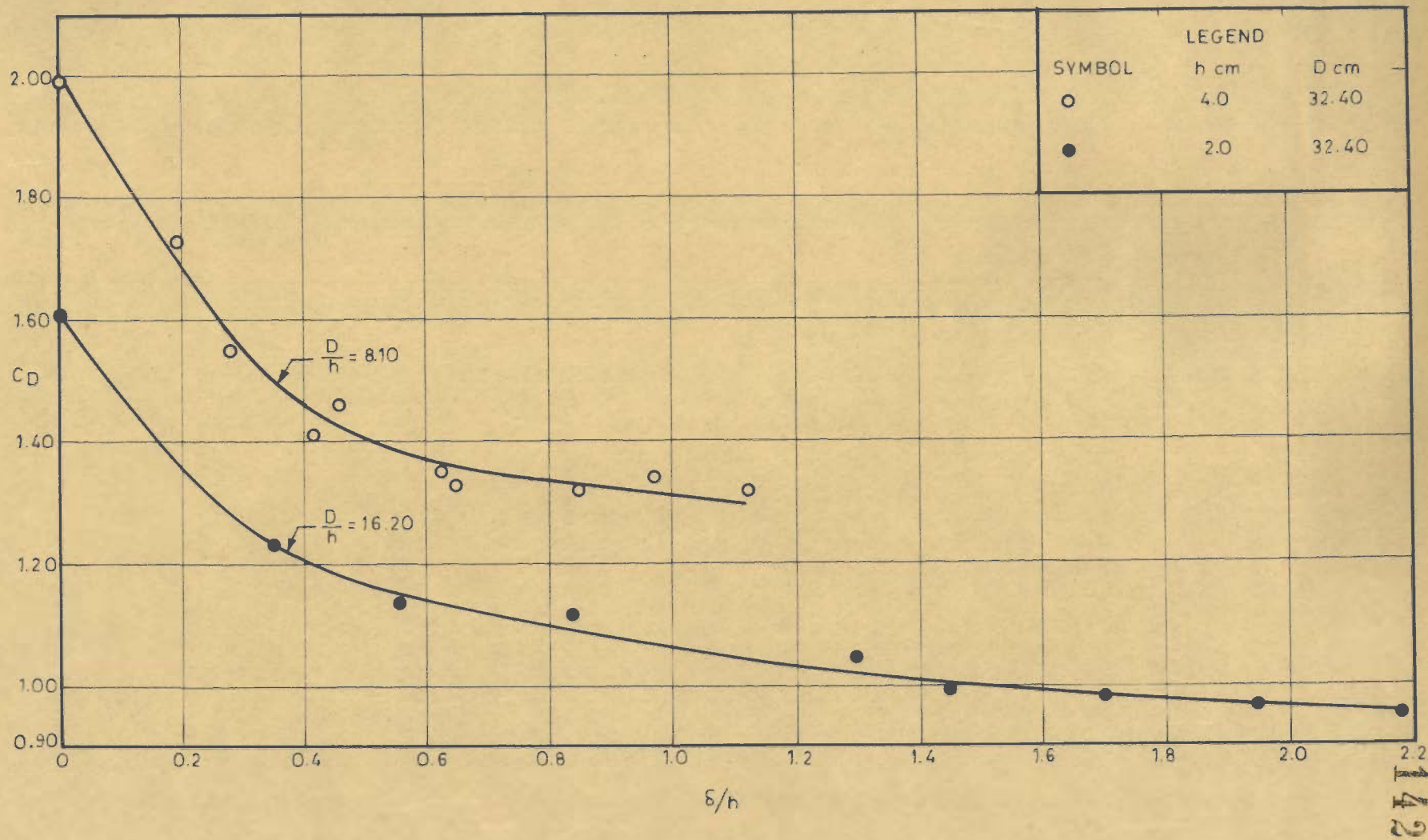

FIG.5.7. VARIATION OF C_D WITH D/h AND δ/h FOR ELEMENT IN BOUNDARY LAYER

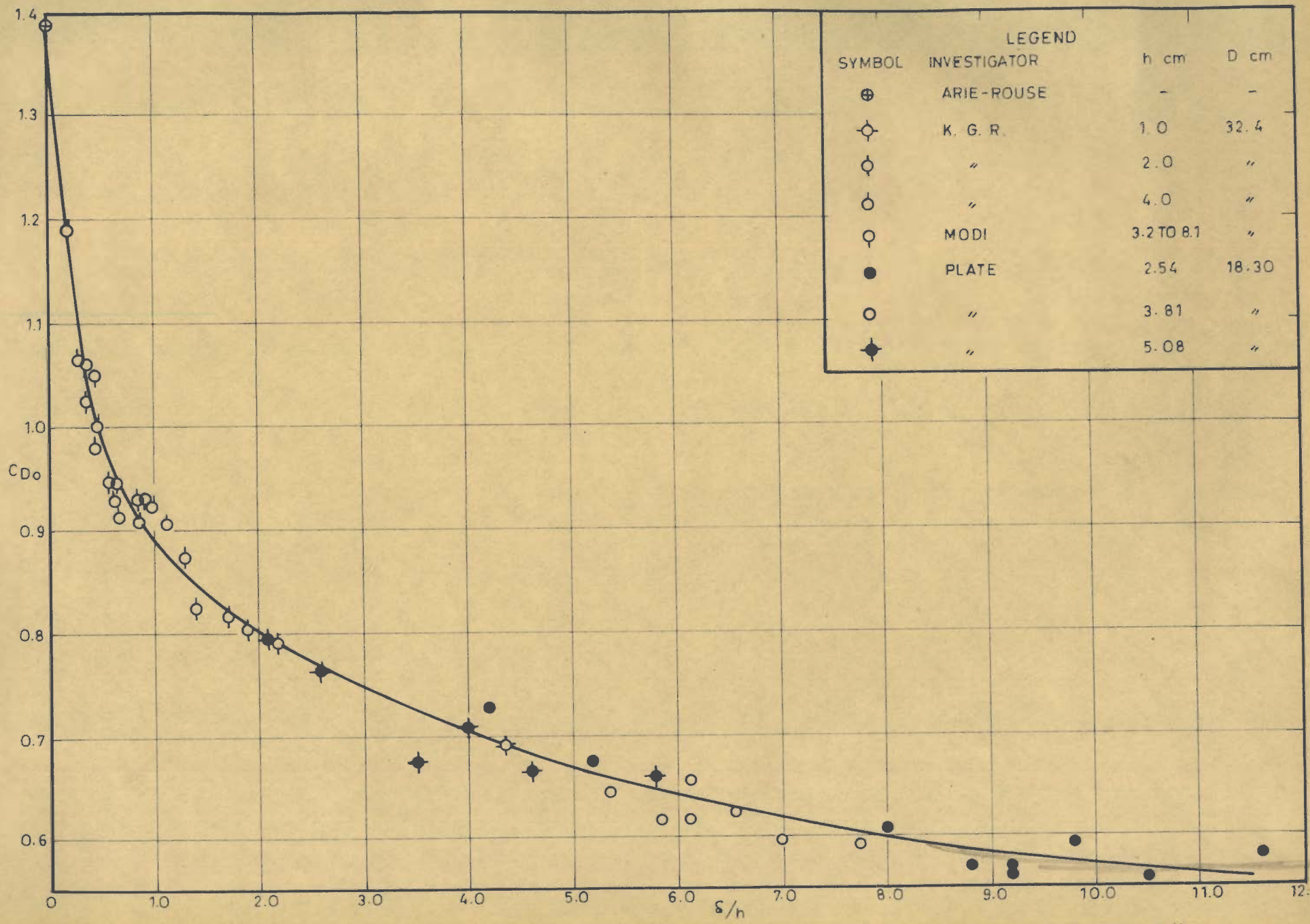

FIG. 5.8_VARIATION OF C_{D0} (DRAG COEFFICIENT CORRECTED FOR BLOCKAGE) WITH δ/h

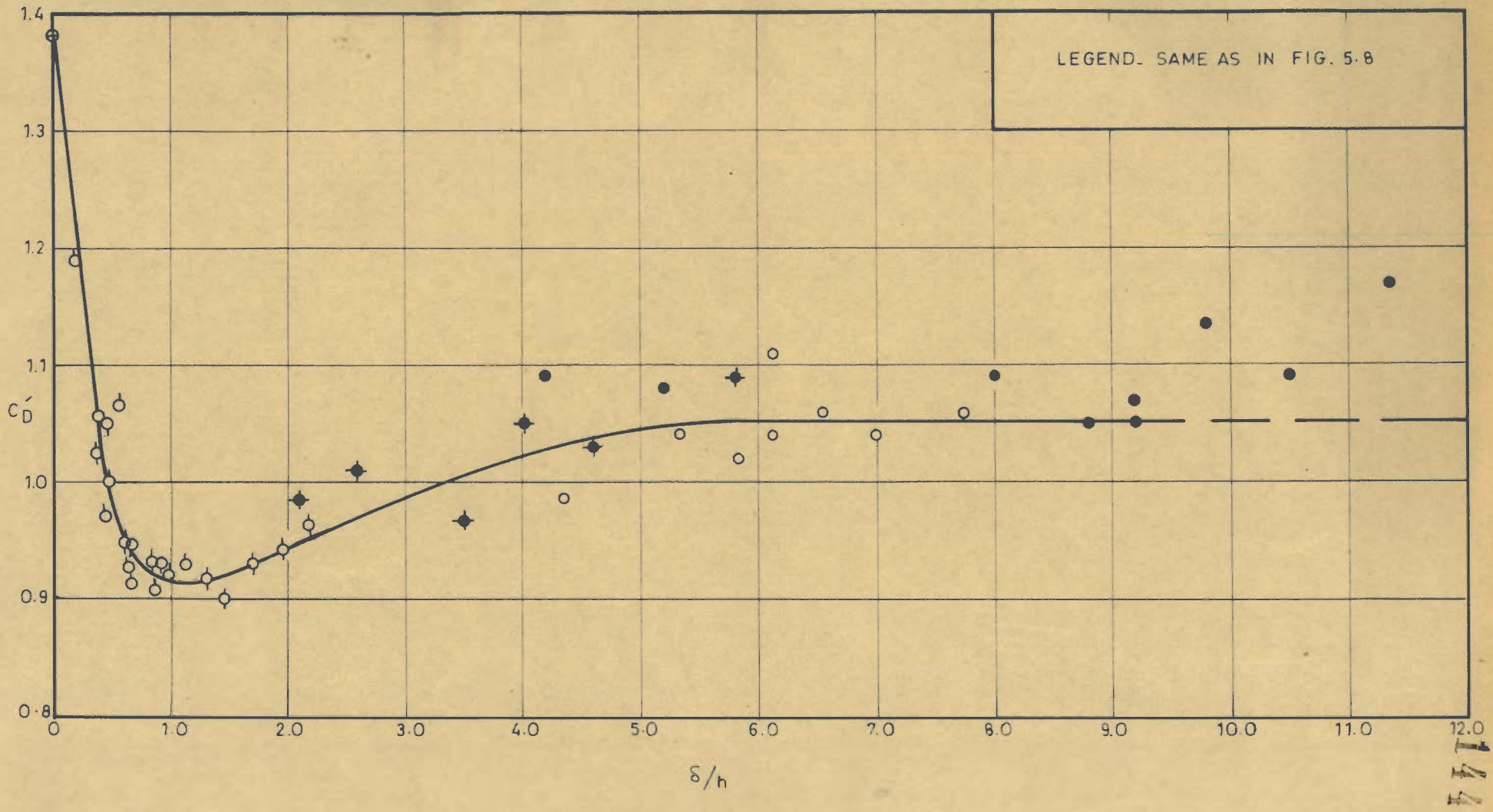

FIG.5.9-VARIATION OF C_D' (DRAG COEFFICIENT W.R.T. VELOCITY AT CREST LEVEL, IN INFINITE STREAM) WITH δ/h

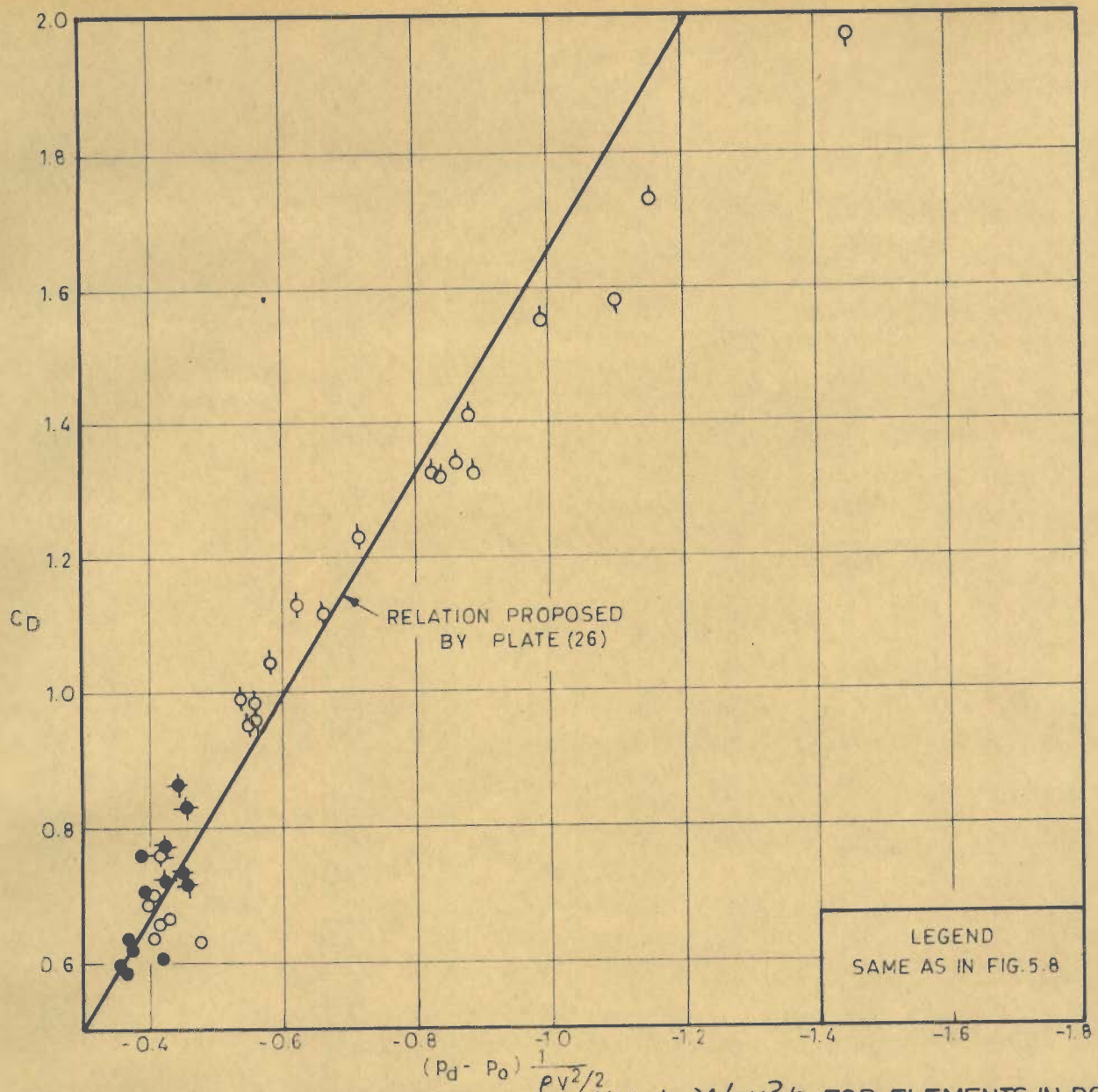

FIG. 5.10 - RELATION BETWEEN C_D AND $(P_d - P_o)1/\rho V^2/2$ FOR ELEMENTS IN BOUNDARY LAYER

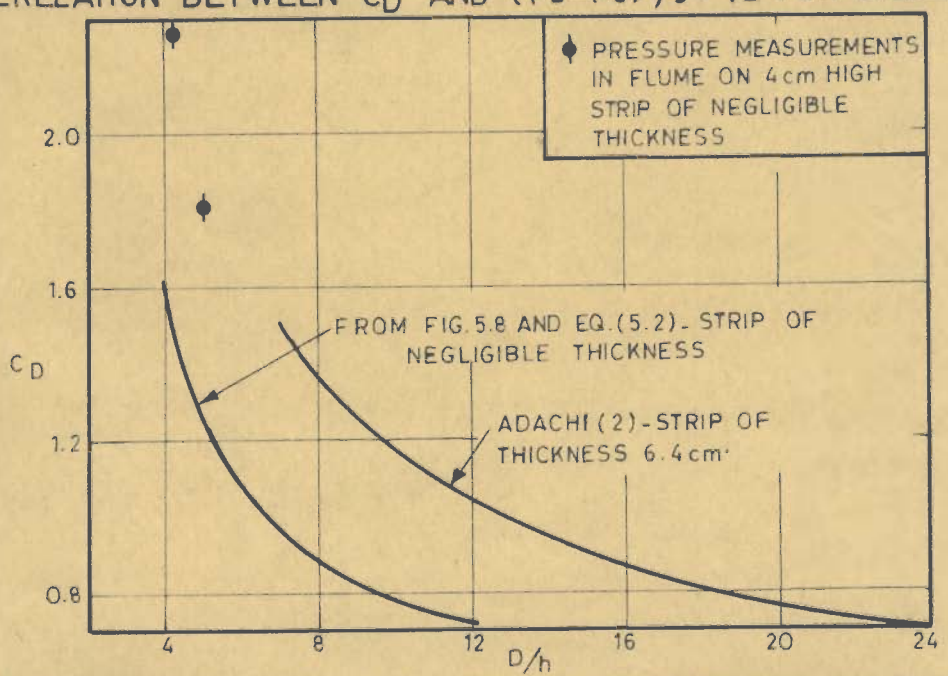

FIG. 5.11 - VARIATION OF C_D WITH D/h FOR ELEMENT ON BED OF AN OPEN CHANNEL

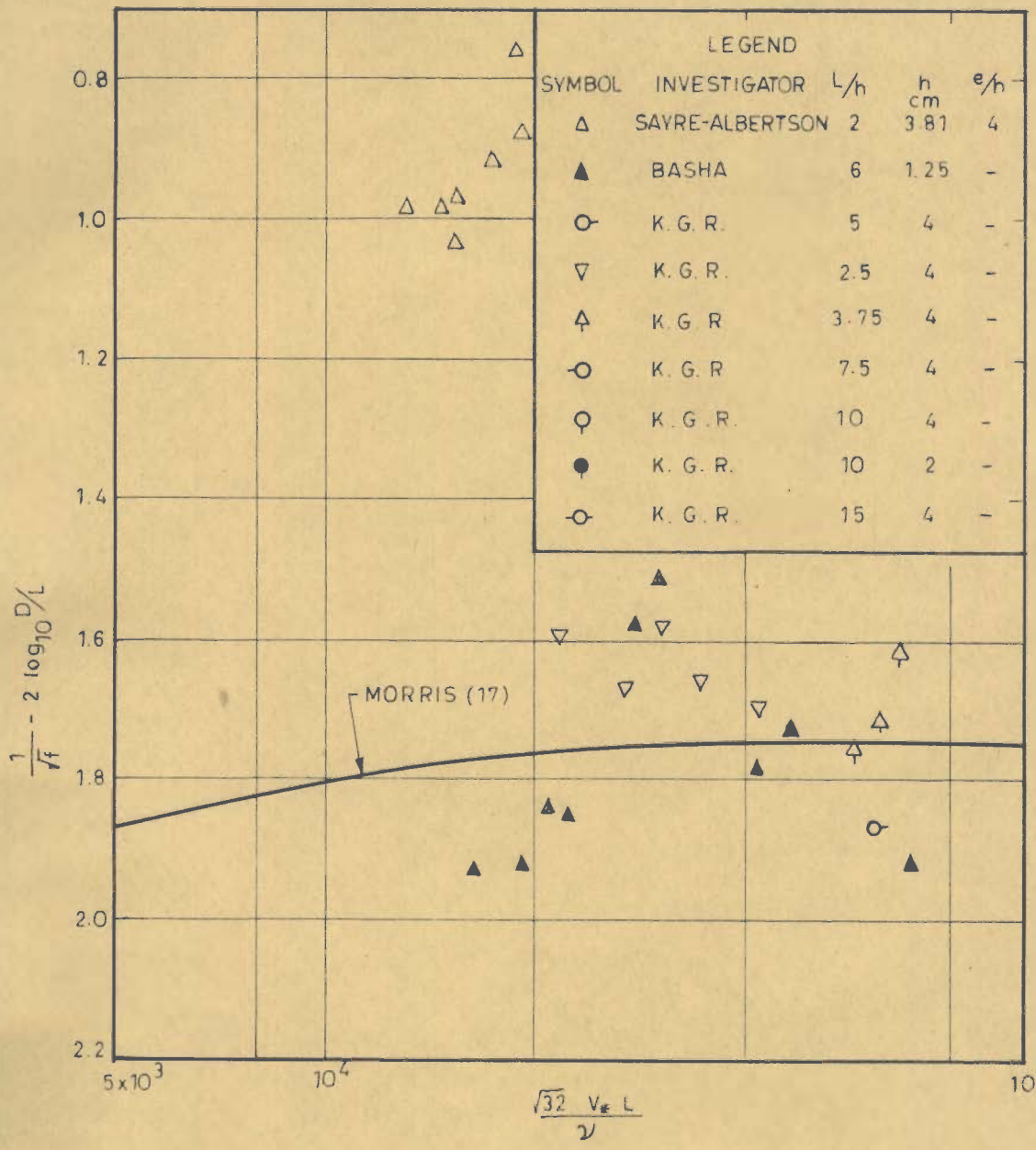

FIG.6.1_FLUME DATA PLOTTED ON MORRIS'S CURVE (REF.17) FOR WAKE-INTERFERENCE TYPE OF FLOW

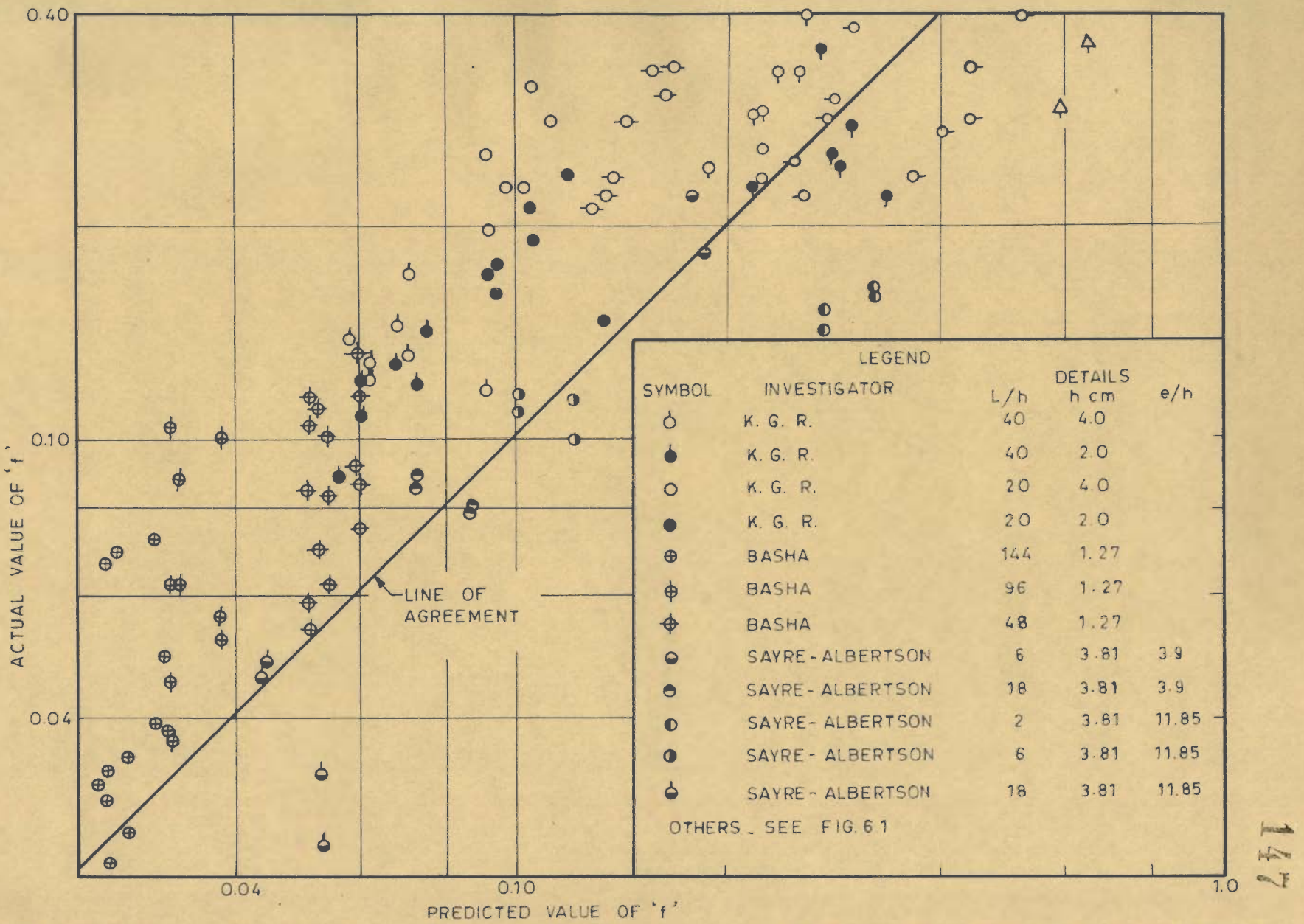

FIG.6.2_COMPARISON OF OBSERVED AND PREDICTED FRICTION FACTORS (BY MORRIS'S METHOD) FOR ISOLATED ROUGHNESS FLOW

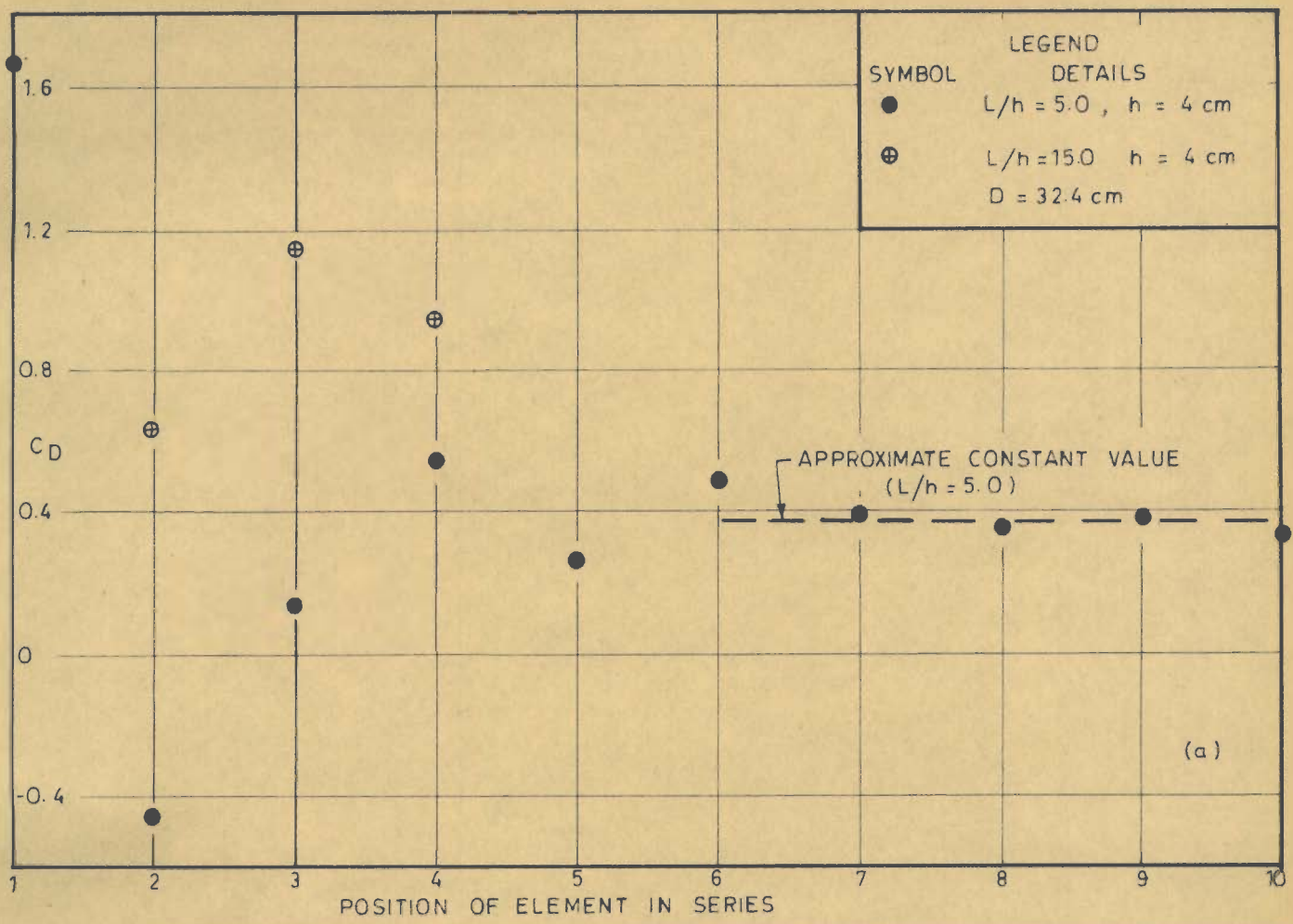

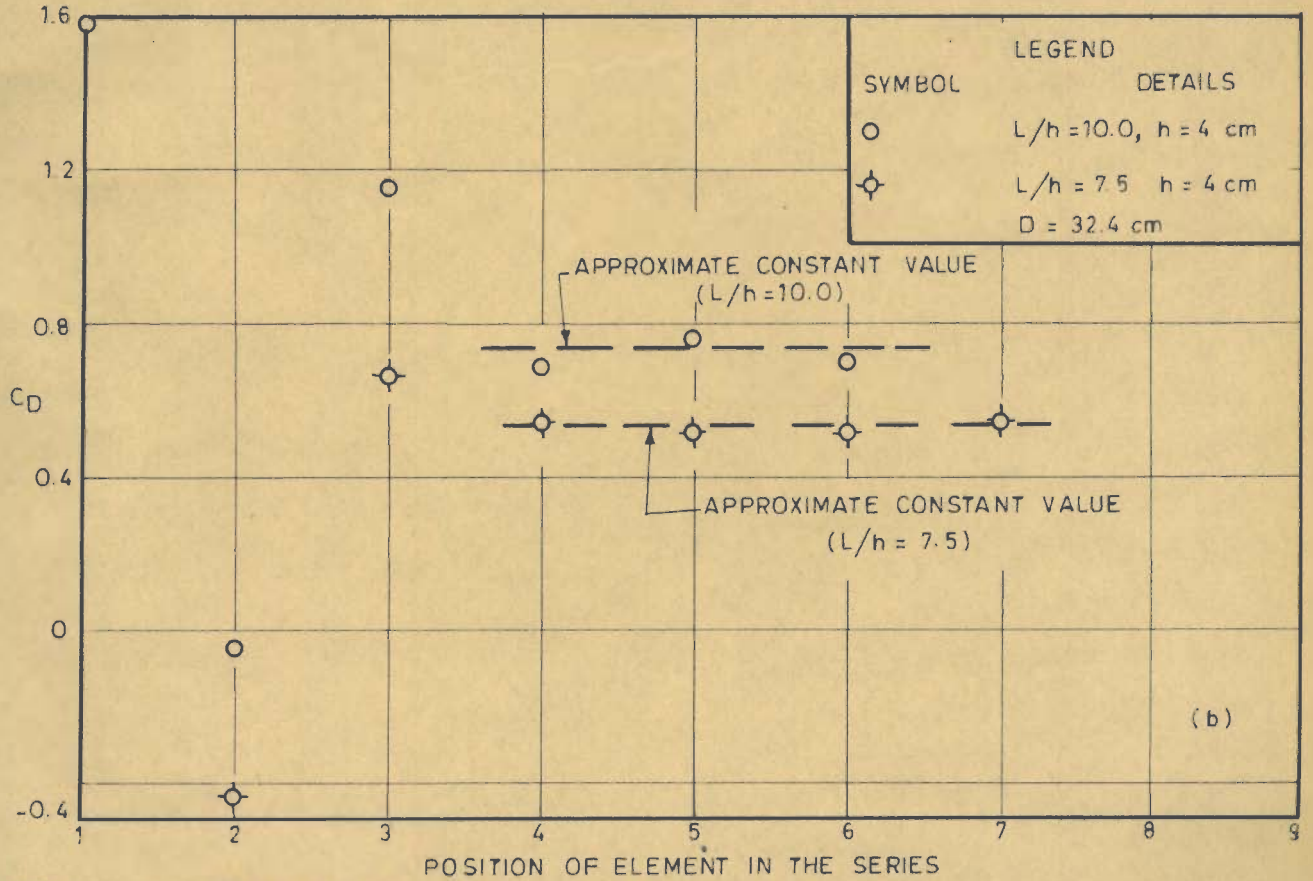

FIG.6.3_VARIATION OF C_D ALONG THE LENGTH FOR ELEMENTS IN SERIES

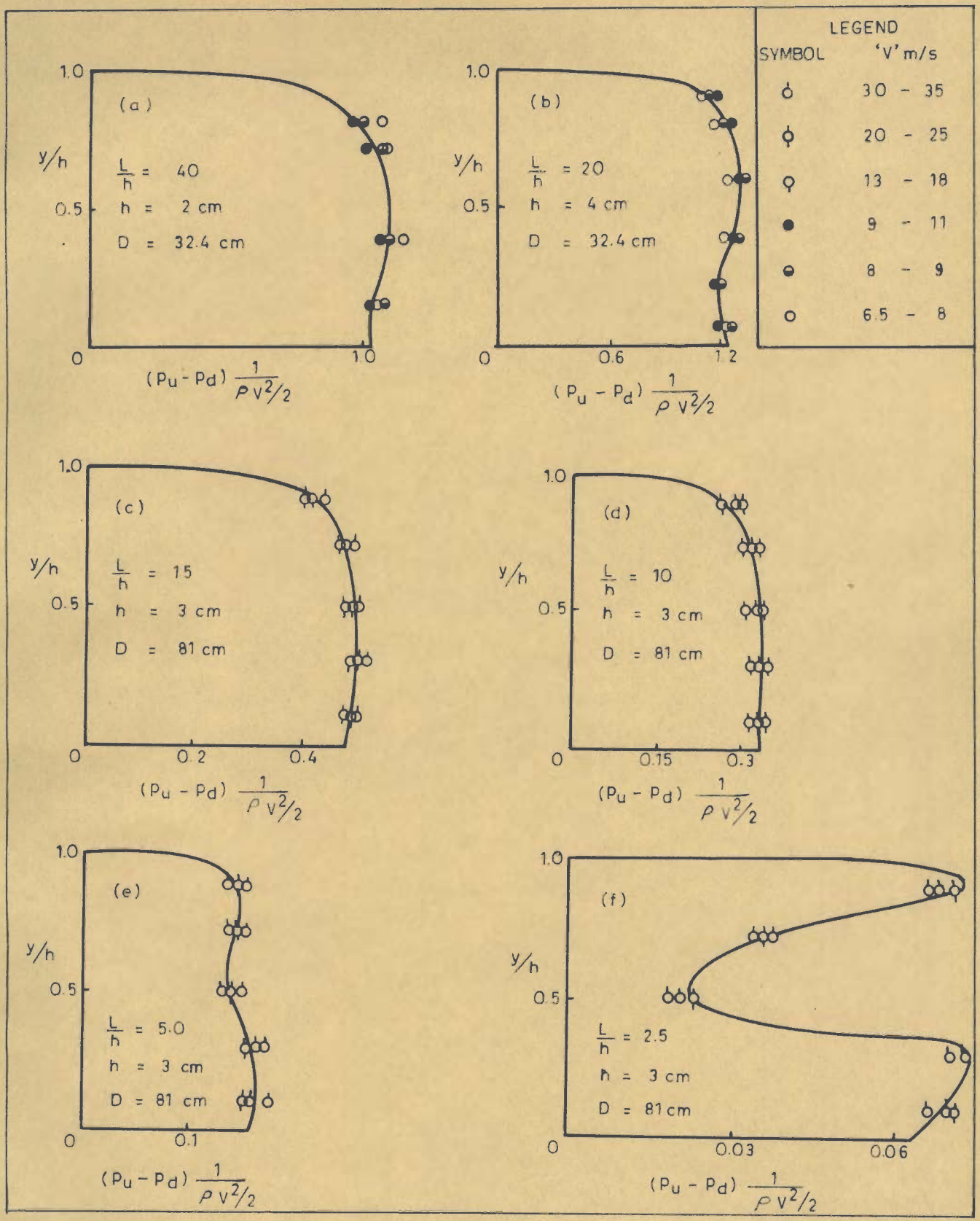

FIG.6.4 PRESSURE DISTRIBUTION AROUND ELEMENT-ELEMENTS IN SERIES

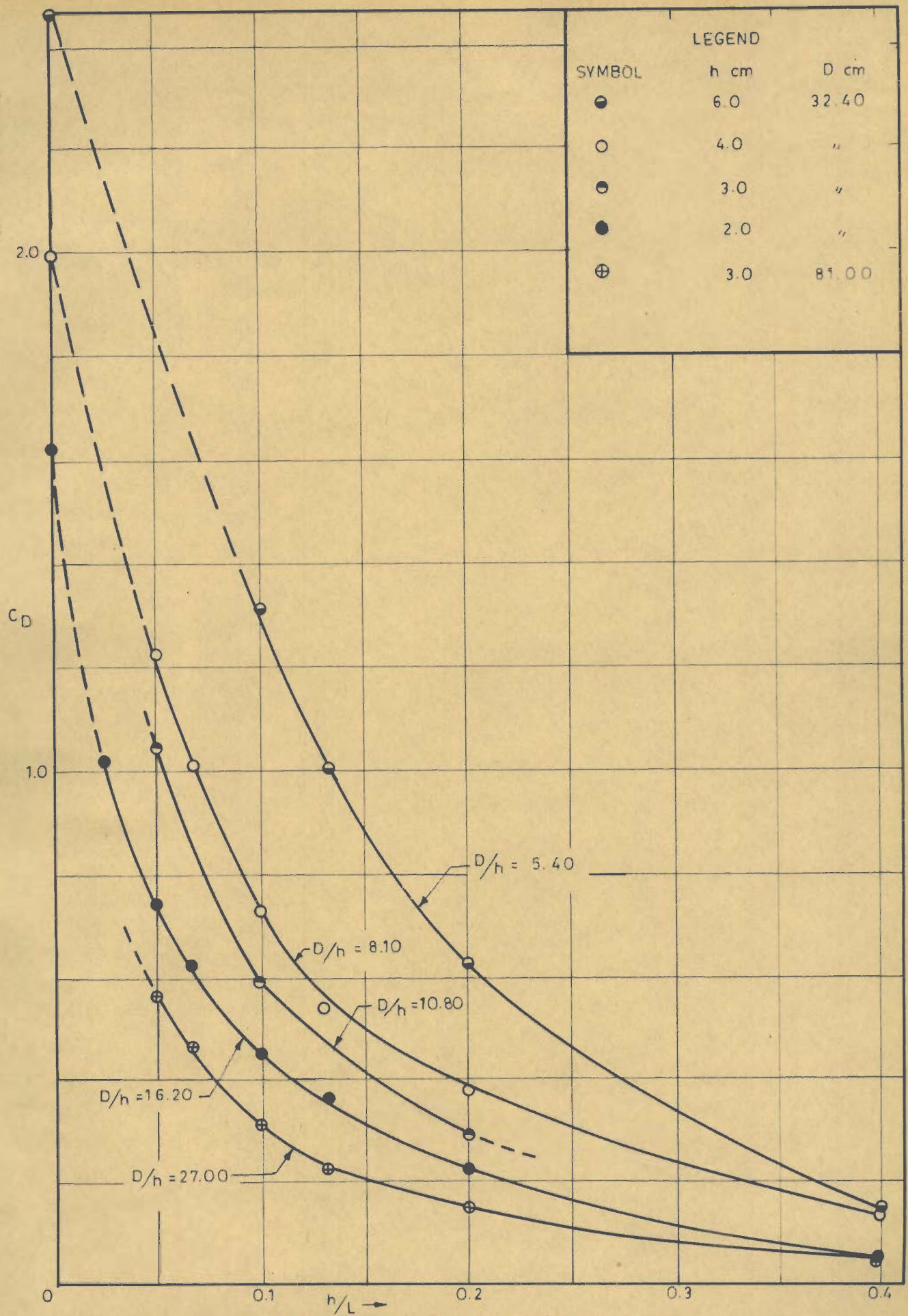

FIG.6.5_VARIATION OF C_D WITH h/L AND D/h FOR TUNNEL DATA

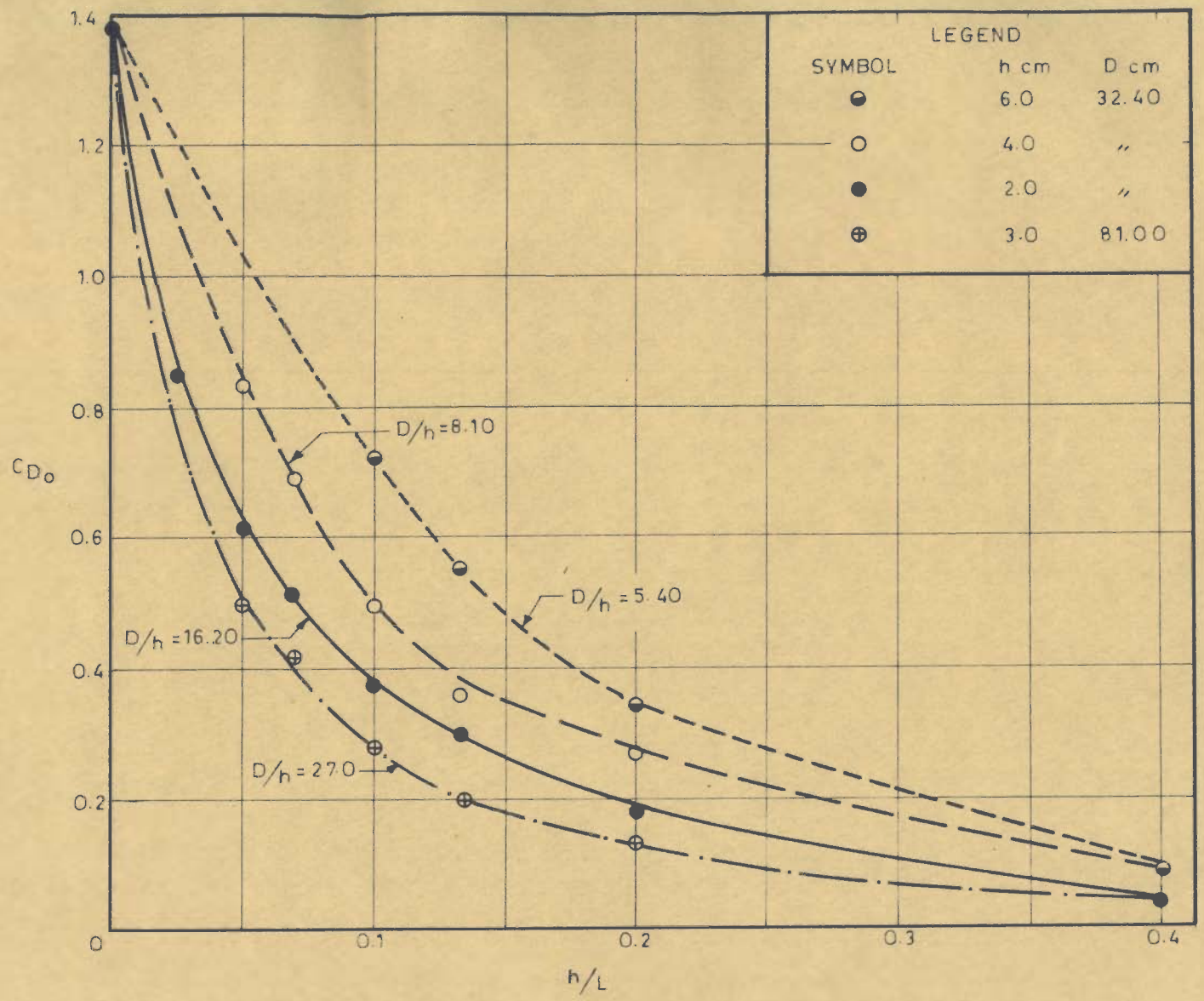

FIG. 6.6_VARIATION OF C_{D_o} (OBTAINED FROM EQUATION 5.2) WITH h/L AND D/h FOR TUNNEL DATA

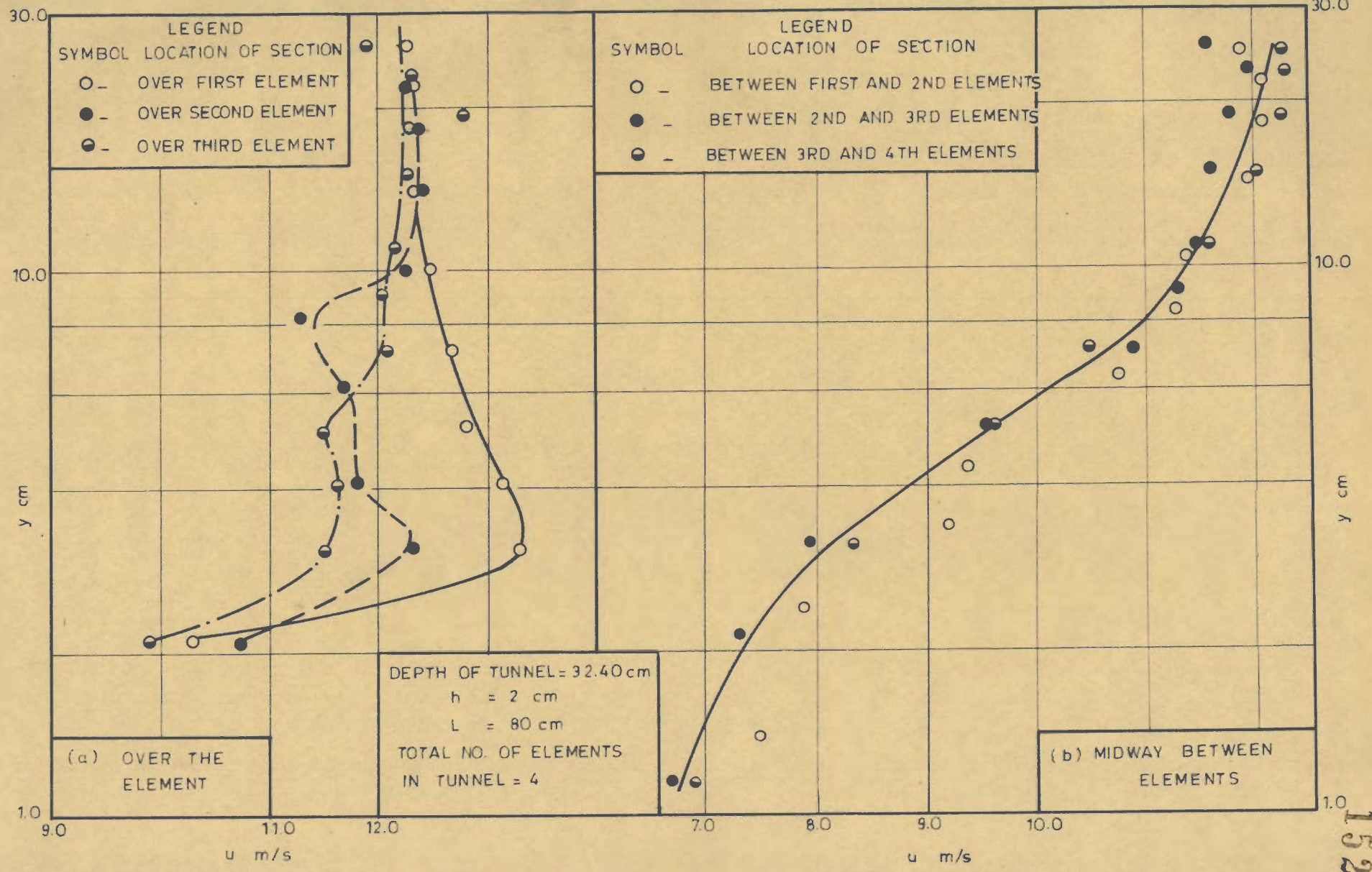

FIG.6.7 VELOCITY PROFILES ALONG THE LENGTH OF TUNNEL FOR ELEMENTS IN SERIES

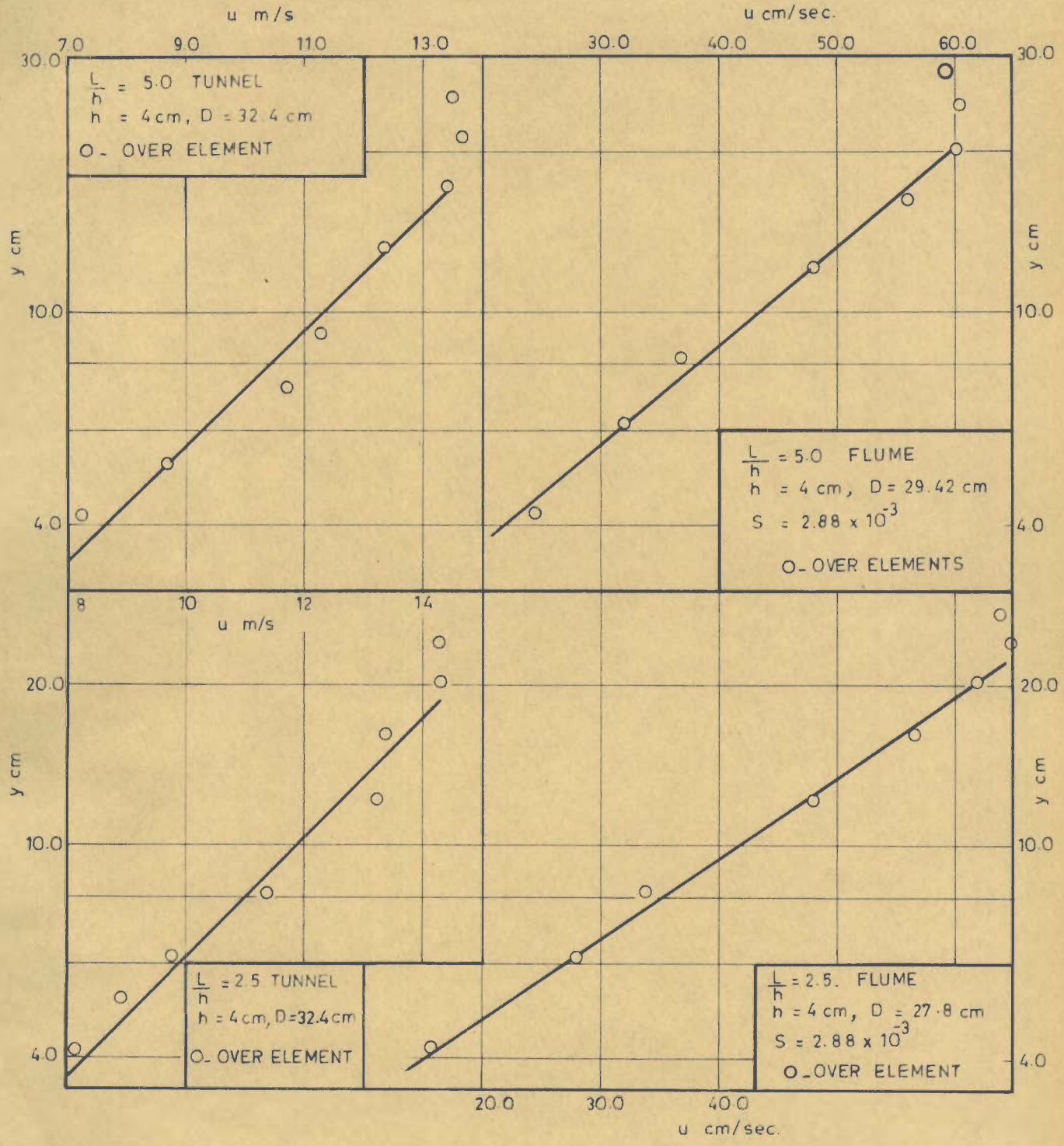

FIG.6.8a.COMPARISON OF VELOCITY PROFILES IN TUNNEL AND FLUME

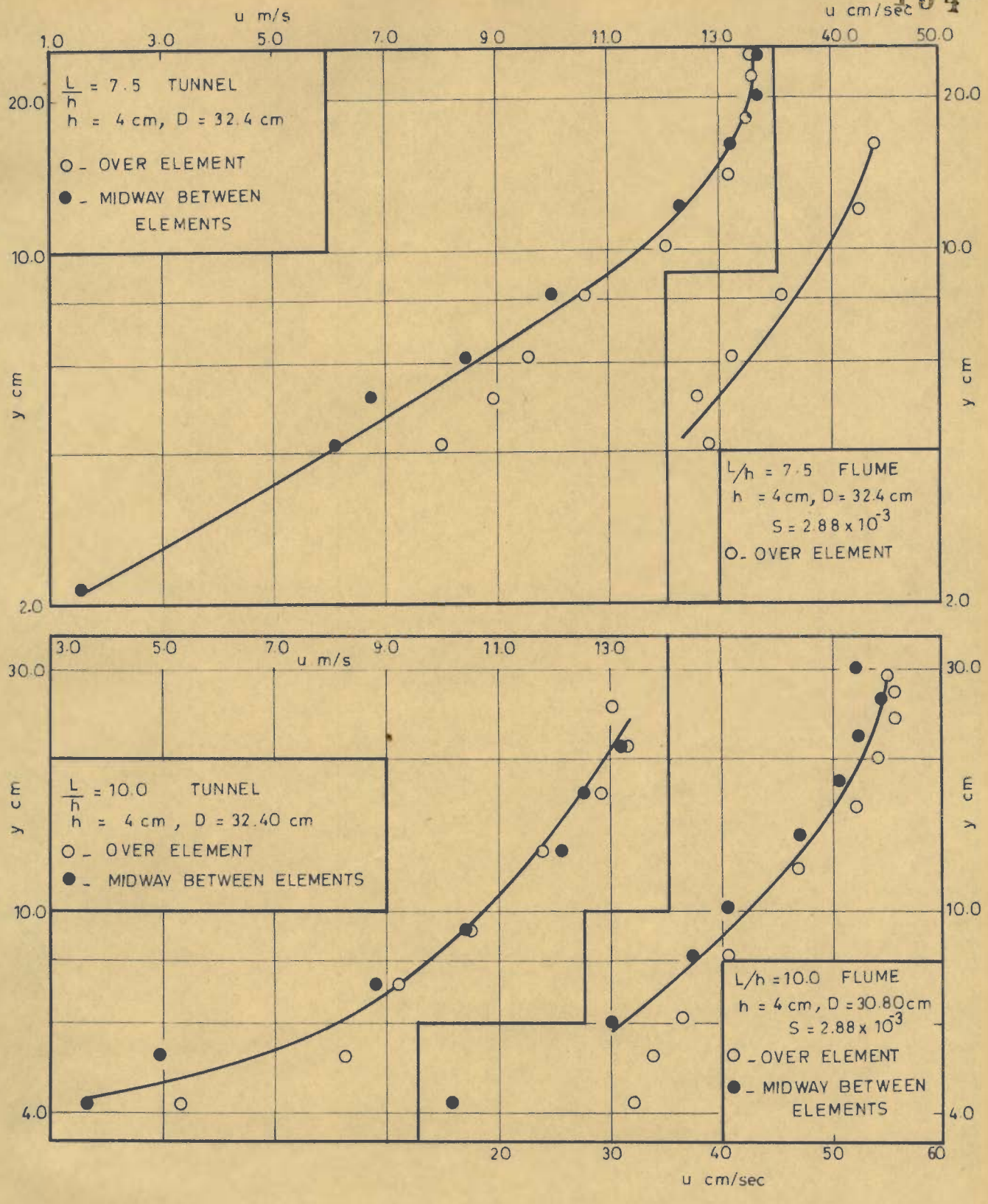

FIG.6.8b. COMPARISON OF VELOCITY PROFILES IN TUNNEL AND FLUME (CONTINUED)

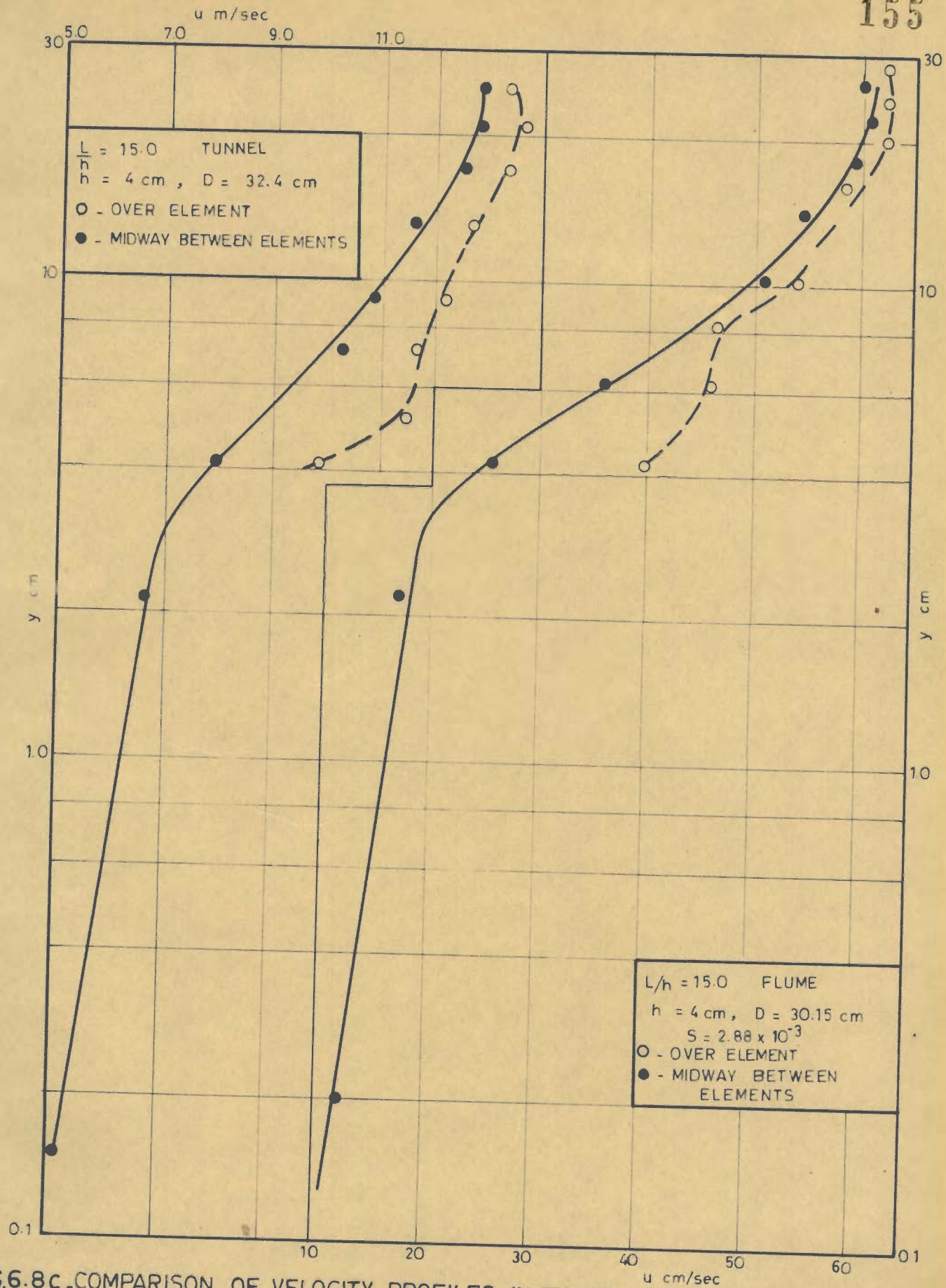

FIG.6.8c COMPARISON OF VELOCITY PROFILES IN TUNNEL AND FLUME (CONTINUED)

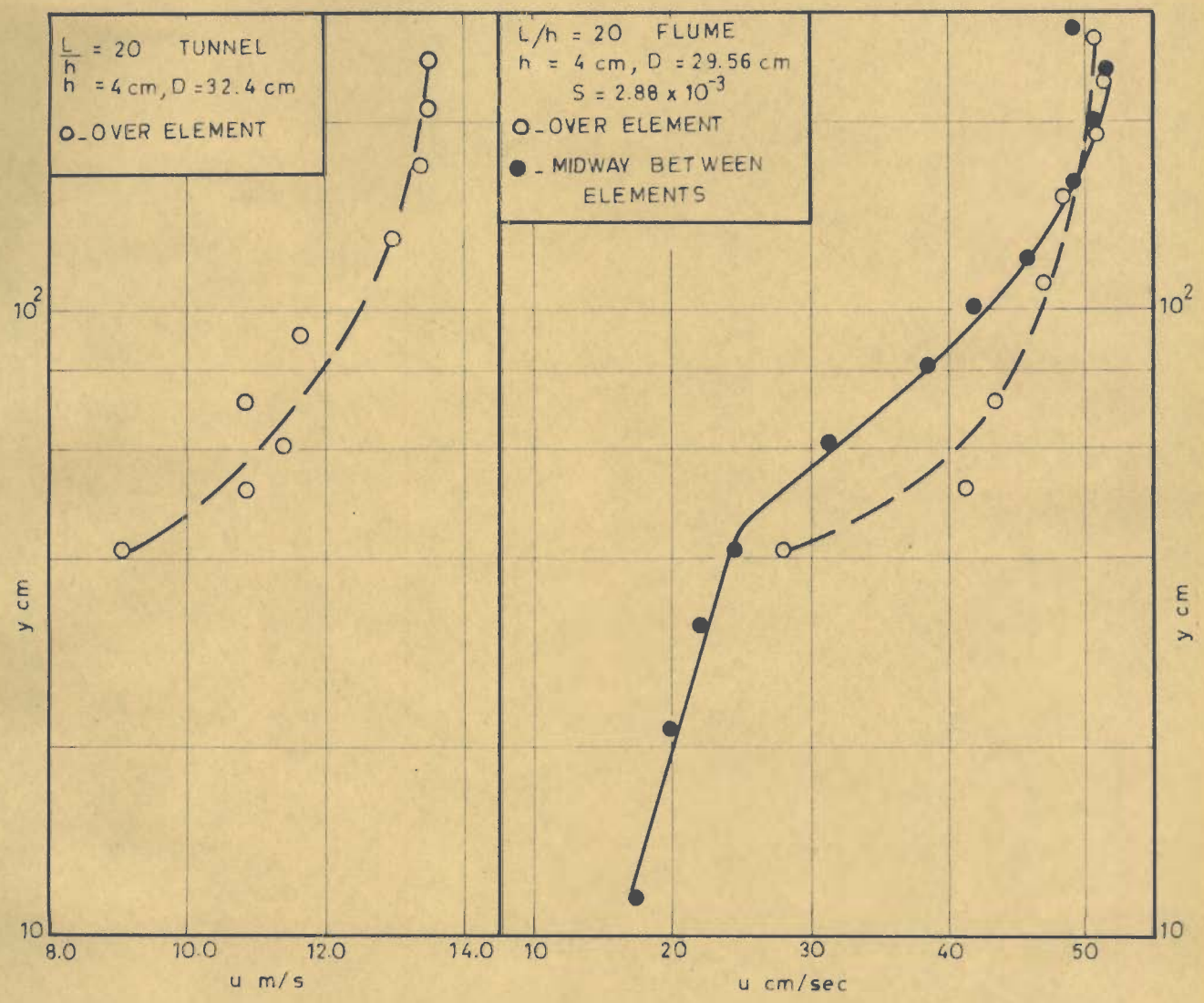

FIG.6.8d - COMPARISON OF VELOCITY PROFILES IN TUNNEL AND FLUME (CONTINUED)

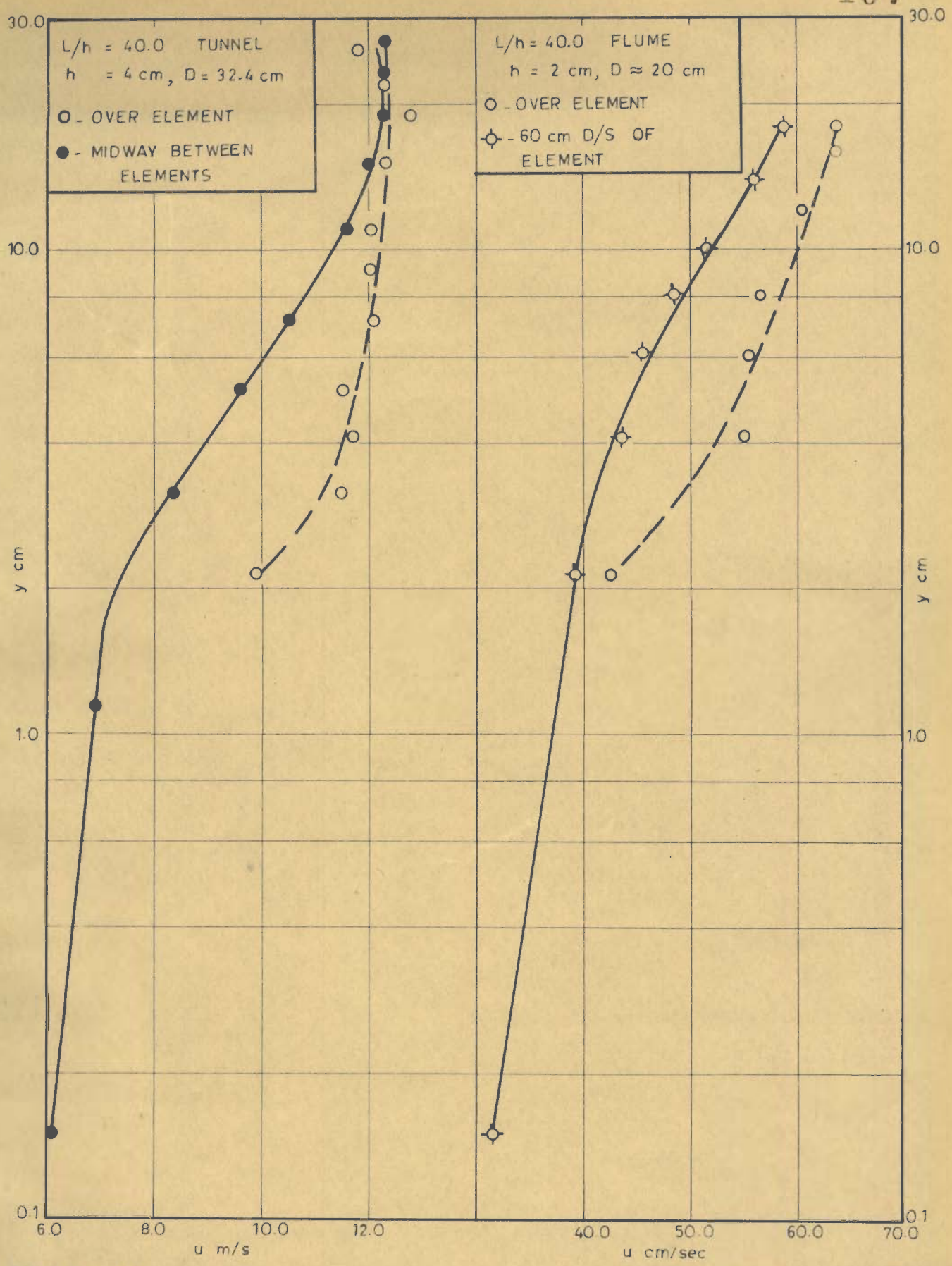

FIG.6-8e - COMPARISON OF VELOCITY PROFILES IN TUNNEL AND FLUME (CONTINUED)

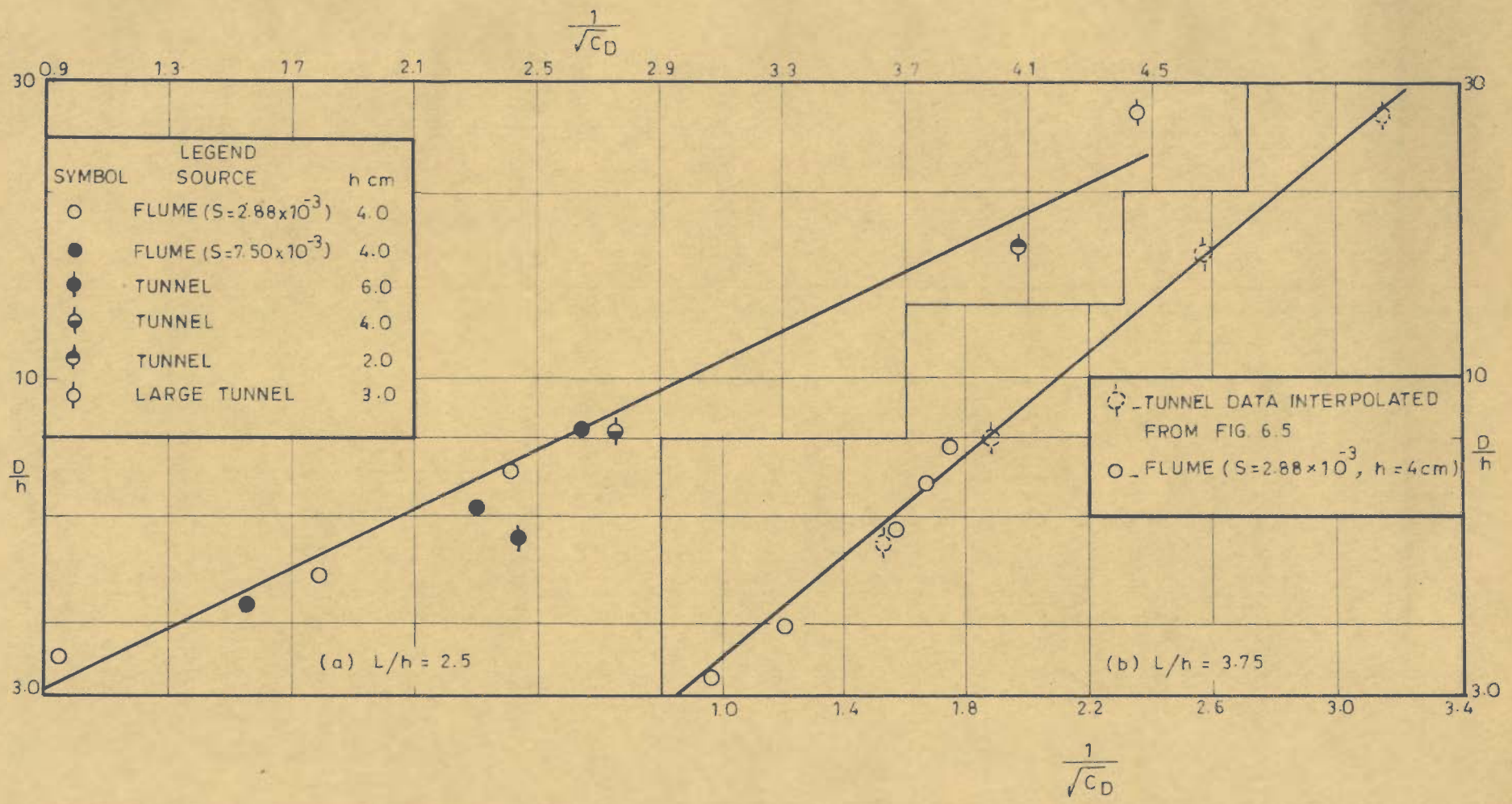

FIG.6.9-VARIATION OF $\frac{1}{\sqrt{C_D}}$ WITH D/h AND L/h FOR TUNNEL AND FLUME DATA

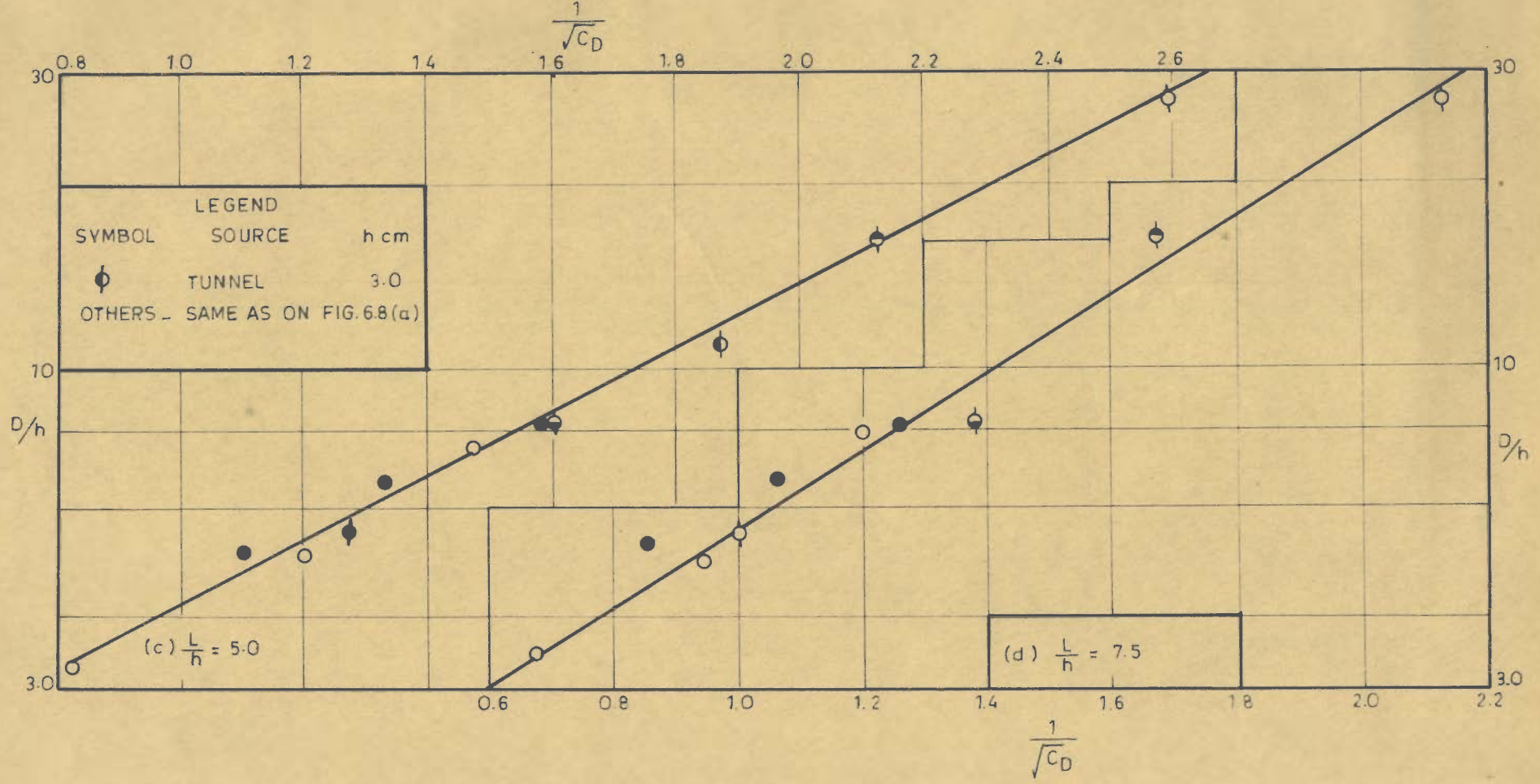

FIG.6.9-VARIATION OF $\frac{1}{\sqrt{C_D}}$ WITH D/h AND L/h FOR TUNNEL AND FLUME DATA (CONTINUED)

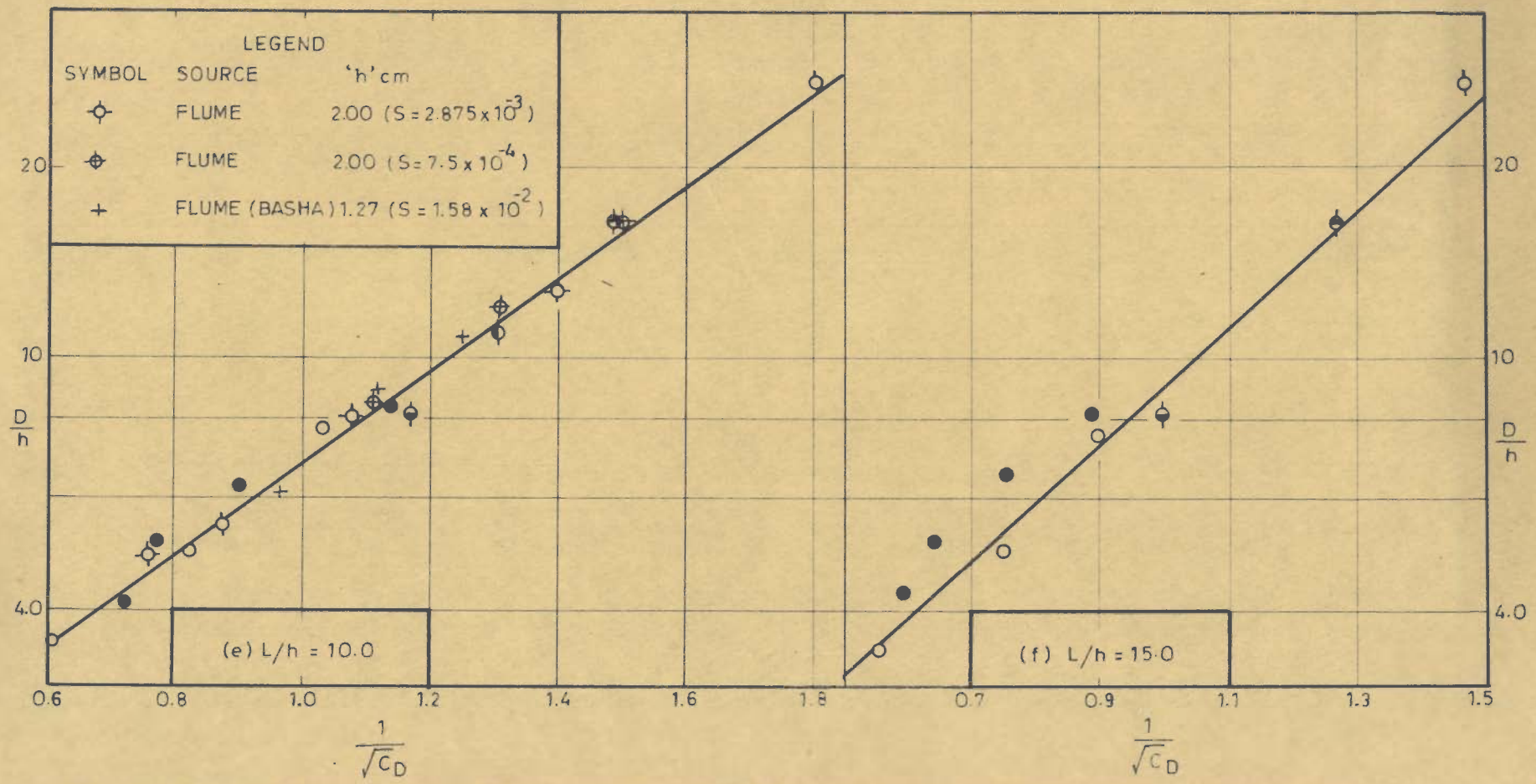

FIG.6.9-VARIATION OF $\frac{1}{\sqrt{C_D}}$ WITH D/h AND L/h FOR TUNNEL AND FLUME DATA (CONTINUED)

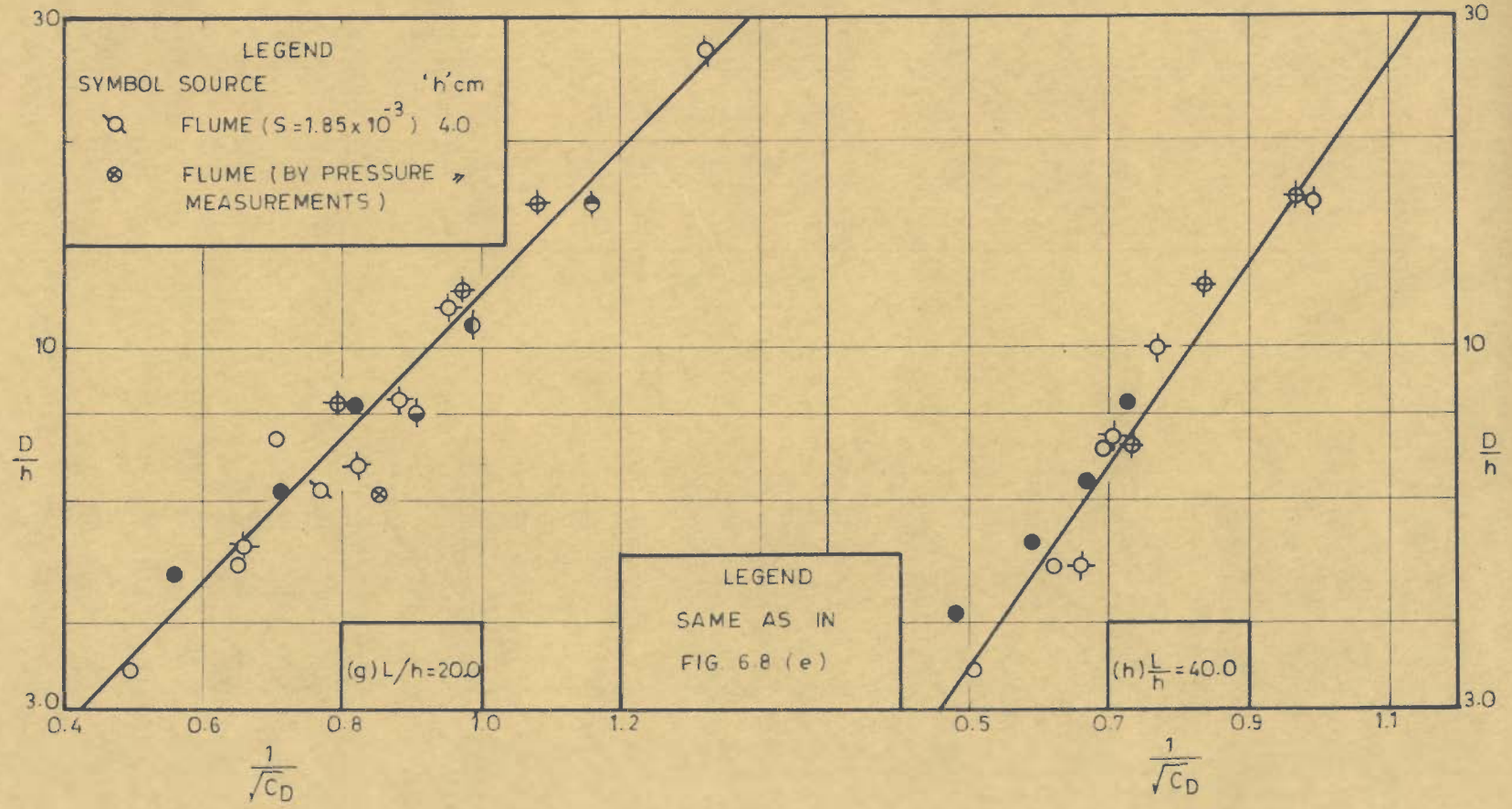

FIG.6.9_VARIATION OF $\frac{1}{\sqrt{C_D}}$ WITH D/h AND L/h FOR TUNNEL AND FLUME DATA (CONTINUED)

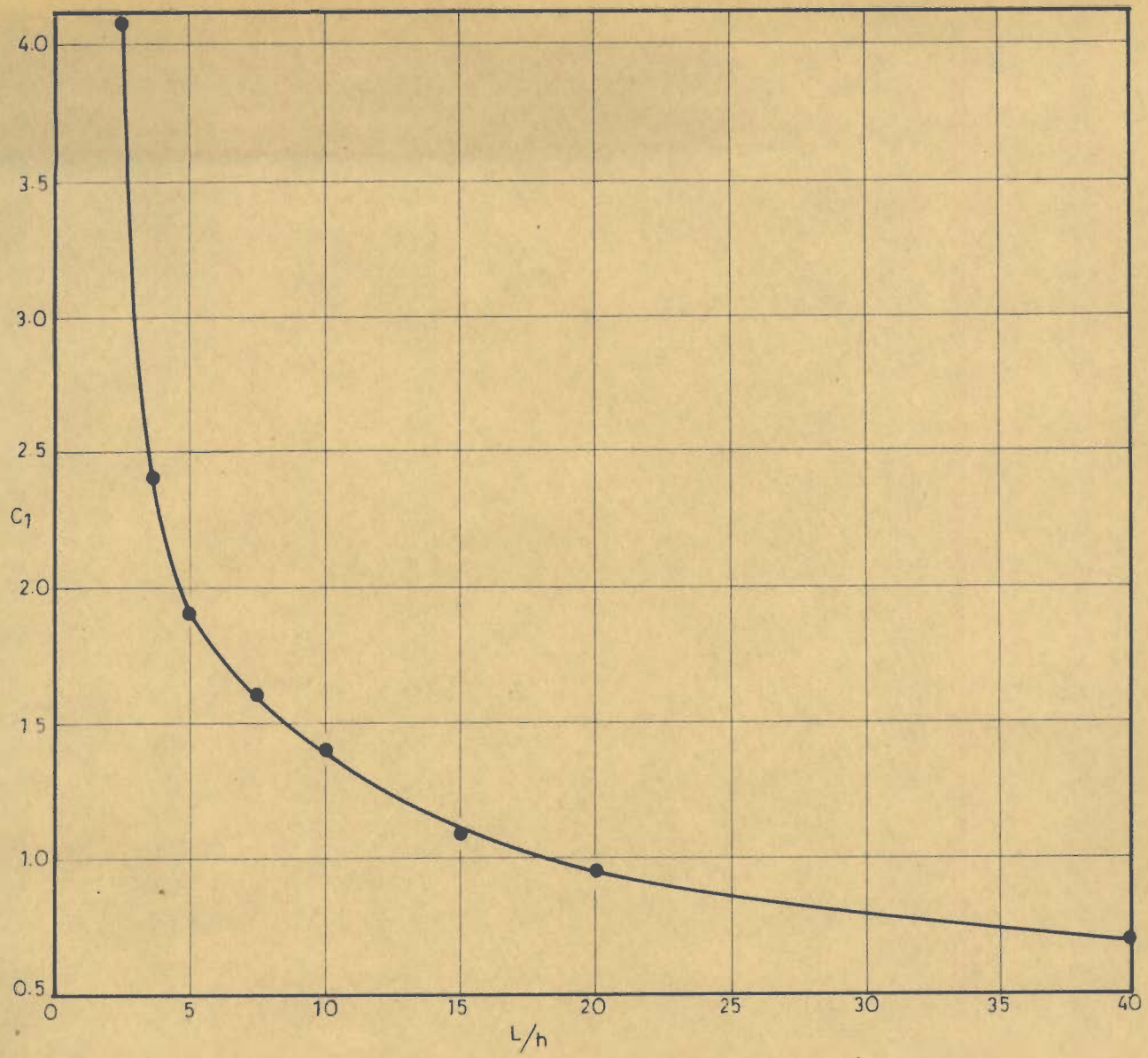

FIG.6.10-VARIATION OF C_1 WITH L/h FOR ELEMENTS IN SERIES

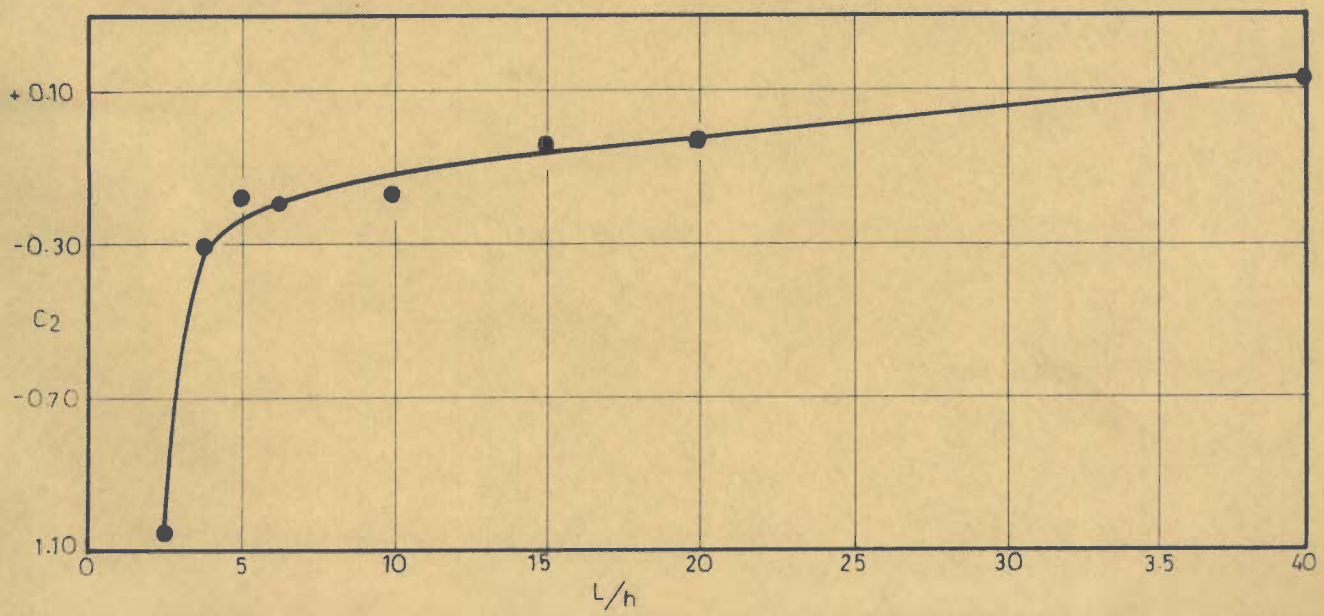

FIG.6.11_VARIATION OF C_2 WITH L/h FOR ELEMENTS IN SERIES

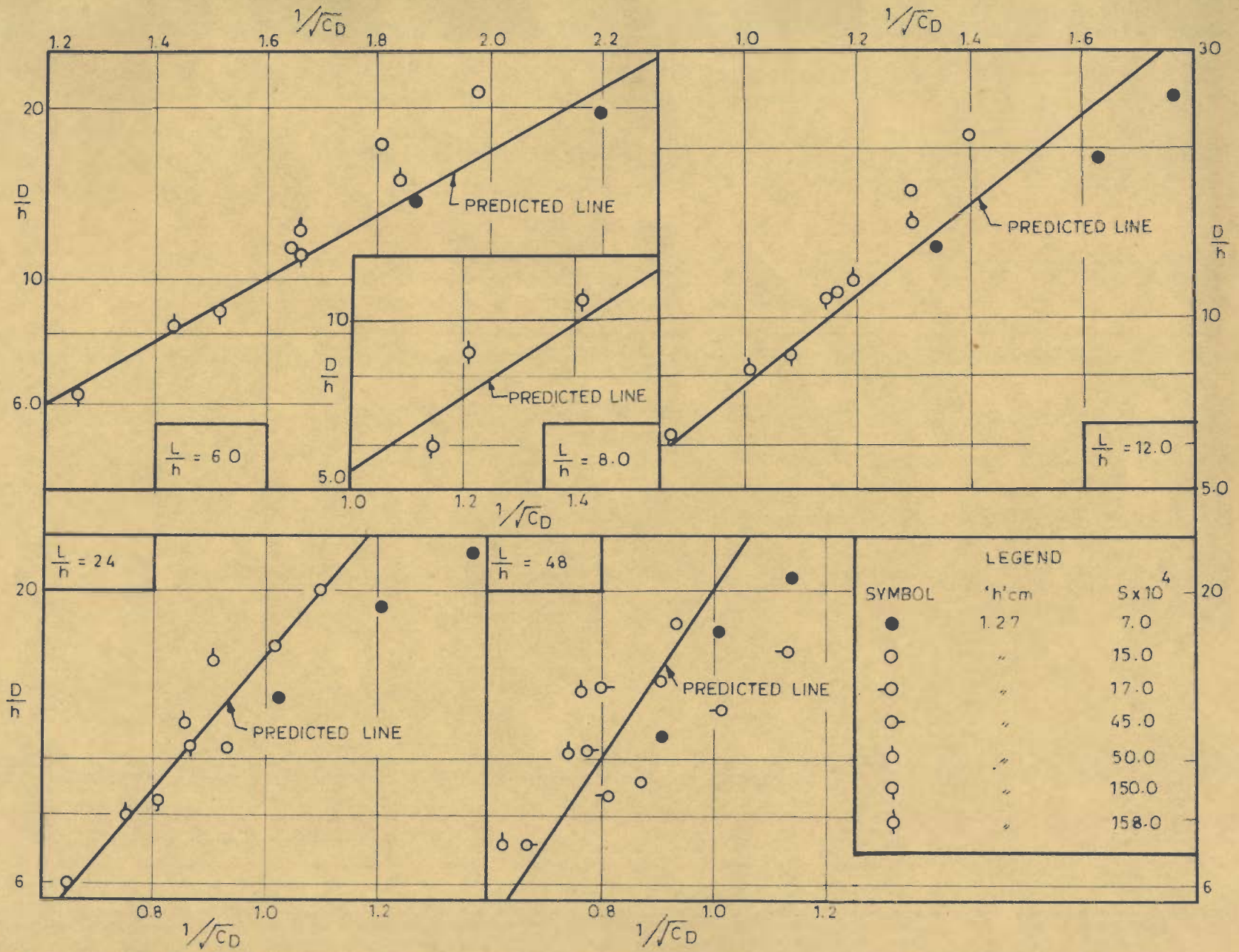

FIG. 6.12 _ COMPARISON BETWEEN OBSERVED AND PREDICTED RESISTANCE FOR BASHA'S DATA (REF. 6)

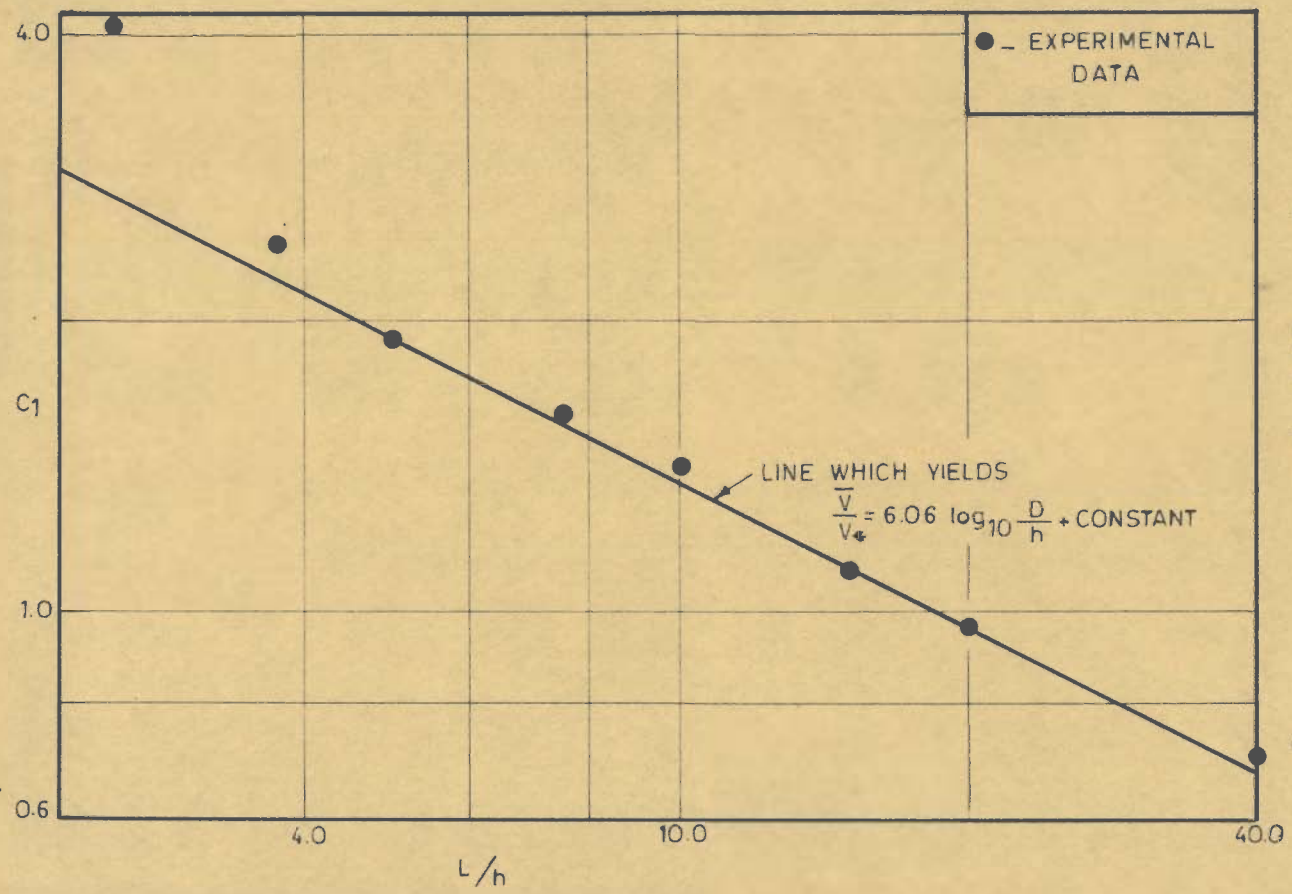

FIG. 6.13_ COMPARISON OF CONVENTIONAL RESISTANCE EQUATION WITH OBSERVED VARIATION

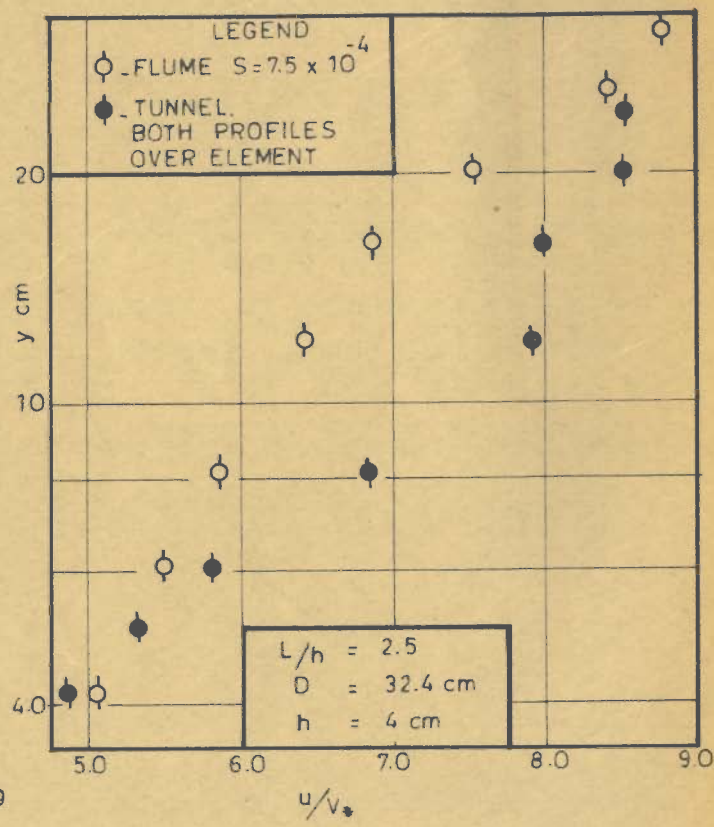

FIG. 6.14_ PLOT OF u/V_* VS. $\log_{10} y$ FOR TUNNEL AND FLUME DATA

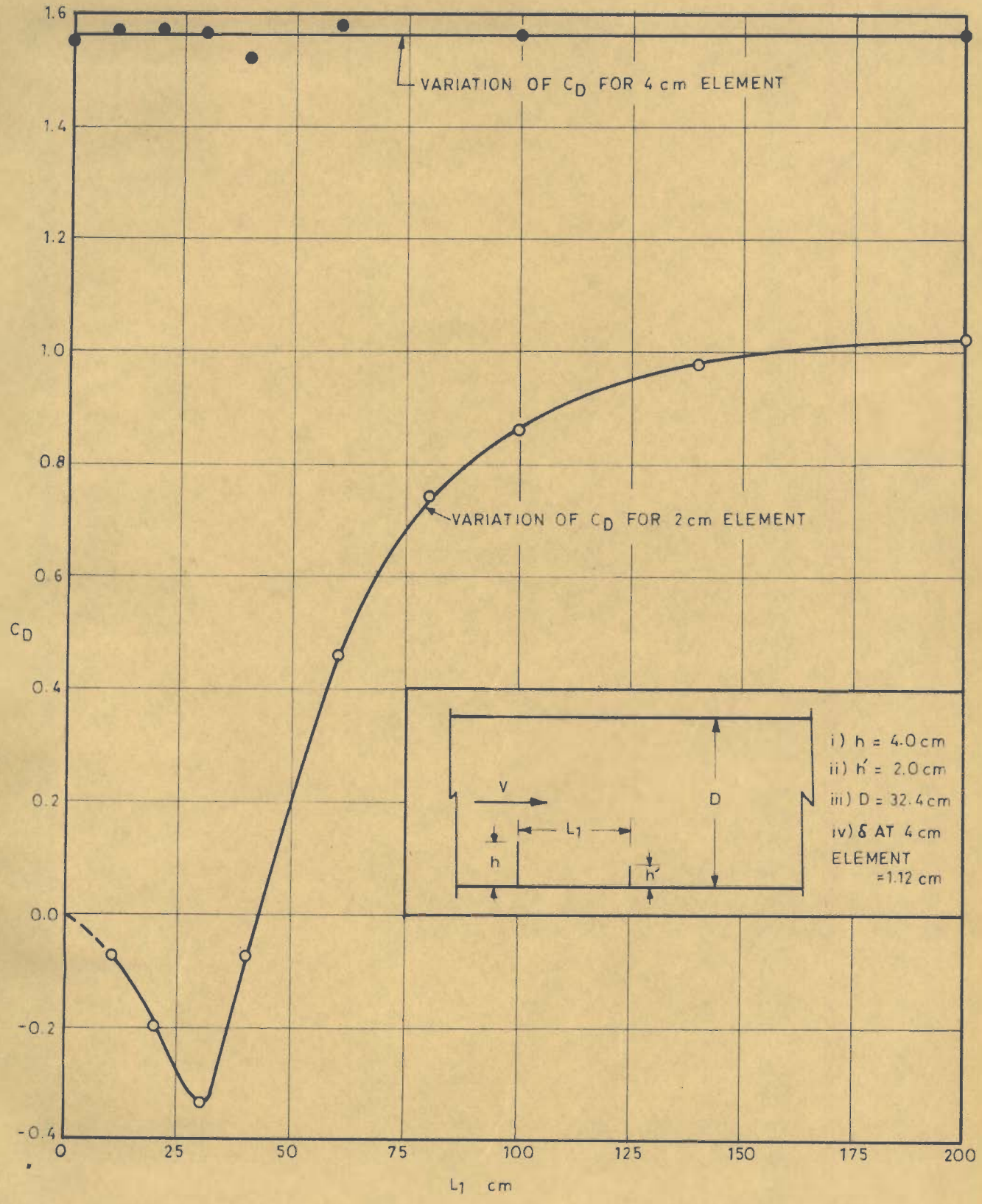

FIG. 7.1_VARIATION OF C_D WITH L_1 FOR CASE OF 2 CM STRIP DOWNSTREAM OF 4 CM STRIP ($\delta/h = 0.28$)

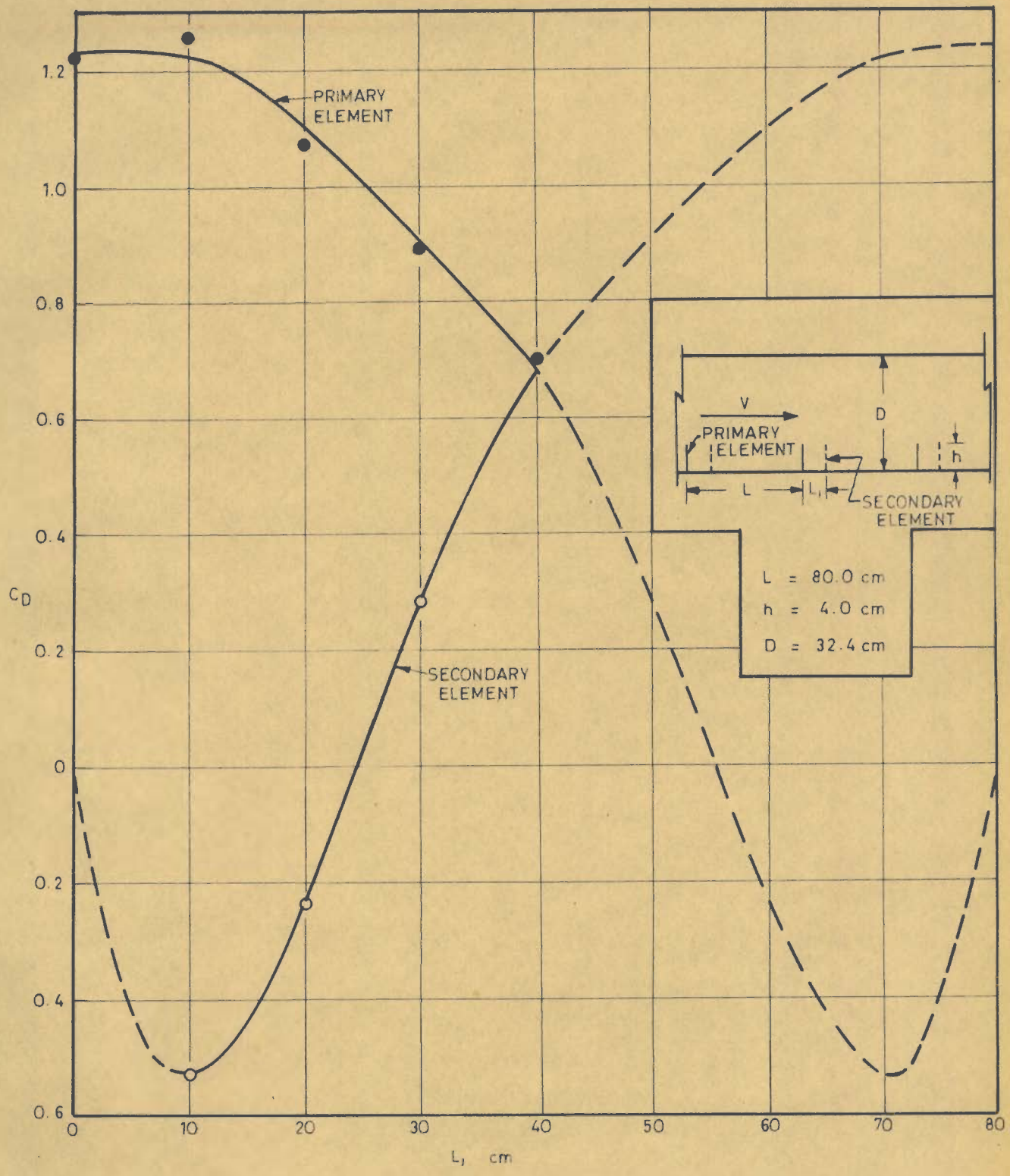

FIG. 7.2(a)_VARIATION OF C_D WITH RELATIVE DISPLACEMENT OF TWO SERIES OF ROUGHNESSES (TUNNEL DATA)

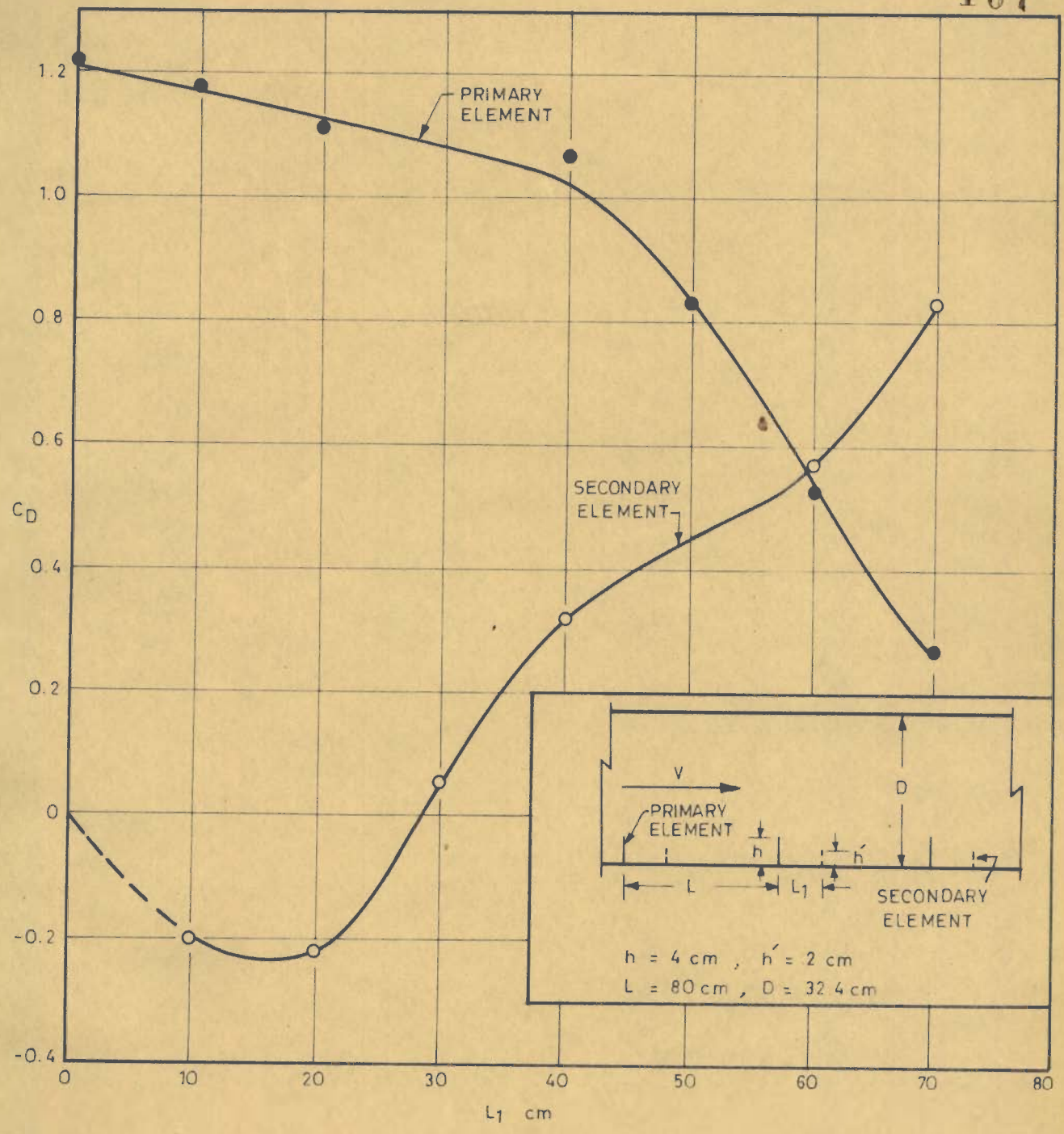

FIG. 7.2(b)_VARIATION OF C_D WITH RELATIVE DISPLACEMENT OF TWO SERIES OF ROUGHNESSES (TUNNEL DATA)

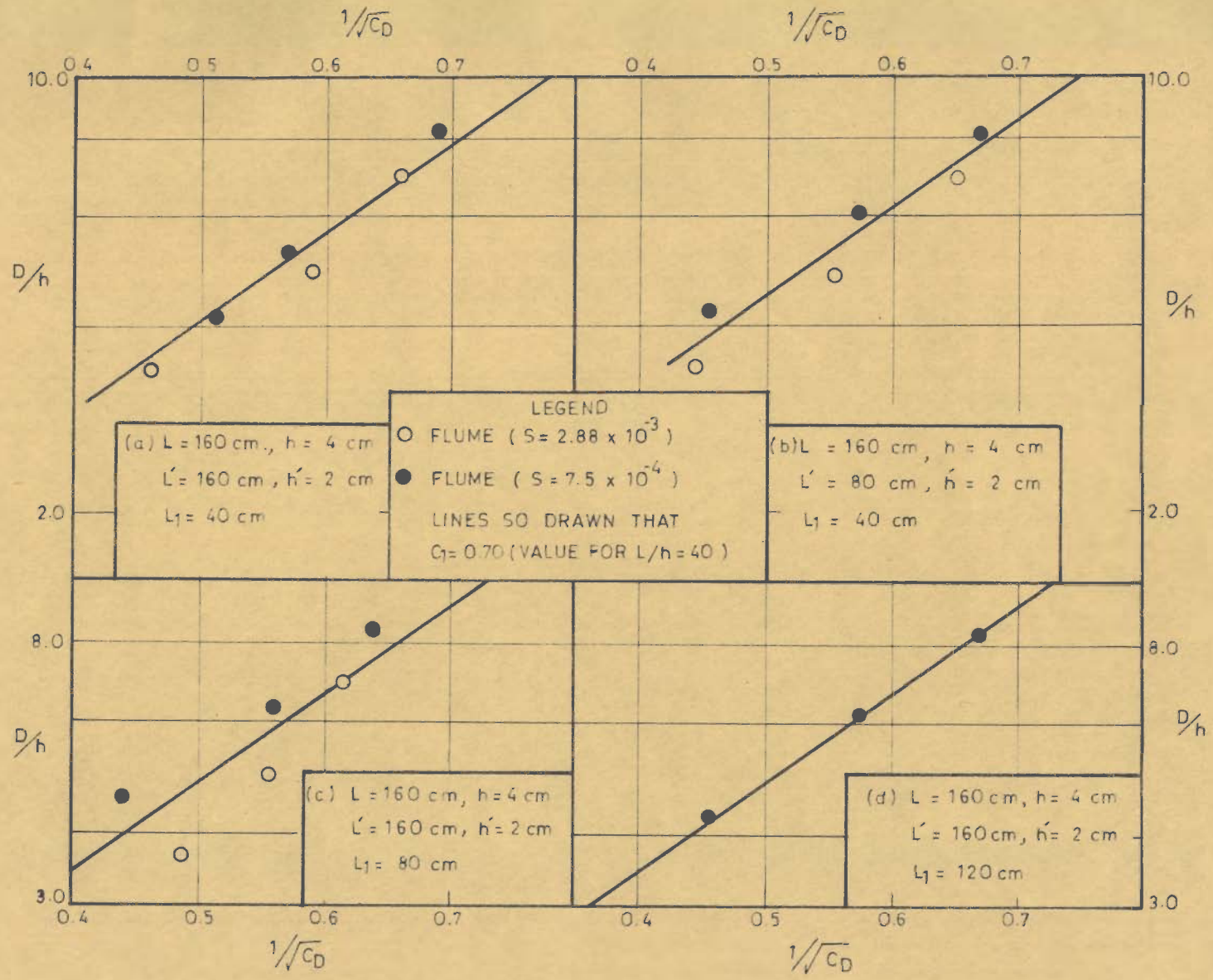

FIG.7.3- VARIATION OF EFFECTIVE C_D' OF AN ELEMENT IN THE PRIMARY SERIES WITH D/h FOR COMBINATION OF TWO ROUGHNESS SERIES

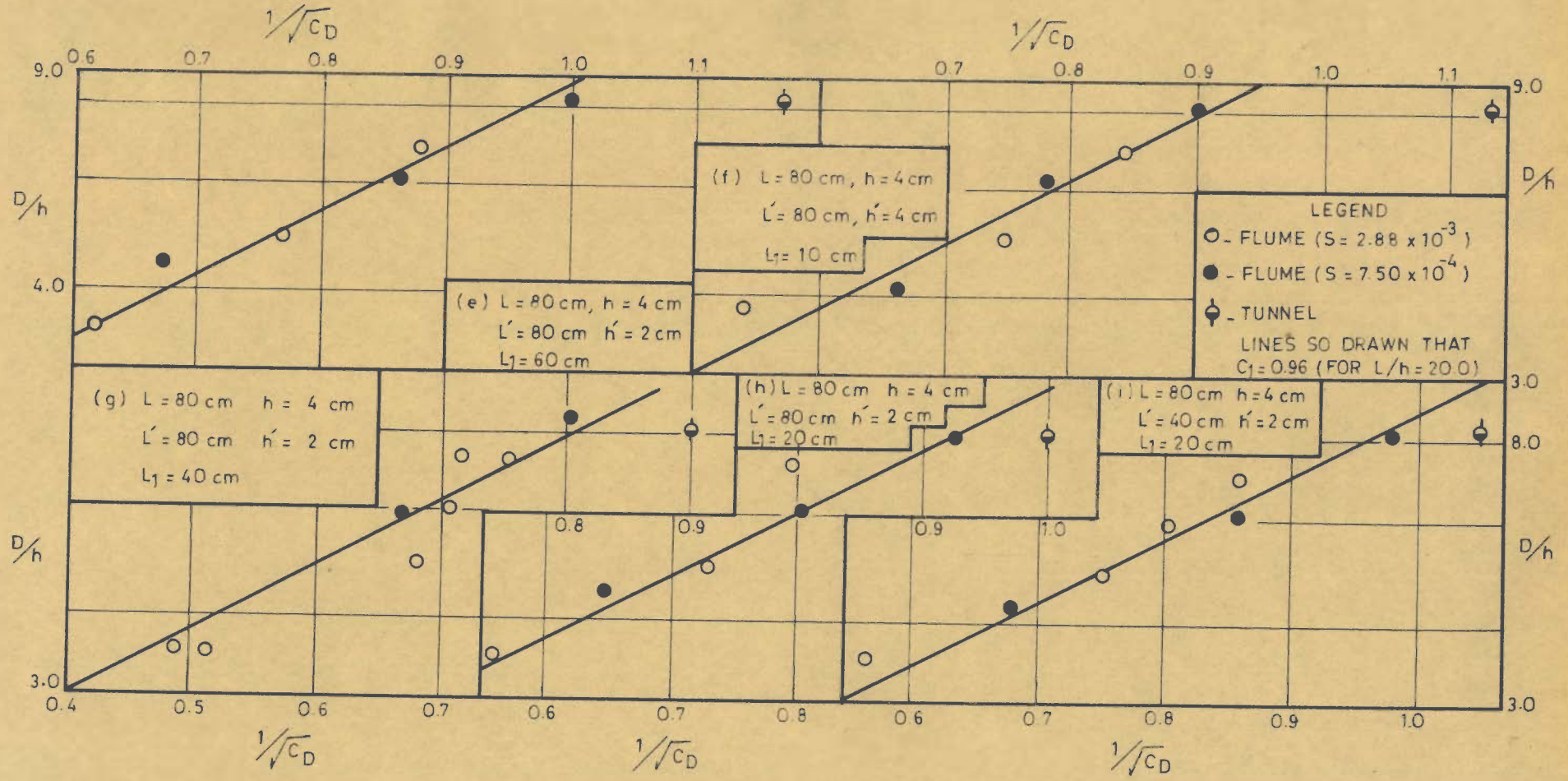

FIG. 7.3_VARIATION OF 'EFFECTIVE C_D' OF AN ELEMENT IN THE PRIMARY SERIES WITH D/h FOR COMBINATION OF TWO ROUGHNESS SERIES

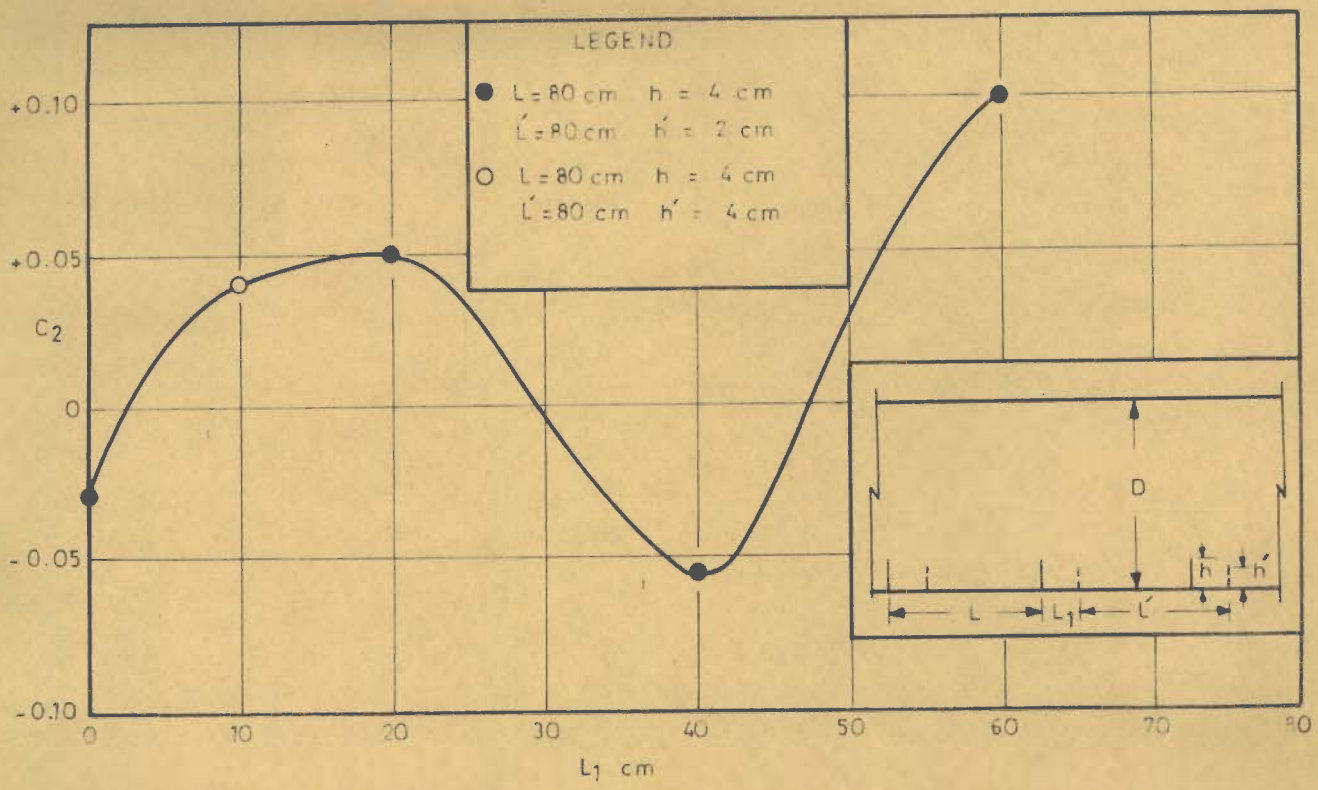

FIG. 7.4 (a)_VARIATION OF C_2 WITH L_1 FOR COMBINATION OF TWO ROUGHNESS SERIES (BASED ON FLUME DATA)

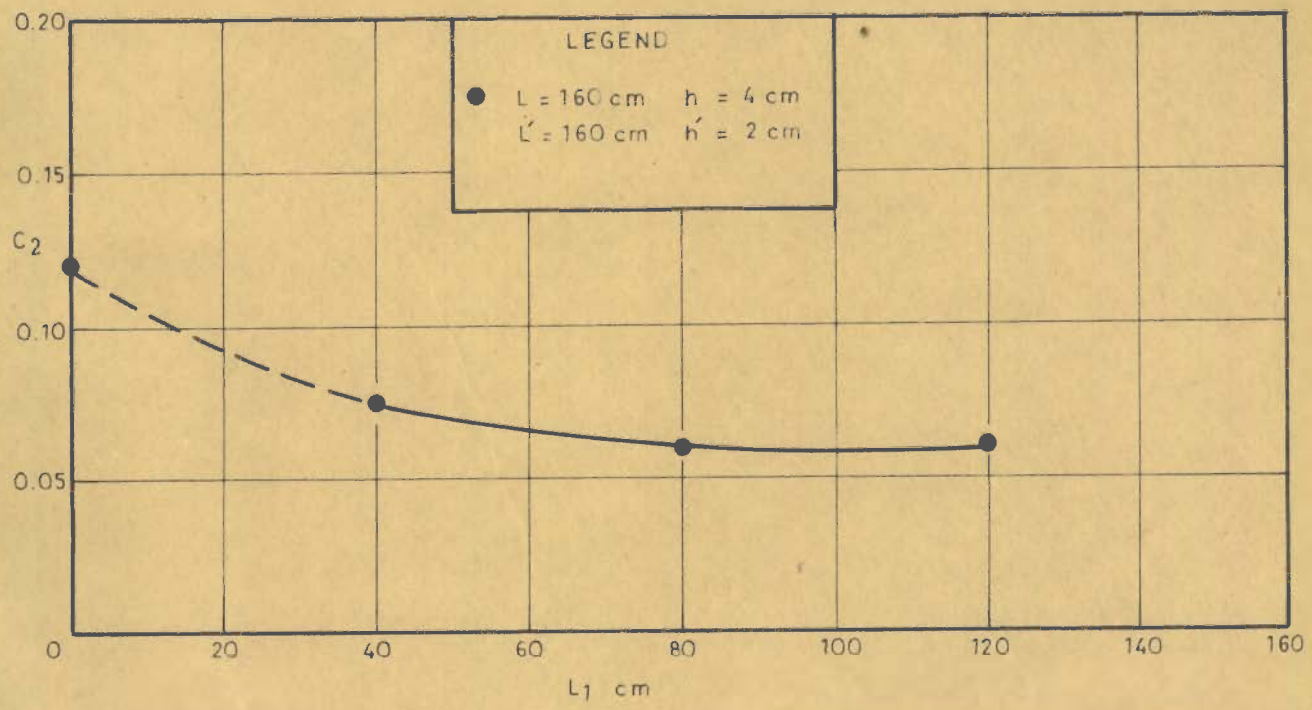

FIG. 7.4 (b)_VARIATION OF C_2 WITH L_1 FOR COMBINATION OF TWO ROUGHNESS SERIES (BASED ON FLUME DATA)

APPENDIX

TABLE - I

SUMMARY OF FLUME DATA COLLECTED BY THE AUTHOR

Width of flume = 47.20 cms. Manning's 'n' for side wall=0.009
Manning's 'n' for wooden bottom = 0.0135
(See Table 4.1 for details of roughness patterns).

Run No	cms D	Sx10^3	Cms/See V	T^{o}C	Cms R_b
A_1 - 1	24.88	2.875	49.50	15.0	22.40
A_1 - 2	19.24	"	39.60	"	17.85
A_1 - 3	13.73	"	27.80	"	13.17
A_1 - 4	16.55	0.75	14.75	31.0	15.80
A_1 - 5	21.00	"	20.10	"	20.10
A_1 - 6	25.66	"	24.80	"	23.10
A_1 - 7	33.18	"	30.00	"	28.65
A - 6	19.56	2.875	30.30	14.5	18.60
A - 7	29.56	"	39.30	15.0	27.45
A - 8	13.57	"	19.20	14.0	13.57
A - 9	33.50	0.75	24.60	29.5	30.20
A - 10	24.99	"	18.80	"	23.40
A - 11	18.98	"	12.75	31.0	18.20
A - 12	25.10	1.85	31.60	15.0	23.30
A_3- 1	13.79	2.875	18.75	20.5	13.40
A_3- 2	19.82	"	30.00	21.5	18.85
A_3- 3	30.12	"	43.50	22.0	27.70
A_3- 4	17.00	0.75	11.30	31.0	16.50
A_3- 5	20.52	"	13.50	"	19.70
A_3- 6	26.29	"	17.70	"	24.70
A_3- 7	32.50	"	22.80	"	29.70
A_2- 1	30.79	2.875	41.30	15.0	28.45
A_2- 2	19.64	"	27.00	14.0	18.80
A_2- 3	14.05	"	16.90	14.0	13.80
A_2-4	16.25	0.75	10.95	31.0	15.75
A_2- 5	20.36	"	13.05	"	19.60
A_2- 6	25.05	"	16.85	"	23.60
A_2- 7	33.17	"	24.00	"	30.00

(Contd)

Run No	cms D	Sx10^3	Cms/See V	T°C	Cms R_b
A_5- 1	31.42	2.875	41.70	19.5	28.70
A_5- 2	19.50	"	26.60	20.00	18.70
A_5- 3	13.84	"	16.20	21.0	13.60
A_5- 4	32.17	0.75	22.80	31.0	29.30
A_5- 5	26.47	"	17.60	"	24.90
A_5- 6	20.80	"	12.70	"	20.00
A_3- 1	13.05	2.875	15.60	15.0	12.80
A_3- 2	19.85	"	27.70	-	19.00
A_3- 3	29.42	"	40.60	16.5	27.20
A_3- 4	32.41	0.75	23.20	31.0	29.50
A_3- 5	26.01	"	17.85	"	24.40
A_3- 6	20.20	"	13.20	"	19.40
A_7- 1	30.73	2.875	42.70	19.0	28.40
A_7- 2	26.92	"	38.50	"	25.05
A_7- 3	22.56	"	33.30	"	21.30
A_7- 4	15.47	"	21.50	"	15.00
A_7- 5	13.08	"	16.35	"	12.80
P - 1	14.82	"	39.20	15.5	13.75
P - 2	19.93	"	49.00	14.5	17.85
P - 3	9.60	"	26.50	14.0	9.25
P - 4	32.54	0.75	38.40	28.0	26.30
P - 5	24.62	"	29.70	"	21.40
P - 6	14.69	"	20.60	"	13.60
P_1- 1	13.47	2.875	30.60	14.0	12.15
P_1- 2	18.87	"	39.30	"	17.50
P_1- 3	25.39	"	48.50	"	22.80
P_1- 4	10.24	"	22.10	"	9.95
P_1- 5	16.63	0.75	17.15	28.00	15.70
P_1- 6	24.11	"	24.60	"	21.85
P_1- 7	32.31	"	30.80	"	27.50

(Contd)

Run No	cms D	Sx10^3	Cms/See $\overline{V}$	T°C	Cms Rb
P_3- 1	9.75	2.875	17.40	22.0	9.36
P_3- 2	16.16	"	32.00	23.0	15.30
P_3- 3	25.33	"	50.00	25.0	22.65
P_3- 4	32.56	0.75	30.60	28.0	28.10
P_3- 5	23.83	"	23.40	"	21.70
P_3- 6	16.85	"	17.00	"	15.90
AAU- 1	14.13	2.875	21.40	16.0	13.70
AAU- 2	19.93	"	35.10	"	18.70
AAU- 3	27.63	"	45.15	"	25.20
AAU- 4	32.18	0.75	26.20	28.0	28.60
AAU- 5	24.57	"	20.30	"	22.80
AAU- 6	16.38	"	14.24	"	15.70
APZ- 1	29.03	2.875	44.00	15.0	26.80
APZ- 2	19.73	"	33.50	14.0	18.58
APZ- 3	14.00	"	22.00	"	13.55
APZ- 4	32.24	0.75	26.90	29.0	28.60
APZ- 5	24.50	"	20.90	"	22.60
APZ- 6	17.86	"	14.50	"	17.05
AP_1Z-1	14.21	2.875	22.40	15.0	13.74
AP_1Z-2	19.40	"	34.40	"	18.25
AP_1Z-3	27.57	"	46.00	"	25.10
AP1Z-4	23.23	"	39.50	27.0	21.25
AP_1Z-5	32.37	0.75	28.80	29.0	28.30
AP_1Z-6	24.08	"	21.60	"	22.20
AP_1Z-7	17.08	"	14.90	"	16.25
APY- 1	27.23	2.875	46.50	15.0	24.60
APY- 2	19.69	"	35.20	"	18.45
APY- 3	13.91	"	24.10	"	13.40
APY- 4	17.63	0.75	15.00	28.0	16.85
APY- 5	24.34	"	22.20	"	22.35
APY- 6	32.80	"	29.00	"	28.60

(Contd)

Run No	cms. D	Sx10^3	Cms/See $\overline{V}$	T^{o}C	Cms Rb
APX- 1	19.69	2.875	31.20	14.0	18.65
APX- 2	23.24	"	39.70	"	27.05
APX- 3	14.12	"	20.30	"	13.76
APX- 4	14.19	"	19.40	27.0	14.00
APX-5	23.88	"	35.40	"	22.40
APX- 6	28.93	"	41.40	"	26.70
APX- 7	33.55	0.75	23.90	27.0	30.30
APX- 8	23.40	"	16.75	"	21.50
A_1P_2W-1	14.42	2.875	27.50	15.0	13.83
A_1P_2W-2	19.41	"	35.90	"	18.20
A_1P_2W-3	27.32	"	46.50	"	25.15
A_1P_2W-4	33.29	0.75	26.70	28.0	29.60
A_1P_2W-5	24.93	"	20.60	"	23.05
A_1P_2W-6	17.78	"	13.84	"	17.00
A_1P_2X-1	27.51	2.875	49.30	15.0	24.70
A_1P_2X-2	19.38	"	37.80	"	18.05
A_1P_2X-3	13.34	"	24.90	"	12.85
A_1P_2X-4	16.45	0.75	15.60	31.0	15.60
A_1P_2X-5	24.99	"	20.90	"	23.10
A_1P_2X-6	32.82	"	28.40	"	28.80
A_1P X-1	13.73	2.875	24.40	14.0	13.25
A_1P X-2	19.14	"	35.50	"	17.95
A_1P X-3	27.64	"	49.00	"	24.80
A_1P X-4	32.41	0.75	27.60	30.0	28.70
A_1P X-5	23.87	"	20.80	"	22.10
A_1P X-6	16.86	"	14.05	"	16.10
A_1P_2T-1	32.92	"	27.60	31.0	29.00
A_1P_2T-2	24.38	"	21.00	"	22.50
A_1P_2T-3	16.75	"	14.05	"	16.05

TABLE - II

SUMMARY OF WIND TUNNEL DATA COLLECTED BY THE AUTHOR

ON NORMAL PLATES KEPT IN MIDSTREAM AND PROVIDED WITH A TAILPLATE

Run No	Cms h	Cms D	m/s V	T_c	C_D	C_D (Average)
K-1	2.10	32.40	12.20	37.00	1.65	
K-2	"	"	9.70	37.00	1.62	1,611
K-3	"	"	8.55	38.0	1.56	
K-4	"	"	6.86	38.0	1.60	
O-1	4.00	32.40	11.90	37.5	2.00	
O-2	"	"	9.61	31.0	1.99	1.97
O-3	"	"	8.35	32.0	1.92	
O-4	"	"	6.82	33.0	1.98	
N-1	5.00	32.40	11.35	29.0	2.24	
N-2	"	"	9.63	31.5	2.26	2.26
N-3	"	"	8.35	33.5	2.29	
N-4	"	"	6.84	34.5	2.25	
M-1	6.00	32.40	10.80	32.0	2.45	
M-2	"	"	9.61	30.5	2.48	2.48
M-3	"	"	8.35	32.0	2.44	
M-4	"	"	6.85	36.5	2.54	
L-1	8.00	32.40	9.91	31.0	3.13	3.07
L-2	"	"	8.23	34.5	2.90	
L-3	"	"	6.80	29.5	3.17	
X-1	14.00	81.00	12.20	28.0	2.32	2.35
X-2	"	"	18.10	32.0	2.34	
X-3	"	"	24.60	39.0	2.40	
Y-1	5.00	81.00	13.10	29.0	1.62	1.63
Y-2	"	"	21.90	25.0	1.62	
Y-3	"	"	18.10	25.0	1.64	
Z-1	3.00	81.00	12.10	28.0	1.56	1.56

TABLE - III

SUMMARY OF WIND TUNNEL DATA COLLECTED BY THE AUTHOR ON NORMAL PLATES IN A TURBULENT BOUNDARY LAYER.

Run No	Cms δ	Cms h	Cms D	m/s V	$T^{o}C$	C_D	C_D (Average)	C_{D_c} (Average)
C-1	4.35	1.00	32.40	12.45	19.0	0.75	0.76	0.69
C-2	"	"	"	10.10	"	0.77		
Pa-1	0.70	2.00	32.40	12.10	28.5	1.24		
Pa-2	"	"	"	9.62	30.0	1.26	1.23	1.03
Pa-3	"	"	"	6.82	31.0	1.18		
P_b-1	01.12	2.00	32.40	12.80	25.0	1.13		
P_b- 2	"	"	"	9.62	30.0	1.13	1.14	0.95
P_b- 3	"	"	"	6.80	30.0	1.16		
P_c- 1	1.68	2.00	32.40	12.69	27.0	1.12		
P_c- 2	"	"	"	9.64	31.0	1.12	1.12	0.93
P_c- 3	"	"	"	6.76	29.0	1.12		
P_d- 1	2.60	2.00	32.40	12.70	29.5	1.06		
P_d- 2	"	"	"	9.57	28.5	1.01	1.05	0.87
P_d- 3	"	"	"	6.76	28.0	1.07		
P_e- 1	2.90	2.00	32.40	12.80	23.5	0.99	0.99	0.83
P_f- 1	3.40	2.00	32.40	12.70	29.5	0.97		
P_f- 2	"	"	"	9.62	31.0	1.01	0.98	0.82
P_f- 3	"	"	"	6.85	34.0	0.96		
P_g- 1	3.90	2.00	32.40	12.65	32.0	0.96		
P_g- 2	"	"	"	9.26	"	0.98	0.97	0.81
P_g- 3	"	"	"	6.82	"	0.96		

(Contd)

Run No.	Cms δ	Cms h	Cms. D	m/s V	$T^{\circ}C$	C_D	C_D (Average)	C_{Do} (Average)
P_h- 1	4.35	2.00	32.40	12.75	29.0	0.97		
P_h- 2	"	"	"	9.83	30.5	0.92	0.95	0.80
P_h- 3	"	"	"	6.82	32.0	0.97		
A_a- 1	0.78	4.00	32.40	11.65	24.0	1.67		
A_a- 2	"	"	"	9.50	"	1.77	1.73	1.19
A_a- 3	"	"	"	6.72	"	1.74		
A_b- 1	1.12	4.00	32.40	11.80	38.0	1.56		
A_b- 2	"	"	"	9.67	38.0	1.55	1.55	1.07
A_b- 3	"	"	"	6.87	39.0	1.54		
A_c- 1	1.68	4.00	32.40	12.05	26.0	1.46		
A_c- 2	"	"	"	9.46	22.0	1.37	1.41	0.97
A_c- 3	"	"	"	6.70	23.0	1.39		
A_d- 1	1.84	4.00	32.40	11.85	12.0	1.42		
A_d- 2	"	"	"	11.65	18.0	1.44	1.46	1.00
A_d- 3	"	"	"	9.41	18.0	1.44		
A_d- 4	"	"	"	6.67	21.0	1.54		
A_e- 1	2.50	4.00	32.40	12.05	21.0	1.37		
A_e- 2	"	"	"	10.5	21.0	1.37	1.35	0.93
A_e- 3	"	"	"	8.13	18.5	1.30		
A_e- 4	"	"	"	5.35	"	1.35		
A_f- 1	2.60	4.00	32.40	12.20	22.0	1.36		
A_f- 2	"	"	"	9.47	22.5	1.28	1.33	0.91
A_f- 3	"	"	"	6.69	22.0	1.35		

(Contd)

Run No	Cms. δ	Cms h	Cms D	m/s V	$T^{\circ}C$	C_D	C_D (Average)	C_{D_o} (Average)
A_g- 1	3.40	4.00	32.40	12.05	21.0	1.27		
A_g- 2	"	"	"	9.42	20.0	1.34	1.32	0.91
A_g- 3	"	"	"	6.72	24.0	1.36		
A_h- 1	3.90	4.00	32.40	12.20	32.0	1.34		
A_h- 2	"	"	"	9.39	32.0	1.30	1.34	0.92
A_h- 3	"	"	"	6.80	32.0	1.38		
A_i- 1	4.50	4.00	32.40	12.00	18.0	1.31		
A_i- 2	"	"	"	9.40	18.0	1.30	1.32	0.91
A_i- 3	"	"	"	6.67	20.0	1.37		

TABLE - IV.

SUMMARY OF WIND TUNNEL DATA COLLECTED BY THE AUTHOR ON NORMAL PLATES (ROUGHNESS ELEMENTS) KEPT IN SERIES ON THE FLOOR .

Run No.	Cms h	Cms D	Cms L	m/s V	$T^{o}C$	C_D	C_D(Average)
P_{40}-1	2.00	32.40	80.00	11.30	29.0	1.05	
P_{40}-2	"	"	"	9.65	30.0	1.02	1.02
P_{40}-3	"	"	"	8.38	32.0	1.01	
P_{40}-4	"	"	"	6.85	33.0	0.99	
B_{20}-1	3.00	81.00	60.00	29.70	40.0	0.60	
B_{20}-2	"	"	v "	25.90	40.0	0.57	0.57
B_{20}-3	"	"	"	20.10	39.0	0.56	
B_{20}-4	"	"	"	13.35	40.0	0.53	
A_{20}-1	4.00	32.40	80.00	9.77	14.0	1.23	
A_{20}-2	"	"	"	8.85	20.0	1.25	1.22
A_{20}-3	"	"	"	8.18	21.0	1.18	
A_{20}-4	"	"	"	6.70	21.5	1.21	
P_{20}-1	2.00	32.40	40.00	11.25	30.0	0.74	
P_{20}-2	"	"	"	9.59	27.5	0.71	0.74
P_{20}-3	"	"	"	8.27	31.0	0.78	
P_{20}-4	"	"	"	6.76	29.0	0.73	
R_{20}-1	3.00	32.40	60.00	10.45	27.0	1.01	1.04
R_{20}-2	"	"	"	8.11	"	1.03	
R_{20}-3	"	"	"	6.75	"	1.07	

(Contd.)

Run No	Cms h	Cms D	Cms L	m/s V	$T^{\circ}C$	C_D	C_D(Average)
B_{15}-1	3.00	81.00	45.00	32.10	43.0	0.48	
B_{15}-2	"	"	"	27.50	43.0	0.46	0.47
B_{15}-3	"	"	"	22.90	42.0	0.46	
B_{15}-4	"	"	"	15.75	41.0	0.46	
A_{15}-1	4.00	32.40	60.00	9.58	21.5	1.14	
A_{15}-2	"	"	"	8.75	16.0	1.14	
A_{15}-3	"	"	"	8.07	12.5	1.08	1.13
A_{15}-4	"	"	"	6.67	20.0	1.14	
P_{15}-1	2.00	32.40	30.00	10.62	19.0	0.62	
P_{15}-2	"	"	"	9.46	22.0	0.64	0.62
P_{15}-3	"	"	"	8.20	23.0	0.60	
P_{15}-4	"	"	"	6.70	"	0.58	
B_{10}-1	3.00	81.00	30.00	32.00	38.0	0.33	
B_{10}-2	"	"	"	28.00	40.0	0.33	0.31
B_{10}-3	"	"	"	24.80	39.0	0.30	
A_{10}-1	4.00	32.40	40.00	9.60	16.0	0.60	
A_{10}-2	"	"	"	8.79	19.0	0.62	0.65
A_{10}-3	"	"	"	8.10	14.5	0.68	
A_{10}-4	"	"	"	6.64	16.5	0.68	
P_{10}-1	2.00	32.40	20.00	11.75	30.0	0.46	
P_{10}-2	"	"	"	9.60	30.5	0.45	0.45
P_{10}-3	"	"	"	8.32	31.0	0.42	
P_{10}-4	"	"	"	6.53	22.0	0.44	

(Contd)

Run No	Cms h	Cms D	Cms L	m/s V	$T^{o}C$	C_D	C_D (Average)
R_{10}-1	3.00	32.40	30.00	10.35	27.0	0.61	
R_{10}-2	"	"	"	8.27	"	0.70	0.62
R_{10}-3	"	"	"	6.75	"	0.57	
M_{10}-1	6.00	32.40	60.00	9.39	17.0	1.27	
M_{10}-2	"	"	"	8.85	22.5	1.34	1.31
M_{10}-3	"	"	"	8.15	18.5	1.30	
M_{10}-4	"	"	"	6.68	21.0	1.33	
$B_{7.5}$-1	3.00	81.00	22.5	33.20	41.0	0.24	
$B_{7.5}$-2	"	"	"	29.80	41.0	0.21	0.22
$B_{7.5}$-3	"	"	"	25.40	40.0	0.21	
$B_{7.5}$-4	"	"	"	17.80	39.0	0.22	
$A_{7.5}$-1	4.00	32.40	30.00	9.45	14.0	0.51	
$A_{7.5}$-2	"	"	"	8.13	17.0	0.51	0.53
$A_{7.5}$-3	"	"	"	6.67	21.0	0.54	
$P_{7.5}$-1	2.00	32.40	15.00	10.60	12.0	0.348	
$P_{7.5}$-2	"	"	"	9.34	14.5	0.301	
$P_{7.5}$-3	"	"	"	8.14	17.0	0.375	0.36
$P_{7.5}$-4	"	"	"	6.64	18.0	0.369	
$M_{7.5}$-1	6.00	32.40	45.00	9.70	15.0	1.02	
$M_{7.5}$-2	"	"	"	8.87	16.0	0.98	1.00
$M_{7.5}$-3	"	"	"	8.14	18.0	0.96	
$M_{7.5}$-4	"	"	"	6.66	20.0	1.02	
B_5- 1	3.00	81.00	15.00	34.30	40.0	0.15	0.14
B_5- 2	"	"	"	30.80	44.0	0.14	
B_5- 3	"	"	"	18.80	35.0	0.14	

(Contd)

Run No	Cms h	Cms D	Cms L	m/s V	$T^{\circ}C$	C_D	C_D (Average)
A_5- 1	4.00	32.40	20.00	9.52	12.5	0.39	
A_5- 2	"	"	"	8.75	16.0	0.35	0.39
A_5- 3	"	"	"	8.15	19.5	0.42	
A_5- 4	"	"	"	6.59	13.0	0.40	
P_5- 1	2.00	32.40	10.00	10.50	18.0	0.22	
P_5- 2	"	"	"	9.44	21.0	0.23	0.23
P_5- 3	"	"	"	6.72	24.0	0.23	
R_5- 1	3.00	32.40	15.00	10.45	27.5	0.28	
R_5- 2	"	"	"	8.27	"	0.33	0.29
R_5- 3	"	"	"	6.75	"	0.27	
M_5- 1	6.00	32.40	30.00	9.13	16.0	0.63	
M_5- 2	"	"	"	8.04	11.0	0.57	0.62
M_5- 3	"	"	"	6.63	16.0	0.65	
$B_{2.5}$-1	3.00	81.00	7.50	34.70	44.0	0.055	
$B_{2.5}$-2	"	"	"	31.10	44.0	0.045	0.05
$B_{2.5}$-3	"	"	"	26.60	44.0	0.051	
$A_{2.5}$-1	4.00	32.40	10.00	10.05	16.0	0.136	0.14
$A_{2.5}$-2	"	"	"	8.15	20.0	0.158	
$P_{2.5}$-1	2.00	32.40	5.00	10.80	23.0	0.056	
$P_{2.5}$-2	"	"	"	9.47	"	0.037	0.05
$P_{2.5}$-3	"	"	"	10.90	13.0	0.053	